Faculdade de Engenharia da Universidade do Porto

Characterizing electrophysiological communication between neuronal populations with known architecture

Pedro Miguel Pinto Teixeira de Melo

Dissertação realizada no âmbito do

Mestrado em Bioengenharia – Engenharia Biomédica

Orientador: José Mateus (PhD)

Co-orientador: Paulo Aguiar (PI, Group Leader)

23th of June of 2024

Resumo

O sistema nervoso é o sistema biológico mais intrincado conhecido pela humanidade, resultado da combinação da sua complexidade natural inigualável, já que coordena a reação à aquisição de estímulos mantendo simultaneamente funções essenciais à sobrevivência do corpo, com as multitudes de processos e dinâmicas que ainda estão por descobrir no que concerne a este sistema.

Contudo, uma informação-chave que está já estabelecida sobre os astutos mecanismos dos neurónios é que a arquitetura das redes neuronais é crucial para determinar os seus níveis de eficiência funcional. Deste modo, compreender as relações complexas entre a conectividade anatómica e funcional é crucial para a compreensão do que sustenta a transmissão de informação neuronal eficaz.

Com este objetivo, estabelecer como as populações neuronais comunicam umas com as outras e como isto se relaciona com o modo como elas se conectam é fundamental. Assim, fazer análise através de métodos alta produtividade, como neuroeletrofisiologia, pode propulsionar ainda mais o nosso conhecimento sobre este tópico. Neste estudo, dados foram retirados de MEAs de 256 elétrodos associados a microfluídica para segregar duas ("source" e "target") populações neuronais, conectadas via microcanais com dimensões proibitivas para processos somatodendríticos mas que permitem que axónios os atravessem. Estes microcanais contêm elétrodos, pelo que permitem o registo de potenciais de ação que se propaguem ao longo dos axónios. Diferentes designs de microcanais assimétricos foram implementados, quer retirados da literatura, como as "arrowheads" e as "tesla valves", quer variações customizadas dos mesmos.

O objetivo do projeto é, então, caracterizar a comunicação elétrica entre estas populações separadas de neurónios hipocampais e recapitular *in vitro* caminhos neuronais hipocampais que são unidirecionais no sentido anterógrado, algo que ainda não foi conseguido. Isto implica novas análises computacionais, tendo em conta a dimensão dos dados.

No global, esta tese contribui com gráficos de leitura fácil e análises que efetivamente demonstram um viés funcional nas culturas neuronais com arquitetura imposta. Recorrendo aos designs assimétricos, foi possível criar um viés funcional efetivo na comunicação entre populações, quer em termos de disparos individuais que se propagam ao longo dos microcanais, quer na comunicação por meio de eventos de maior sincronicidade.

Quase todas as medidas diretas e indiretas de bloqueio funcional indicam os "Rams" como o melhor. De facto, este design teve uma média de 2.634 relativamente à razão na direccionalidade

"Source"-"Target" da atividade global dos microcanais e uma média de 92% no que diz respeito à propagação de eventos nesse mesmo sentido nos microcanais, validando-o como uma forte alternativa em forçar um caminho preferencial para o fluxo de informação na comunicação neuronal.

No final, este trabalho tem o potencial de alargar o nosso conhecimento de investigação fundamental sobre a comunicação entre populações neuronais, mas também facilitar a criação de recriações mais realistas de chips relativos ao hipocampo.

Abstract

The nervous system is the most intricate biosystem known to mankind, which is a result of the combination of its unrivalled natural complexity, being responsible for coordinating the reaction to simultaneous stimuli acquisition while maintain vital functions to the body's survival, and the multitudes of processes and dynamics which are still uncharted regarding this system.

Nonetheless, one key information that has been established about the mischievous mechanisms of neurons is that the neural networks' specific architecture is crucial in determining neural function. Therefore, comprehending the complex relationships between anatomical and functional connectivity is crucial for the understanding of what underpins effective neuronal transmission of information.

To this end, establishing how neuronal populations communicate with one another and how does this relate to how they connect is quintessential. On neuroelectrophysiology studies, high throughput methodologies are common and in particular the use of *in vitro* systems which propel further the knowledge on this topic. Here, data was retrieved from 256-electrode MEAs with microfluidics to segregate two ("source" and "target") neuronal populations, connected via microchannels whose dimensions are prohibitive for somatodendritic processes but allow for axons to cross. This combination allows for these microchannels to encompass electrodes, thus enabling the recording of action potentials propagating along the axons. Different designs of asymmetric microchannels were implemented, either retrieved from literature, such as "arrowheads" and "tesla valves", or custom variations of those.

The goal of this project is, then, to characterize the electrical communication between these segregated populations of hippocampal neurons and recapitulate *in vitro* feed-forward hippocampal pathways which is still an issue to be addressed. This implied the use of novel computational analysis, considering the size of the data.

Overall, this thesis contributes with easy-to-read visual outputs and analyses that effectively demonstrate a directionality bias in the neuronal networks with imposed architecture. With the use of the asymmetrical designs, it was possible to create an effective functional bias in the communication between populations both in terms of individual spikes propagating along the microchannels and in the communication through higher synchronicity events.

Almost all of the direct and indirect measures of functional blockage returned the "Rams" as the best performer. In fact, this design had a mean of 2.634-fold-change in the "Source"-to-"Target" directionality of overall activity in the microchannels and a 92% mean of forward spiking bias on the

Commented [jo1]: vital functions?

Commented [jo2]: Isto representa um conjunto de métodos, tenta rever esta frase

Commented [PMPTdM3R2]: Feito!

Commented [jo4]: This combination allows...

Commented [PMPTdM5R4]: Feito!

microchannels, validating it as a strong alternative on enforcing a preferential path for information flow in neuronal communication.

In the end, this work has potential to widen our knowledge on fundamental research of the neuronal population' communication but also eases the creation of more faithful recreations of hippocampus-on-a-chip.

Commented [jo6]: Quanto tiveres concluído os resultados, volta aqui para complementar com algo mais bem definido

Commented [PMPTdM7R6]: Já o fiz, vê por favor se achas que deva adicionar mais alguma coisa

Agradecimentos

Este trabalho não estaria completo sem, acima de tudo, uma estrutura de suporte e carinho, à qual ao longo destes últimos meses, recorri um sem-número de vezes para me motivar e onde me apoiei. Acredito que muitas vezes nem se aperceberam da importância da vossa ajuda, e também, por isso, estou-vos a todos eternamente grato.

Primeiramente, gostaria de agradecer ao meu orientador Doutor José Mateus por todas as vezes em que um "é só uma pequena dúvida…" se tornou uma manhã inteira de discussão à volta de temas e de análises que poderiam fazer sentido ou ser interessantes. Obrigado pela paciência, pela disponibilidade e pela confiança, sobretudo quando nem eu estava muito seguro do trabalho que fiz. Acima de tudo, obrigado por me incutires um gosto por pensar as neurociências de uma forma muito mais biológica que a que um ~~(futuro)~~ engenheiro está habituado a pensar.

De seguida, agradecer também o voto de confiança ao 'líder do barco', Professor Paulo Aguiar, não só por ter sempre o conselho certo em momentos de aperto, mas também pelo entusiamo com que faz pautar a ciência que se faz no NCN. Gostaria também de agradecer a todos os restantes NCNers por momentos dentro do contexto académica, como bons conselhos e várias sugestões, como fora. Termino com o sentimento de uma missão cumprida e a sensação de ternura de alguém que encontrou neste grupo um pequeno porto de abrigo. Sem vocês, esta dissertação não estaria completa.

À minha família, que, apesar da sua ~~(loucura)~~ excentricidade, é sempre casa. Em particular, aos meus pais, por sempre me lembrarem que a vida não é só isto, é um monte de coisas (bem arrumadas, por favor!) mas, nem por isso, menos certos no seu incansável apoio. À minha irmã, que gozava que só trabalhava em "linhas e pontos", mas que não deixou que nenhum tivesse fora do sítio ou com a cor errada. E aos meus primos mais velhos, por me levarem a espairecer quando precisei e por terem uma palavra sábia de quem passou algo parecido não há muito tempo.

Por fim, aos meus amigos, que felizmente são muitos. Aos meus *day one* do Luso, obrigado por estarem sempre lá para mim. À Ana Martins, por ser uma amiga que por mais que passe tempo desde o último momento juntos, é como se tivesse sido há minutos. Ao Castro, por ter sempre o timing certo no que diz respeito a ser sério e sensível ou brincalhão e idiota, à Marta, por ser a minha *deskie* independentemente de já não partilharmos carteiras, à Bia, por nos lembrar sempre de ver o lado bom e divertido das coisas, ao Migas, por ter sempre um suspiro e por estar em todo o lado (ou pelo

menos um sósia qualquer), ao Alves, por ser o Alves, e à Rita, por ter sempre uma palavra amiga ou um riso contagiante.

À Ana Sousa, minha presidente, 'prima' e 'hiperlino', por todo o companheirismo e apoio em todas as situações, mas sobretudo na parte académica.

Às amizades, colegas e atletas que o voleibol me deu deixo também o meu agradecimento. Neste sentido, um obrigado especial à Patty, que é a minha fã número 1 e que me apoia incondicionalmente e à Rita Teixeira, do qual serei sempre treinador adjunto seja de que aventura/projeto for.

Por último, mas não menos importante, um obrigado sentido aos meus amigos de um mestrado (de Neurobiologia) emprestado. O quanto vocês me fizeram sentir parte de algo que foi meu apenas por pouco tempo não se põe em palavras. Agradecimentos especiais à Ritinha, o meu porta-chaves, designer gráfica e parceira de aventuras de última hora, e ao Rúben, por ser psicólogo - quando as coisas na minha cabeça começam a ser demasiado – e me ajudar a rever tudo no final.

"*Magic is just science that we don't understand yet*"

Arthur C. Clarke

Index

List of figures

Abbreviations

Commented [PMPTdM8]: Voltar aqui para adicionar algumas abreviaturas que estão em falta

AAV	*Adeno Associated Virus*
AP	*Action Potential*
BCI	*Brain-Computer Interfaces*
DG	*Dentate Gyrus*
DIV	*Days in Vitro*
DRG	*Dorsal Root Ganglia*
EC	*Entorhinal Cortex*
IBeI	*Inter Burst Event Interval*
iPSCs	*Induced Pluripotent Stem Cells*
ISI	*Inter Spike Interval*
MEA	*Micro-Electrode Array*
MFR	*Mean Firing Rate*
MF	*Mossy Fibers (Pathway)*
NB	*Network Burst*
PDE	*Population-Driving Events*
PE	*Propagating Event*
PDMS	*Polydimethylsiloxane*
PP	*Perforant Pathway*
SC	*Schaffer collaterals*
SFR	*Summed Firing Rate*
Sub	*Subiculum*
TA	Temporoammonic *(Pathway)*
TTX	Tetrodotoxin
µF	*Microfluidics*
µEF	*Microelectro arrays combined with microfluidics*

Chapter I

Introduction

The brain is the ultimate structure of biological complexity, coordinating a myriad of processes. What is most remarkable is its ability to simultaneously guarantee the survivability by maintaining involuntary vital functions, to execute acquisition and processing of different kinds of stimuli and, finally, to integrate them on higher level and, thus, ensuring the build-up for knowledge, memory and other cognitive abilities. In this sense, it is fundamental on maintaining homeostasis and for environmental perception, facilitating the interactions with one another and with the environment in the day-to-day life.

Despite extensive research, many aspects of neuronal dynamics and interconnectivity remain enigmatic, posing a significant challenge to neuroscientists. Neurosciences are a growing field of research that attempts to unveil the mysteries which the nervous system are still enshrouded on.

In vitro neuronal circuitry is a fundamental tool for understanding the complex dynamics of their *in vivo* counterparts, especially regarding their basic principles: more often than not, studying the neuronal system (or part of it) integrated into the human body is a virtually impossible task, due to its inaccessibility, the complexity of their mechanisms when considering the system as a whole and the lack of control on the experimental variables. Thus, mimicking *in vivo* systems through *in vitro* techniques means, in general, a lower level of complexity and a more controlled and accessible environment for understanding neuronal functionality, without compromising the significance of the results. In fact, reviews have already been made ensuring that a lot can be extrapolated about *in vivo* function, in this sense, from this *in vitro* neuronal data [1].

These platforms generate a colossal amount of complex yet valuable data, raising the need to create new advanced tools for their analysis and visualization. Several work has already been done on the processing of neural data obtained from Micro-Electrode-Arrays (MEAs) recordings, particularly, studying metrics that characterize the propagation of the signal. Likewise, the relationship between neuronal signal and its encoded function, in particular, what concerns to coordination of events also known as bursting activity has been studied vastly and it's critical to understand spatiotemporal dynamics of the networks.

This type of activity is a result of the presence of functional neuronal communities with recurrent local connections [2], [3], [4], [5], [6], [7], meaning spatial and temporal profiling of the networks are paramount to understanding these dynamics [8], [9], [10]. There were also some papers where

Commented [jo9]: Opinião geral: Acho que estás a entrar em assuntos muito específicos cedo demais. Aproveita esta secção para dar um contexto mais geral do trabalho da tese

Commented [jo10]: Acho que podias começar com um parágrafo mais geral da função cerebral, como no abstract

Commented [PMPTdM11R10]: Depois vê se concordas como isto ficou?

Commented [jo12]: tools?

Commented [pm13]: For submission, this should be put as [3-8], right?

Commented [jo14R13]: Sim, o mendeley deveria fazer isso automaticamente. Possivelmente é algo que se tem de alterar nas definições do estilo de ref

Commented [PMPTdM15R13]: Ok, vou deixar o comentário ativo para me lembrar de rever isso no final

the properties of the signal were related to neurological disorders [11], further extending the interest of this kind of work to clinical.

Furthermore, in-depth studies on axon communication profiling could prove crucial to a better understanding of the underlying mechanisms of the neural system [12]. Currently, solutions are designed to characterize communication at network levels and therefore are lacking the capacity to describe details concerning the communication on the parts of the neuron [13]. This issue becomes particularly interesting when considering, for one, that axons are an essential piece of neuronal communication, able to perform by themselves some degree of signal processing [14], [15] – a task which up until now was thought to be only related with the somatodendritic section of the neurons - but also when the structure of the Microfluidics' chambers and channels entails changes on the development of the networks and, therefore, on their activity.

On the one hand, for a complete understanding of these methods is necessary to understand the correlation between the activity on the soma and axonal part of the neurons, eventually, raising the need to comprehend how these structures behave at the synaptic level to establish how signal propagation is performed from population to population.

On the other hand, recent studies have shown that different designs of the channels connecting population's condition differently the networks' behaviours/activity. Hence, the characterization of how these Micro-Electro-fluidic (μEF) designs are capable of reproducing feed-forward networks (similar to the ones found *in vivo*) is relevant.

It is relevant, thus, to review the current solutions' utility and specifics on neuro-electrophysiology studies to develop a software solution that performs the analysis specifically, on the properties of the propagation of action potentials (APs) within a single cell and the way they relate to the communication at the network and population-wide levels, while accounting for the effect of structural motifs on them.

1.1 - Motivation

The primary objective of this research project should be academic, as there is a considerable degree of novelty. Indeed, while various studies on neuronal network dynamics have already been performed, as explained, work concerning signal propagation at the subcellular level is still lacking.

For instance, a primary goal of the work done for this thesis is enhancing the understanding of neuronal network dynamics through the development of a software tool capable of performing a higher-level of analysis, thereby contributing to the foundational knowledge of neuronal communication. This involves increasing the knowledge on the network connectivity by performing a functional data analysis, bridging the gaps between the different levels of the neuronal system.

The second main goal of this project is to emulate the predominantly unidirectional flow of information, similar to that occurring in vivo in the perforant pathway (PP) of the hippocampus (Fig. I.1). By achieving this, the project aims to gain deeper insights into the mechanisms governing neuronal interactions. These efforts are intended not only to advance the scientific understanding of neuronal communication but also to pave the way for new therapeutic approaches to neurological disorders, thereby bridging the gap between fundamental research and clinical applications.

Acquiring this knowledge of neurodynamics is relevant not only for the sake of itself but also has, to some extent, clinical value, which can, later on, be translated into the development of brain-computer interfaces (BCI) and neurostimulation systems. Furthermore, the creation of a tool with these potentialities would also address a very important component, which is the existing shortage of

Commented [jo16]: Acho que tens várias frases na seccção anterior que ficariam melhor aqui na Motivation

Commented [PMPTdM17R16]: Estás a pensar nas frases que dizem respeito à parte clínica? Deixei as com realce amarelo mas já aqui nesta secção

Commented [PMPTdM18]: Sounds like motivation

Commented [jo19R18]: Concordo (1º paragrafo)

Commented [PM20R18]: Feito e adaptado! Como te parece?

software that conducts a thorough standard analysis on subcellular data, making it attractive for future investigations on neurophysiology.

A particular use-case to be performed also on the scope of this thesis is the study of how different designs for the microchannels will affect neuronal communication, enforcing (or not) the desired directionality. Indeed, this would, then, allow for the creation of in vitro models of tri-synaptic pathway in the hippocampus (Fig I.1). Here, there's evidence of a bias towards feed-forward propagation between the entorhinal cortex (EC) and the dentate gyrus (DG) – information tends to flow from the EC to the DG, through the perforant pathway (PP) [12]. The PP pathway is the main input of the DG and no pathway pertaining to the signal starting on the DG going to the EC directly was ever found.

Instead, projections from the DG follow to the CA3, in the mossy fibers pathway (MF) and from there to CA1, through Schaffer collaterals (SC) and, finally, there are CA1-EC connections – both direct and projections that go through the subiculum (Sub), thus closing the loop [16], [17]. Pathways from CA1 to EC are still not really defined and neither is the role of subiculum on this communication on the hippocampus, even if this is empirically proven to be relevant.

However, information flows output by layer III of the EC to area CA1 follow the temporoammonic (TA) pathway [18], which is already a known and studied process of the hippocampal information modulation.

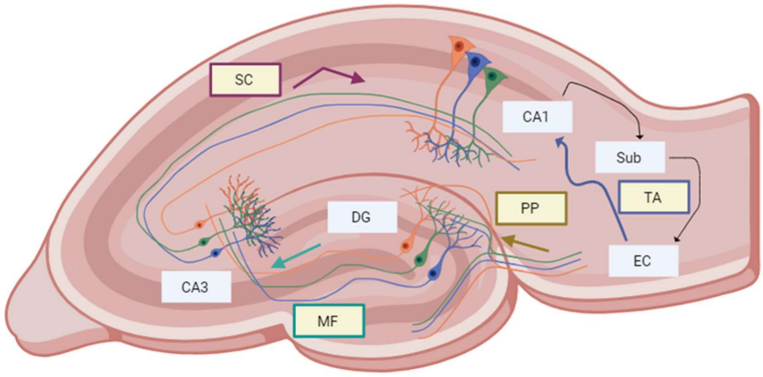

Figure I.1 - Schematic of the Hippocampus and its neuronal pathways. The grey rectangles represent the main nuclei of the hippocampus while the yellow ones represent the pathways established between them. For the sake of comprehension, arrows are displayed to show the preferential direction of communication. Adapted from [12], [16], [17], [18]

As such, "brain-on-chip" technologies, namely the use of Microfluidics in Neuronal circuitry design, allow for known architecture and connectivity defined by the investigator [19], allowing to comprehend how structure-function relationships are establish in neuronal settings and, in particular, to create *in vitro* analogous for these pathways.

Nevertheless, there's also to consider a degree of clinical relevance and the fact that recent studies have shown that, in neuropathological settings associated with networks reconfiguration, symptomatology is only observed after irreversible and irreparable damage on the neuronal networks, meaning it is fundamental to assess this information prior to the presence of symptoms [20], which is something that might be easier after the studies here elaborated.

Commented [jo21]: Acho demasiado cedo para aparecer estas ideias de BoC, structure-function...

Commented [PMPTdM22R21]: Mas achas q devo retirar completamente ou só passar por exemplo para secção de motivation?

Commented [JM23R21]: Acho que fica melhor depois desta parte da fisiologia/anatomia do hipocampo... No sentido de BoC poderem ser utilizadas para mimetizar esta organização in vitro

1.2 - Challenges

Most studies concerning the use of MEAs for retrieval of neuronal activity data are focused on processing spiking activity from the neurons registered in the electrodes and correlate it to get information on network activity. In this case, population-to-population propagation is not analyzed because there is only a single subject of study. Even when there is a small number of populations, separated either in different wells or different chambers on the same MEA, this evaluation is not extensive, mainly due to the lack of electrodes pertaining to the means of communication or the lack of communication between the populations altogether.

Consequently, the shortage of studies relating to the relationship between somatic and axonal activity posed a significant hurdle in defining parameters for the functions and operations used in this thesis. This necessitated a trial-and-error approach for parameter selection, especially in the network burst detection algorithm, due to the lack of supporting material to justify specific values. Additionally, unlike the prevalent unidimensional analyses found in the literature, this work involved a multi-level analysis encompassing somal, axonal, and population levels of activity. For this holistic approach, no existing parameters could be found in the literature, further complicating the signal analysis process and making it more time-consuming.

Additionally, the processing power needed to work with the data of the raw voltage directly obtained from the 256-MEA (~1 GB/min), considering its size and the computational operational cost, is not possible in a day-to-day personal computer. Therefore, they require the use of one of the lab's workstations, meaning management of the availability of the hardware equipment was also necessary. These operations also take their time, which considering the time given to do the project can also be named as a hindrance.

Finally, one must consider that in vitro neuronal networks show high values of inter-culture variability as the connections between their nodes are intrinsically different. Likewise, intra-culture variability over time is also a key factor in neuro-electrophysiology as synaptic and network plasticity occur. In summary, as with most of the disciplines involving cell studies, one cannot ignore these factors which heighten the importance of doing statistical analysis to avoid making the mistake of assuming a relationship to be found when it is due to chance alone.

1.3 - Objectives and Contributions

The purpose of this master's thesis is integrated on a bigger project inside the research group. In fact, works with standard microchannel designs (i.e., straight) and neuronal cultures had already been done, in order to achieve a higher level of comprehension of how the propagation of the neuronal signal occur in the axons [21].

However, this earlier study left a question to be answered: are the antidromic events on the axons a result of the neuronal population lacking a target population to communicate with? So, to test this hypothesis it was essential to ensure, firstly, the existence of said second neuronal culture to work as a synaptic target of the first and, secondly, to devise a way to keep the microchannels free of activity related to axons growing from the target population.

While the first part was rather easy and meant only adding a second chamber on the previous developed devices, for the other part, research was necessary to understand how to condition the

Commented [jo24]: ?

Commented [PMPTdM25R24]: Creio que agora está mais claro, mas confirma pf

Commented [jo26]: this evaluation is not extensive

Commented [jo27]: Revê esta frase ou apaga mesmo. Acho que é algo comum a toda a biologia...

Commented [PMPTdM28R27]: Concordo, talvez seja inespecifico, mas acho que é importante recordar aqui que foi um desafio no sentido em que exige mais que só procurar relações

Commented [jo29]: Aqui podes referir que a tua tese faz parte de um trabalho maior e especificar a tua contribuição (software e análise de resultados de eletrofisiologia)

Commented [PM30R29]: Não o tinha feito por comparação às restantes teses disponiveis na pasta do NCN mas totalmente de acordo em adicionar isto aqui se por ti também estiver ok

creation of modular networks and, hence, the concept of the asymmetric designs of the microfluidics used in this work was implemented, following data from the literature [22], [23], [24], [25] .

Preliminary structural studies were run on these devices by other elements of the group to assert if structural bias were generated by implementing the designs on the channels. These studies demonstrated that ~75%, ~40% and ~25% of the microchannels with "Rams", "Arrows" and "Tesla-valve" motifs, respectively, completely blocked axon growth. After this screening, there was a need for the development of new methodologies for the analysis of neuro-electrophysiologic recordings retrieved from μEF devices that integrated these microchannel designs.

Indeed, the aim of the work for this dissertation is to characterize the conditions in which there is neuronal population communication, in terms of the response delay, synchronicity of events and the effects of the microchannels' design on these. Ultimately, this project helps to better understand how neuronal cultures' population-to-population signal propagates, by integrating multi-scale levels of the culture, namely cellular and network levels of the analysis, and how it can be modulated, in further studies.

1.4 - Document Structure

This document is organized into five chapters. Chapter I presents a briefing of the topic of this dissertation, while also listing the goals and main hurdles associated with this study. Chapter II looks at the past and current state-of-the-art solutions for capturing the signal of neuronal cultures. In this chapter, studies of how the networks behave in both physiological and pathological settings *in vivo* and *in vitro*, particularly how structural constraints condition their dynamics, are also visited. It is also a review on the computational methods used on the analysis of *in vitro* neuro-electrophysiology recordings, exploring their strong suits and weaknesses. Chapter III describes the methods and materials implemented on the presented work, ranging from the description of the equipment used for the recording to the development of the functions in the software for the analysis. A novel approach to do Network Burst (NB) detection is proposed and its pros and cons debated. Chapter IV discusses the outputs returned by the software. In the end, Chapter V concludes what are the impacts of this work on the scope of future research on the field, while pointing out in what directions should further studies head on.

Chapter II

Literature Review

Establishing how neuronal communication is performed is a task very much sought-after by neuroscientists worldwide, as there's still much uncharted territory to be explored. As such, it is a field whose interest has skyrocketed in the past decades, namely in what concerns the understanding of how neuronal populations interact and convey information to one another. This chapter aims to provide a comprehensive overview of the state-of-the-art of the current understanding on the way neurons communicate, by gathering the relevant studies which characterize the mechanisms and methods and discuss the implications related to these neuronal interactions.

First, basic concepts and initial definitions of how the neuron activity is recollected are reviewed, detailing the different techniques used to record it and their pros and cons, as the first step for a good interpretation of the obtained information can only be achieved after getting a good grasp of the principles underlying these methodologies.

Another critical point addressed in this section regards, precisely, the methodologies of the processing of the gathered data, which involves data analysis algorithms of different sorts to obtain also different kinds of information about the neuronal dynamics. The definition of the most commonly used metrics and the way their changes reflect on neuronal function and dysfunction are briefly discussed too.

Finally, the gaps identified in the current literature and their relationship with the motivations and goals for this project are presented.

Commented [PMPTdM31]: Is it really a good idea to have this here?

Commented [jo32R31]: Não vejo problema

2.1 - Neurophysiological recordings

The neuronal system and the mechanisms neurons establish between themselves, and other cells of the nervous system have still a lot to be uncovered. As such and given the complexity of the system itself, scaled-down *in vitro* studies, where biochemical environment and neuronal architecture may be measured or set, are crucial to better understanding these dynamics, which are expected to primarily manifest at the electrophysiological level. Hence, in this section, topics such as the means and the details of the systems associated with the neuronal action potentials' data acquisition, the devices, frequently μEF ones, that condition the functional connectivity of the neuronal networks and the most recent discoveries on how axons modulate action potential propagation and communication are discussed.

2.1.1) Electrophysiological neuronal data recording

Neurons are a particularly interesting cell type for electrophysiology, due to their ability to produce a measurable extracellular field potential. Indeed, they are one of the few intrinsically excitable cell types, as highlighted in the research. Neuronal ensembles, coactive groups of neurons, play a crucial role in perception and behavior, forming through changes in excitability that lead to the establishment of functional circuits [26].

They can be cultured over electrodes, and, over time, neuronal cultures will grow and form cohesive networks. Afterward, these networks will present an electrophysiological profile, descriptive of their functionality [2]. Evidence was found that some neurodegenerative disorders could be linked to changes in the parameters of spiking neuronal activity [11]. In terms of the systems implemented in the studies of the activities and dynamics of neuronal networks, MEAs are the go-to technology. These devices are microscopic electrode grids implanted on a substrate, typically arranged in a 2D grid or less frequently in 3D structures, depending on the application [19].

Commented [jo33]: Podes referir que são um dos poucos tipos celulares intrinsecamente excitáveis

Commented [PMPTdM34R33]: Feito e referenciado!

These systems can be further divided into rigid (rMEAs) or flexible (fMEAs) according to the nature of their substrate. For *in vivo* studies, the polymeric matrix of the substrate – based on parylene, polyimide, polydimethylsiloxane (PDMS), or hybrid polymers - in fMEAs and their comparatively lower thickness, makes them the preferred choice over metallic-based rMEAs, avoiding host tissue damage [27].

The interest in using MEAs in neuroscience studies is raised due to their ability to record extracellular electrical signals – both in the form of action potentials (APs) and local field potentials (LFPs) – simultaneously from multiple electrodes, providing high spatial and temporal resolution [28]. On the one hand, state-of-the-art is established by using high-density MEAs which, alongside the miniaturization of the technology, allows for a more refined degree of spatial sampling [5]. Nonetheless, these systems are also designed to endure long-term recordings, revealing how the network activity changes throughout time [9]. Therefore, this type of system is used in *in vitro* studies, where network activity is categorized through a range of metrics [7], [10] - for further details on the algorithms behind them and the metrics themselves, read subsection *Neuronal action potential data processing*.

This analysis is done to extract insights on network behavior, synchronization, and connectivity in neural circuits, aiding in understanding complex brain functions. Companies, namely, Netri, Axion Biosystems, and 3Brain offer this hardware in the form of a closed system with an in-built well. The well size ranges from grids with 8 to 4096 electrodes and the system is available with software that integrates both hardware setup and data analysis functions [28], [29], [30].

However, the solutions presented to this point cannot analyze data from an *in vivo* system. For those scenarios, optimal equipment consists of neural probes such as the Neuropixels probe [31]. These are fMEAs designed in extremely narrow shanks with metal oxide semiconductor (CMOS) technology, which provides a silicon-integrated-circuit-like approach to neuronal studies, allowing for a drastic decrease in wire width and the probes to perform, on par with data acquisition on 960 recording sites in the 70x20µm shank, amplification, digitization, and multiplexing.

This technology could be an important breakthrough in neurosciences, bringing about the exploration of *in vivo* neuronal systems to an integration level: their ability to sample densely, simultaneously, isolates single neuron activity while recording data from multiple layers of the same brain structure [13].

As such, APs can be traced to their origin which leads to a better description of how the components communicate inside neuronal structures. This could ease our understanding of the mechanisms through which they are processed/implemented.

Alternatively, recordings can also be performed using patch-clamp. This technique consists of using a glass pipette whose tip is sealed to the surface of a cell membrane, thus, isolating a *patch* of the neuronal cell's membrane [1]. This technique allows for detailed studies on the electrical properties of individual neurons and mRNA harvesting for gene expression analysis, being for these reasons the single-cell level technique most frequently used in neuroelectrophysiology [32] .

These are highly invasive methodologies, usually done *ex vivo*. Following the euthanization of the animal, its circulatory system is infused with a fixative agent to preserve the tissue. The brain is then retrieved and sliced in a vibratome with a micrometer precision. The slices are subsequently immersed in artificial oxygenated cerebral fluid (ACSF) and allowed to recover for 1-2 hours. Once the tissue has stabilized and appears viable under microscopic examination, a glass pipette is used to clamp the cell membrane, which coupled with electrodes provides critical information of the functions of ion channels' current flowing through the cellular membrane, in very region-specific settings [33].

Commented [jo35]: Referir que é a tecnica de eleição à escala single-cell

Commented [PMPTdM36R35]: Feito e referenciado!

Commented [jo37]: Formaliza isto :)

Commented [PMPTdM38R37]: Está melhor assim não?

2.1.2) Alternative methods for Neuro circuitry mapping

Alongside neuro-electrophysiology, there are other techniques worth mentioning for being frequently used to complement these studies (or to similar ends) – calcium imaging, neuro-tracers and optogenetics.

Firstly, neuronal calcium imaging has emerged as a powerful tool for investigating the spatiotemporal dynamics of intracellular Ca^{2+} concentrations in neuronal cultures. This imaging modality is relevant due to the role of calcium ions in AP propagation, synaptic plasticity and the survivability of neuronal cells. Furthermore, Ca^{2+} ions have undeniable roles in multiple signal transduction pathways [34].

In these methods, fluorescent tags are used to, through alteration of their properties caused by binding with calcium ions, quantify changes in intracellular calcium dynamics. In fact, the indicators, currently in vogue, can be of two types: either they are synthetic dyes - small molecules which can be loaded into cells to manifest, in such scenarios, fluorescence - or induce specific cell types to express genes coding for proteins engineered to emit fluorescence (e.g., GCaMP family) [35].

Fluorescence changes can then be tracked, in general, in terms of fluorescence intensity or wavelength, using a microscope. If the intensity of the signal is registered, the analysis of the data is very similar to the one done on electrophysiological recordings and the conversion to spikes could follow a similar conventional threshold-based methodology.

Microscopy techniques range from confocal microscopy to two-photon microscopy [36], and wide-field imaging [37]. The choice of imaging modality depends on factors such as spatial and temporal resolution requirements and the specific characteristics of the experimental setup [38].

In what regards to spatial resolution, calcium imaging is most likely the best alternative as single-cell spatial resolution can be achieved. Nevertheless, calcium dynamics are slower than the propagation of electrical signals in the neurons, meaning that if the temporal resolution must go below the dozens of microseconds, much like the case in this study, electrophysiology prevails as the best alternative.

Furthermore, the neural circuit mapping through neuro-tracing techniques is crucial for investigating the structural and functional connectivity of the network. These methods rely on the

cellular transport proteins to, after endocytosis, transport along neural pathways and label neurons. Depending on the goal of the project, there are several types of tracers, each offering a distinctive perspective on neural connectivity.

Regarding the type of transport, neuro-tracers are divided into anterograde, whenever the transport occurs from the somatodendritic part to the axonal terminal, and retrograde, if the transport is in the antisense. There is also the possibility for them to be trans-synaptic, enabling cross-synaptic abilities [39].

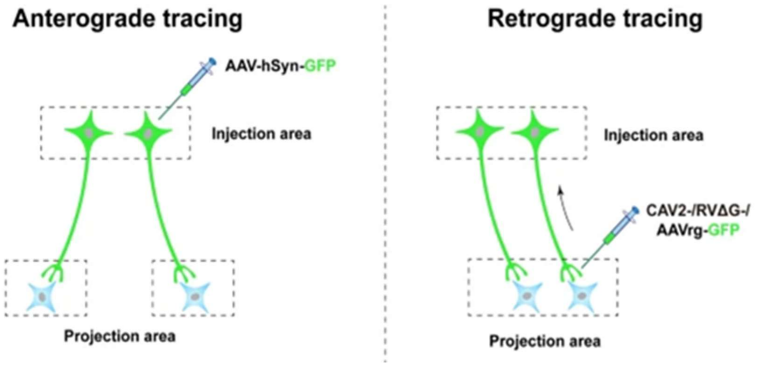

Figure II.1 - Comparison between Anterograde and Retrograde tracing using adeno-associated-virus (AAVs) in what concerns to the labelled neurons, the injection and projection area, Adapted from [39].

Integration of these molecules with optogenetics pave the way for the current state-of-the-art connectivity studies. Optogenetics makes use of, for example, channelrhodopsins or halorhodopsins, which are protein-based ion channels of the neuronal cell membrane, which are activated by laser beams with specific wavelengths. The first ones, when active, let cations in, promoting the neuron depolarization, hence, inducing the propagation of AP, meanwhile the others, are chloride pumps, which reinforce the membrane potential in the active state [40].

This allows for precise *in situ* neuronal modulation with stunning spatiotemporal precision, because of the possibility to genetically target neurons to express these proteins, enabling the marked neurons to be excited or inhibited, respectively.

Deepening the research on the studies of the relationships between network architecture, in particular brain anatomy, and its functionality is critical to the understanding of the pros and limitations of some clinical targeted neurotherapies. For instance, it could improve the results of approaches such as deep-brain stimulation (DBS), which is a procedure where electric pulses are delivered to certain brain areas, aiming to lessen the movement disorders symptoms associated with certain neurological conditions such as Parkinson's disease [41].

Commented [jo39]: melhorar esta frase

Commented [PMPTdM40R39]: Melhor assim?

2.1.3) Microfluidics design in Neurocircuitry

The architecture of the neuronal networks is fundamental to their function [19]. Nevertheless, the neuronal system is very intricate and complex to study systemically. To ensure its understanding one may, attempt a bottom-up approach and simplify the neural circuitry to a scaled-down version.

This eases the process of pinpointing signal sources and could offer a generalizable understanding of their dynamics.

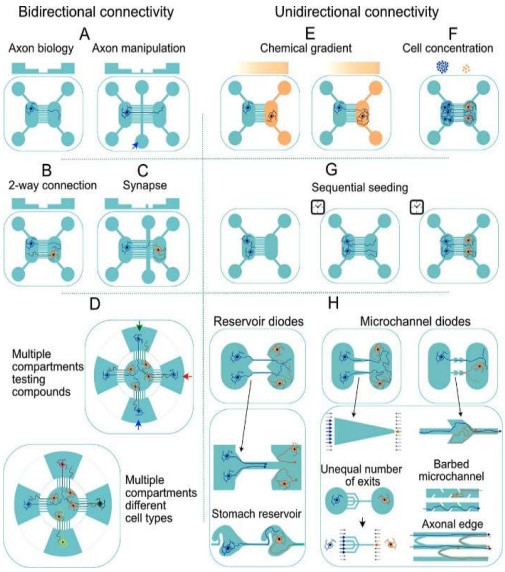

Figure II.2 - Main approaches for engineering neuronal circuits in microfluidic devices: axonal isolation (A), creation of bidirectional networks (B), synaptic isolation (C), design of multiple interconnected population neuronal circuits (D) and creation of unidirectional networks (E-H). Taken from [19]

In neuronal studies, it is not uncommon to have, thus, Microfluidic chambers be associated with MEA to maximize the control of the architecture of the network. When allied with Microfluidics, the systems are referred to as Micro-Electronic-Fluidic (μEF) devices, formulating the current state-of-the-art. These, due to the more controlled environment and the ease of building specific architectural organization, are a growing trend in neurosciences [19].

Neural-engineering 3D approaches have also been revolutionized by Microfluidics. In fact, they were decisive in creating layered neural circuits with oriented connectivity (control over the neuronal cell polarity), which allows the creation of organ/organoid-on-chip technologies for neuronal structures [19].

Lastly, another functional study that was possible through the use of Microfluidics was cell sorting/profiling. This technique can be based on genomic, transcriptomic, and/or proteomic properties of the population.

Cell sorting is interesting for the development of studies on tissue and cell characterization. For the neuronal system, this translates into the depiction of tissue-specific sensory neurons, interneurons, and cells of the neuronal system, such as the glial cells and astrocytes [19]. Microfluidics are a relevant tool for building in vitro systems to do electrophysiology studies of various kinds. Firstly, it's worth noting that their control over network architecture, which conditions not only cell separation in specific tissues but also influences cell growth and differentiation, makes them useful for between-distinct populations communication studies. In Fig. II.2 are depicted the main approaches

for engineering neuronal circuits in microfluidic devices. A crucial takeaway from it is that connectivity, synapse formation and strength are influenced by the architecture. leaving room to explore different types of microstructures in the channels that would condition this connection between architectures.

Another message to consider, also described in Fig. II.2, is the possibility of, through the definition of microchannel's dimensions, isolating axons in them, the microchannels functioning as a physical barrier to cell bodies. This condition is particularly relevant for evaluating the methods of axonal conduction of APs. This was the case in [21], the paper that motivated this project. A simple circuit design where a µEF device was built with two compartments connected via a set number of microchannels with an MEA system aligned beneath it.

In the first approach, a single neuronal cell population was cultured in one of these compartments. Conditional elongation exclusively of the axon in these channels (the channels' size are prohibitive for somatodendritic components) and the correct alignment of the MEA under it, allowed for the recollection of APs that fall only on the axonal domain. Thus, the difficulty of researching an overly complicated environment was overcome: the information processing core is in the compartment, while the electrophysiological communication tools are clearly segregated in the channel. The results of the analysis of axonal AP propagation proved interesting and will be described in the *Neuronal action potential data processing* section.

2.1.4) State-of-the-art axonal communication studies

Finally, after delving into the intricacies of how neuronal coding is decoded in electrophysiological settings, it is necessary to explore the most recent studies on cellular and, more specifically, subcellular neuronal communication.

Indeed, a pivotal discovery has emerged that challenges the traditional view of this communication. Recent research has unveiled unequivocal evidence of bidirectional communication among neurons, extending beyond the conventional orthodromic propagation, which follows the cell body-soma-axon direction. This phenomenon includes the intriguing concept of antidromic conduction [21], where the APs are initiated in the distal part of the axon, leading to a fundamental question: What mechanisms underlie and execute antidromic propagation?

Further exploration highlights the intriguing role of ectopic action potentials (EAPs), which occur in reverse of the typical soma-axon pathway. Recent studies suggest EAPs are significant in processes such as acetylcholine-induced dopamine release, linked to motor control [42], and in conditions of hyperexcitability associated with neurological disorders like epilepsy [43].

Acknowledging the existence of EAPs challenges the traditional view of the axon solely as a transmission cable, suggesting it also plays a role in processing and signal initiation. Understanding EAPs in both physiological and pathological contexts could offer new insights into bidirectional neuronal communication and its implications for neural information processing in health and disease.

The importance of axon communication profiling is even further increased as a result of the findings in recent studies: axonal computations go far beyond the propagation and/or replication of somatodendritic electrical signaling. In other words, axons can modulate their own activity through the regulation of ion channels, myelination, direct and indirect coupling with other axons and signaling with glial cells, in mechanisms that are yet to be completely unveiled [14].

Another key factor that should be considered as a functionality of the software is the online spike sorting. This corresponds to the sorting process of spikes in an extracellular recording based on their neuronal sources simultaneous to the acquisition, being relevant since spikes in the voltage trace

might appear overlapping and erroneously be pinpointed to the same source. But currently, there is a lack of tools to perform it while data is being acquired, hindering the development of closed-loop systems such as BCIs where patients' neuronal network activity is monitored and there could be precise stimulation of specific brain regions [44].

Lastly, there is also the point of having the analysis perform connectivity inference, which is the comprehension of the mechanisms of the neuronal circuitry and how information is encoded in this system. Data regarding these topics allow clinicians to predict how their patients' neuronal network behaves and, therefore, can modulate activity, based on previously processed neuronal network activity [45].

2.2 - Neuronal action potential data processing

After reviewing the means to do the recollection of neuronal signal in both *in vivo* and *in vitro* context, it matters to understand what the current state-of-the-art algorithms and methodologies are in what regards to their processing. Over the years, the techniques and methodologies to obtain the spatiotemporal motifs hidden in the neuronal data have been evolving: the evolution of the MEAs has brought along increasingly more complex and larger datasets meaning the analysis of said data can be performed more in-depth and it's more insightful.

The aforementioned methodologies, often, include core elements, namely, spike sorting, feature extraction, network connectivity analysis, spatiotemporal mapping, information theory, and other metrics.

Spike sorting refers to the grouping of neuronal spikes according to their source [44]. It is commonly a neglected aspect of MEA analysis commercial software, being often their downfall when used on more intricate architectures [46]. The first step is, in general, a threshold-based method to identify spiking activity in an electrode. In conventional methods, threshold selection is based on multiples of standard deviation values for noise/baseline level of activity [47].

Secondly, after initial detection, to ensure a palpable distinction between spikes' sources, features of the waveforms, like spike amplitude and duration, and more complex ones associated with time-frequency analysis are extracted. An alternative is to perform wavelet-template matching [48]. The result is later clustered to distinguish different profiles that can be associated with their respective source. Afterward, an analysis of the temporal and spatial characteristics of the network can be performed on the post-sorted data.

Multiple articles were written on the analysis of electrophysiological recordings. On them, investigators attempted to establish profiles of network activity, looking for spatial and temporal motifs. Profiling neuronal activity is crucial to the understanding of how distinct neuronal populations communicate with one another.

Thus, in this section, the implemented algorithms to establish parameters describing the neuronal communication are explained further, with an emphasis on the methods for NB detection, but also including the most recent breakthroughs in how this communication is evaluated, in terms of both spatial and temporal features, expressed through metrics specifically used in this type of studies.

2.2.1) Network Burst Detection algorithms

In vitro neuronal networks present a coordinated spontaneous spiking activity that propagates spatiotemporally – whenever this activity generates a "wave" where most of the neurons fire

simultaneously or in close succession, the event is called a network burst [2]. *In vitro* systems have the plasticity of rearranging themselves to maintain NB activity towards months of development, making them ideal to study these and, in particular, their role on population-to-population communication.

However, *in vivo* systems, after early development stages, change their regime to asynchronous spiking [2], only maintaining this large-scale neuronal co-activation in many neurological and mental illnesses states, including epilepsy, depression, and anxiety [11]. For this reason, it is important to comprehend this synchronous firing regime and identify, even anticipate, the source of NBs in order to treat these pathologies more effectively, particularly when employing therapies based on neuromodulation, such as the case with brain-computer interfaces (BCIs) or when deep brain stimulation is known to be effective.

When considering NB detection, one should be remembered that the vagueness of the definition of firing *in close succession*, without a set time interval, or a specific threshold of units of activity whether it be neurons or electrodes, makes it hard to find consensus even if it were to be done by visual analysis of each event. Nonetheless, a myriad of methods has already been implemented for this detection with varying degrees of adaptability to different networks. There are essentially 5 types of NB detection algorithms:

- **Threshold-based methods -** Network bursts are identified every time the activity surpasses a preset amplitude or frequency threshold. Its simplicity and is easy to compute, however, may miss bursts with variable amplitudes. While the majority of these algorithms make decisions based of hard thresholds, some set it as a result of the networks firing pattern statistics, increasing its self-adaptiveness in comparison with the previous [49].
- **Principal Component Analysis (PCA) methods -** Assuming linear relationships between the dimensions of the neuronal data, applies dimensionality reduction, identifying bursts through variations of the principal components [8] .
- **Wavelet-based methods -** Frequency analysis of the wavelet transformed signal, with bursts corresponding to the presence of certain frequency components [50].
- **Machine/Deep Learning methods -** Although it requires labeled/annotated data and a good performance is only achievable with good training set, it may be the best alternative to deal with complex non-linear burst dynamics [8].
- **Hidden Markov Models -** Neural activity is modeled as sequence of states, each with a certain probability to move to one of the others. Some specific states are network bursts. In the one hand, it is also good to capture complex burst patterns but is very demanding computation-wise. Besides that, its performance is conditioned to parameter fine-tuning [51].

Among all the available options, the most frequently used are probably adaptive threshold-based approaches, where it is defined through calculated properties of the networks. One subset of these types of algorithms resort to inter-spike intervals (ISI) statistics to define the adaptive threshold. In this study, one of such kind – the Pasquale's method [49] - was used as a reference to create a custom version.

Two main motivations are considered to base an algorithm on the Pasquale's method: first, it is rather simple to compute, which is interesting on the implementation part but also eases its usage by researchers with little to no coding expertise. Secondly, the self-adaptive claims of the algorithm are sustainable, as primary analysis with some of the recordings, output good results for textbook examples.

Commented [jo41]: muito bem!

Commented [PMPTdM42R41]: Obrigado!

Commented [jo43]: and lacks self-adaptation

Commented [PMPTdM44R43]: Expliquei melhor para acomodar essa ideia

Commented [jo45]: may be?

Commented [PMPTdM46R45]: Yup!

Unfortunately, for more complex dynamics of neural activity, Pasquale's method underperforms, either grouping a set of small bursts or missing them all together. Hence, some improvements were needed to get a methodology which would perform well on all scenarios – explained further on the respective section.

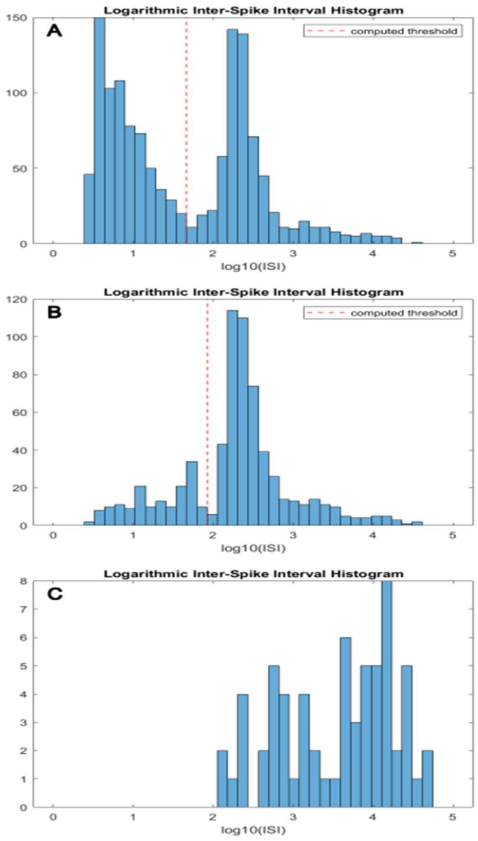

Figure II.3 - Distribution of the Log-Inter-Spike Interval in 3 different scenarios. A - Standard Bimodal distribution histogram; B - Pseudo-bimodal distribution histogram ; C - Non-Bimodal distribution histogram. The red line indicates the calculated *ISITh*.

As for Pasquale's, the first step is the definition of a threshold – *ISITh* – which is selected from the logISI histogram, calculated from the spike train of each electrode. In general, this plot should follow a bimodal distribution, with a primary peak pertaining to the intra-burst spikes and another, to the inter burst ones. Even if there are no guarantees, a semi-log approach is considered to get a clearer distinction between the peaks, as observed in Fig II.3-A.

Nevertheless, the method has a fail-safe for cases where the distribution is not so clearly separated, like the one on Fig. II.3-B , which is the *voidParameter*. This value can be interpreted as percentage of how well separated should the peaks be, to consider a good value of *ISITh* and are calculated according to Eq. 1 [49] for all the candidate minima.

$$void = 1 - \frac{g(minimum)}{\sqrt{g(peaks_1)g(peaks_2)}} \quad (1)$$

where $g(x)$ is the distribution of x = log(ISI).

Please note that *ISITh* corresponds to the first peak corresponding to a validation of sufficiently separated peaks, if at least one minimum has a void parameter that is greater than the predetermined threshold. Usually, the void parameter threshold is set at 0.7, however, it is adjustable by the investigator depending on the activity of its neuronal cultures [49].

If everything else fails, the electrode is not taken into account for the following steps. Besides, after thorough inspection of recordings, "lost" electrodes generally represent electrodes with so little activity that their loss is neglectable, much like in Fig. II.3-C.

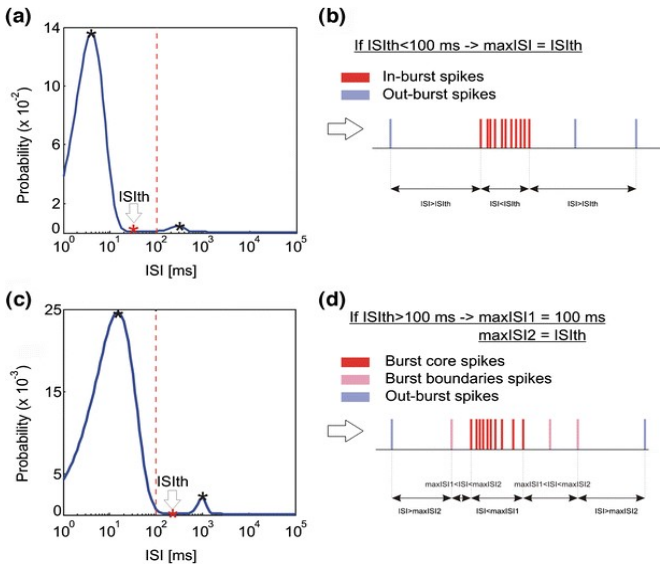

Figure II.4 - Illustration of the Pasquale's Burst Detection algorithm, taken from [49]. (A,B) if *ISITh* is lower than 100ms, it is used to determine the maximum ISI threshold within a burst. (C,D) if *ISITh* is higher than 100ms, two thresholds are used – the first for detection of burst cores and the second for extending them at the boundaries. The red line marks the 100ms and the red asterisk the calculated value of the *ISITh* which separates the peaks marked with the black asterisks.

The next step is the burst detection in each electrode. For each pair of spikes in an electrode, their time distance is calculated. A spike is considered as part of a burst if following spikes occur at ISI lower than the *ISITh*.

Moreover, the latest standard defined in the literature [3], [49] for electrode burst detection is the definition of second threshold: the first one referring to spiking activity in the burst core which corresponds to the previously calculated *ISITh*, and the second, to the spiking activity on the boundaries, *maxISI*.

Hence, in essence, the latter serves the purpose of extending the boundaries of the burst core to include spikes which otherwise be considered of out of burst, whenever the *ISITh* is in the [100, 450] ms window. This is particularly relevant considering that the setup used in this work has nearly 4 times more electrodes than the ones used in Pasquale's original manuscript, so is more likely that nearby electrodes catch residual activity of neighboring neurons. Additionally, one needs to assert the *minSpikes* which is the minimum number of consecutive spikes in a channel to consider it a channel burst.

Thus, in terms of parameters of the algorithm for this step, Pasquale defined *maxISITh* = 100 ms, *maxISImax* = 450 ms and *minSpikes* = 5. If *ISITh* is less than *maxISITh*, then sets of at least 5 consecutive spikes within a time interval smaller than *ISITh* are defined as electrode bursts. On the other hand, if it is higher than that, the difference is that burst cores have a maximum distance between their spikes of *maxISITh* and they are later on extended at their boundaries until the calculated *ISITh* (or in limit cases until *maxISImax*). For visual reference, see Fig II.4.

Following detection of burst activity in the electrodes, the algorithm steps to a network level of analysis: if one considers the sum of all the electrode burst event trains recorded condensed in a cumulative burst event train, NBs appear as clusters of tightly packed channel burst events separated by relatively long periods. Hence, applying the same semi-log histogram approach to the said cumulative burst event train to evaluate the distribution of the Inter-Burst event Interval (IBeI), it is possible to obtain a *IBeITh*, a threshold to distinguish between peaks corresponding to intra-NB and inter-NB intervals, as observed Fig II.5.

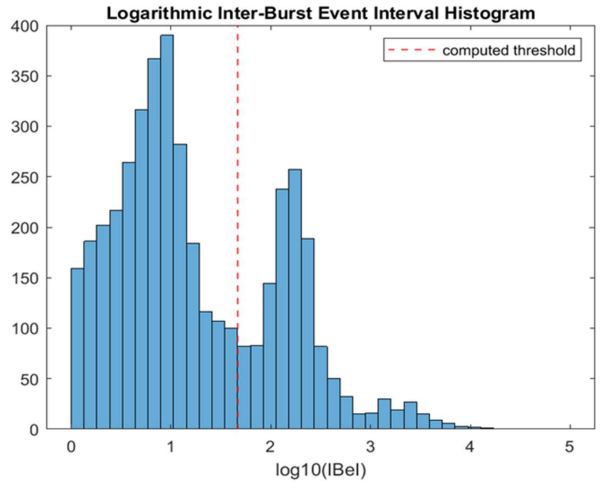

Figure II.5 - Distribution of the logarithmic Inter-Burst Event Interval in the form of a histogram. The red line is indicative of the threshold *IBeITh*.

Eventually, the NB detection algorithm consists in scanning the cumulative burst event train looking for sequences of at least *minPercElec* consecutive electrode burst events spaced less than *IBeIth*. The preset value for *minPercElec* = 10%. This percentage takes in consideration only active electrodes on each population, to ensure that the algorithm is self-adaptive for cultures with different levels of activity.

These algorithms are, in these scenarios, important (as it is their accuracy) due to the fact that NBs have shown clear signs of being a hallmark of activity on *in vitro* networks and, therefore, short delays between these events in connected cultures might be used as a proxy of communication.

Commented [PMPTdM47]: I feel like at this point this idea came out of mind only

Commented [jo48R47]: penso que podes dizer que são um hallmark da atividade das networks in vitro e a sua propagação numa janela temporal curta é um proxy para conetividade

2.2.2) Metrics for Neuro-Electrophysiology

As mentioned, there's a multitude of different analysis that can be done on electrophysiological recordings, in an attempt to discover temporal and spatial patterns in the neuronal activity. In the scope of the work documented on this thesis, it has an added interest as these profiles might be related to how the neuronal populations in this study communicate.

Starting with temporal profiling, techniques like cross-correlation are the most relevant and common. Cross-correlation is a convolution operation between two signals, where one is timed-shifted, that is calculated as per Eq. 2.

$$C(f,g)(\tau) = \int [f(t) * g(t-\tau)]dt \qquad (2)$$

Here, τ represents the time lag or delay applied to one of the signals (g(t)). The result, C(f, g)(τ), is a function that provides a measure of similarity between the two signals as a function of the time lag τ. It is commonly used to assert similarity between electrode activity or between an electrode and a certain event or even between events [2], [52], [53]. In fact, studies of electrophysiology data analysis often resort to this to relate activity between neurons and, in particular, on *in vivo* studies, this metric is used to assert how neurons activation are related to certain events or functions [54].

Commented [jo49]: between neurons?

Commented [PM50R49]: Já referenciei e expliquei de modo mais claro

Furthermore, temporal motifs can also be looked for in terms of the activity preceding a NB event. Recent studies have identified that these events are linked to the activation of certain electrodes which remain consistent in the majority of the spiking activity across time. As such, these electrodes are called Major Burst Leaders (MBLs) and have enough statistical relevance to be considered in NB prediction algorithms [9], [55].

Spatial profiling is achieved by resorting to network analysis algorithms that explore connectivity strengths in the network. Likewise, graph theory intends to describe functional connectivity in neuronal networks: the basic principle is to define neurons as nodes and their connections as edges, which are directed or not, according to the type of directionality, they establish between themselves [56].

Frequently, neurons are not by themselves capable of driving events and, as such, is important to consider as a functional unit of the networks what are called ensembles. Ensembles are, as per [57], regardless of their level of anatomical connectivity, groups of neurons which express above average levels of synchronous activity, so, in other words, functional clusters of the neuronal networks. Indeed, in studies like the one documented on this paper, it is not uncommon to look for these clusters [58].

Bringing together both temporal and spatial information is also important, considering the time dependency of functional connectivity – varies continuously due not only to the changes in sensory inputs both in internal and external environments [56], [57] but also because of the changes in neuronal and synaptic plasticity. Evidence has shown that neuronal system information flows are about the right neurons firing at the right time [59], [60].

An easy-to-implement, intuitive descriptor of the dynamic activity of neuronal networks is the Center of Activity Trajectory (CAT) analysis. It is a representation over time of the Center of Activity,

as can be seen in Eq. 3, analogous to the center of mass but takes into consideration the weighted activity of the electrodes in the event [61].

$$CAT = CA(t) \tag{3}$$

For 2D MEA, the equation can be simplified for a given t to the result in Eq. 4.

$$CA = \begin{bmatrix} CA_x \\ CA_y \end{bmatrix} = \begin{bmatrix} \frac{\sum_i (Act_i \times row_i)}{\sum_i Act_i} \\ \frac{\sum_i (Act_i \times col_i)}{\sum_i Act_i} \end{bmatrix} \tag{4}$$

where Act_i is a measurement of activity of the electrode *i* and row_i and col_i are the row and column, respectively, of the electrode *i* in the electrode grid, for example, assuming conventional grids, B1 corresponds to row 2 and column 1. The summation operator runs across all the electrodes *i* that are active in the considered interval.

A drawback of this approach is that the averaging of the center of activity measurement might be noxious when the activity is generated through multiple ignition sites – the spatial location where the spiking activity of an NB starts – is sparsely located [61].

Likewise, there's also the possibility of pinpointing certain regions of the MEA, for instance the previously mentioned functional clusters, and check whether their activity inside an interval event can be cross-correlated within themselves.

Other metrics about the activity should be collected, which are the standard activity parameters and results regarding information theory. The first ones, such as the *mean firing rate* (MFR), *inter-spike interval* (ISI), *coefficient of variation* (CV) and *inter-burst interval* (IBI) are essential for characterizing the baseline firing properties of individual neurons. In fact, they support conclusions on the neuronal health of the network, as abnormal firing regimes can be indicative of neuronal dysfunction [11].

The latter include measurements which, for instance, describe how much information is encoded in a spike train and they reveal further details on temporal and spatial patterns of activity. Three reasons can be named to include this type of analysis [62]:

1) in neuroscience, experiments include analysis of multidimensional data, which is commonly also multivariate;

2) the nonlinear relationships variables can establish between themselves might be otherwise difficult to define;

3) lastly, the possibility of variables that might seem unrelated but, in fact, are not, is avoided.

Once more, the relevance of studies with Microfluidics is emphasized, because of the work still to be done on characterizing neuronal communication on different oriented structures. Additionally, metrics like Granger causality and transfer entropy are applied to explore the direction of information flow and causal relationships between neurons [63].

Granger causality refers to a statistical analysis of how much predictive power there is in the past values of a time series in what concerns to another, considering a linear relationship between them. This causality is not expressed, however, in a physical way, such as events in X causing events in Y, but rather changes in previous values of X equating to high chances of seeing responses in future values of Y. For neuro-electrophysiology, this is, therefore, a tool to better define the influence, both in terms of temporal relationships and directionality, between different sections of the object of study.

Likewise, transfer entropy is a similar type of analysis but extends the search to more complex, non-linear relationships, meaning that it is necessarily more computationally demanding. As such, it is a measurement of the amount of uncertainty reduction about future states of Y given the previous states of X. High values of this variable indicate that there are effective connections between the different regions in analysis.

In summary, the decoding of neuronal activity and if the goal is to effectively get to a point where the behaviours of a studied neuronal network become predictable, metrics need to be calculated which translated its activity in ways that are (more easily) understandable.

2.3 - Summary

Despite the numerous advances in the studies related to neuronal communication, the mechanics underpinning the propagation of information in neurons still hold many mysteries. A key challenge is, firstly, the incomplete understanding of neuronal network dynamics. Even if the static connections between neurons, namely, structural and anatomical ones already have been extensively mapped, their ability to dynamically change and present different profiles under changes of the physiological and pathological conditions is still something very undocumented.

Furthermore, issues pertaining to the capacity to monitor neuronal activity with the temporal and spatial resolution needed for the comprehension of the mechanisms of neuro-electrophysiology persist, even when using state-of-the-art technology. Additionally, the inaccessibility associated with *in vivo* recordings is still a hurdle to surpass as it hinders the ability of recording extensive neuronal populations on these settings.

The conjugation of both factors does not allow for researchers to effectively capture the intricate, transient nature of the neuron-to-neuron interactions in real-time, limiting therefore the depth of insights one can obtain pertaining to neuronal communication processes.

Alongside the already mentioned problematics, the development of the already existing technology has led to the recollection of larger and more complex volumes of data, which in turn raised substantial difficulties in the processing as this progress as not being accompanied by advancements in algorithms for the data analysis. In fact, the shortage of algorithms makes it hard for achieving accurate detection of temporal and spatial patterns inherent in neuronal data.

It is fulcral to create novel and improved computational algorithms that not only manage these datasets efficiently but also streamline the integration of data across different scales. Indeed, there's a lack of studies which correlate activity on the molecular and cellular levels to network and population levels.

An important idea defended in this thesis is that a comprehensive understanding of neuronal activity requires a holistic approach, integrating data from various levels of analysis. Specifically, by combining information from the activity within microchannels with the activity of the broader neuronal populations, insights into how *in vitro* neuronal cultures communicate ought to be revealed.

Indeed, microchannels provide a controlled environment to study axonal activity and signal propagation between modules, while recordings from neuronal populations reveal the network dynamics and functional connectivity. Their integration is, hence, essential for understanding how structural motifs influence functional outcomes and for learning about the mechanisms underlying neural transmission.

This kind of multi-scale integration, in spite of its importance, is seldom employed in functional data analysis, highlighting the need for novel computational tools and methodologies to facilitate such comprehensive studies and to allow for a more complete picture of *in vitro* neuronal interactions.

Closing this gap will deepen our understanding of neural networks and how they dynamically respond to various environments, ultimately contributing to both basic neuroscience and the development of cutting-edge neurotechnological applications.

Commented [jo51]: Não percebi

Commented [PM52R51]: A ideia aqui era dizer que para de facto perceberemos a comunicação entre as populações de neurónios temos de tentar relacionar informação que tirarmos da análise dos canais com o que tivermos da análise das populações para, de facto compreendermos… v-e pf se fica mais claro assim

Chapter III

Materials and Methods

To comprehend in all its essence the work output as a result of this thesis, it's fundamental to review the different methods used in all aspects of the electrophysiological experiments, ranging from acquisition to data processing and analysis. Hence, this chapter gathers details on both the experimental setup and the computational strategies implemented, showcasing the reader the means to eventually reproduce the described results.

3.1 - Neuronal action potential data processing

Initially, it matters to describe the experimental setup for the acquisition - the recordings were done using µEFs, which are devices composed by the integration of MEAs with Microfluidics, as previously mentioned – and, consequently, the means to prepare them.

Firstly, the MEAs used (Multi Channel Systems (MCS), Germany) were of 16x16 planar grid with 4 internal reference and 252 titanium nitride recording microelectrodes. Their electrode diameter is of 30 µm. As for the Microfluidics, they were PDMS chambers with 2 separate compartments, where later the neuronal populations were cultured on, connected with each other through 16 microchannels. These microchannels had a 10x1000x3 µm (width-length-height), to maintain the microchannels' property of being axon-exclusive and to ensure long-term axon viability [21]. Additionally, they were also interspaced 200 µm of each other and each encompassed 5 electrodes.

PDMS chambers production was based on replica molding and the substrate was prepared of a mixture of silicone elastomer and its curing agent (Sylgard 184, Dow Corning). The degassing process was achieved through vacuum desiccation and polymerization was done for 3h at 70 ◦C. Finally, the PDMS molds were cut and had their medium reservoirs manually punched with a steel biopsy punch (Ø 6 mm) [21].

The preparation of the µEFs followed protocols already established in previous work done within the group [21], [64], meaning the components were bound in a reversable manner, to preserve the use of the MEAs for further experiments. However, there was also the need to confirm the tight coupling, by checking lack of medium leakage or axonal outgrowth under the PDMS.

A bath of 70% ethanol had to be prepared to submerge both elements for a small interval of time. Then, they were put in a laminar flow hood to air dry and were sterilized by UV. To ensure precise alignment of the columns of electrodes and their respective microchannel, it was necessary to use a

stereomicroscope. Following this step, the newly formed µEFs were, once more, air dried and air plasma-cleaned for 1 min at 15 W to allow for surface hydrophilization. In order to promote cell adhesion, a coating of poly-D-lysine (20 µg/ml) was applied to the µEFs [21].

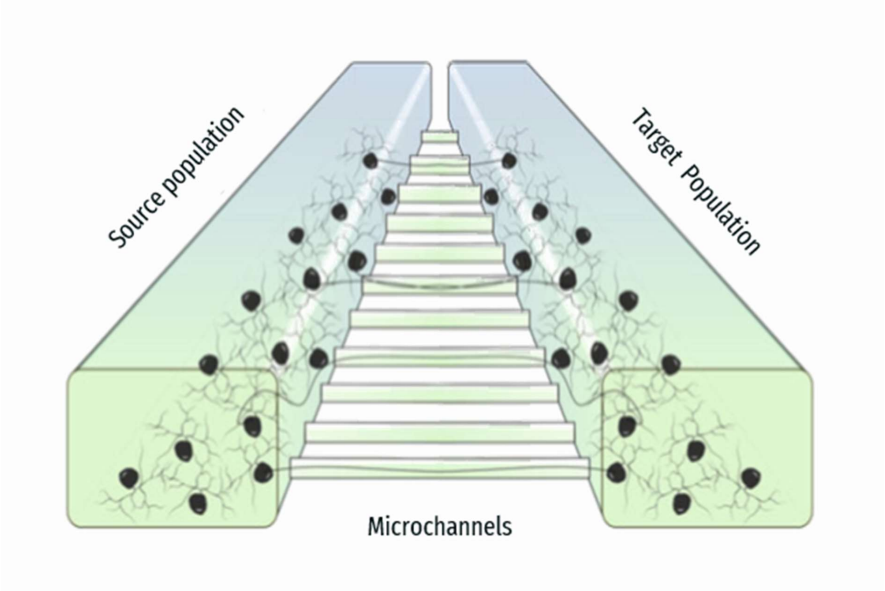

Figure III.1 - Depiction of the microfluidics setup used for the experiments, with two PDMS chambers for the neuronal populations to be cultured on. Those are interconnected with very thin microchannels, whose dimensions are prohibitive for sommatodendritic processes, making them axon-exclusive. Adapted from [64].

3.2 - Structural designs on the microchannels

Structure-oriented microchannels were designed with the goal of exploring the effects of the structural constraints on the network communication. In the end, the aim is to reproduce simplified models for neuronal network with preferred signal propagation directionality, which are known to occur *in vivo* in specific pathways such as the projections of the EC to the DG, as seen in Fig I.1.

To this extent, the microchannels had, considering their length, in the 600 µm closest to the top chamber a linear profile and in the remaining 400 µm asymmetric designs which were expected to condition signal propagation in the back-to-top-chamber directionality. For that reason, the neuronal population on the top chamber is also identified as “Source” population, while the bottom one, as “Target” population.

As for the structural motifs, three designs were tested: tesla valves and arrowheads (Fig III.2 C, D) which were already suggested in the literature, but also a custom variation of the arrowheads - named rams (Fig III.2 E) due to its resemblance with the animal.

The first one was an invention of Nikola Tesla, known for his works on electrophysics, in an attempt to create in his circuits a valvular component, which would condition the flow of a fluid to be unidirectional. Thus, this design is now in vogue, specially in micro and nanofluidics’ studies where

Commented [PMPTdM53]: Revisiting this section, I think I'm lacking here an explanation on how the microfluifics setup looks like in general. I think I should get back that picture presented on IJUP (the one adapted from the paper from Estrela Neto)

Commented [PMPTdM54R53]: Maybe it should be on the electrophisiology recordings?

Commented [jo55R53]: Não percebi a pergunta

Commented [PMPTdM56R53]: Pus na parte de cima ! Vê se faz sentido pf

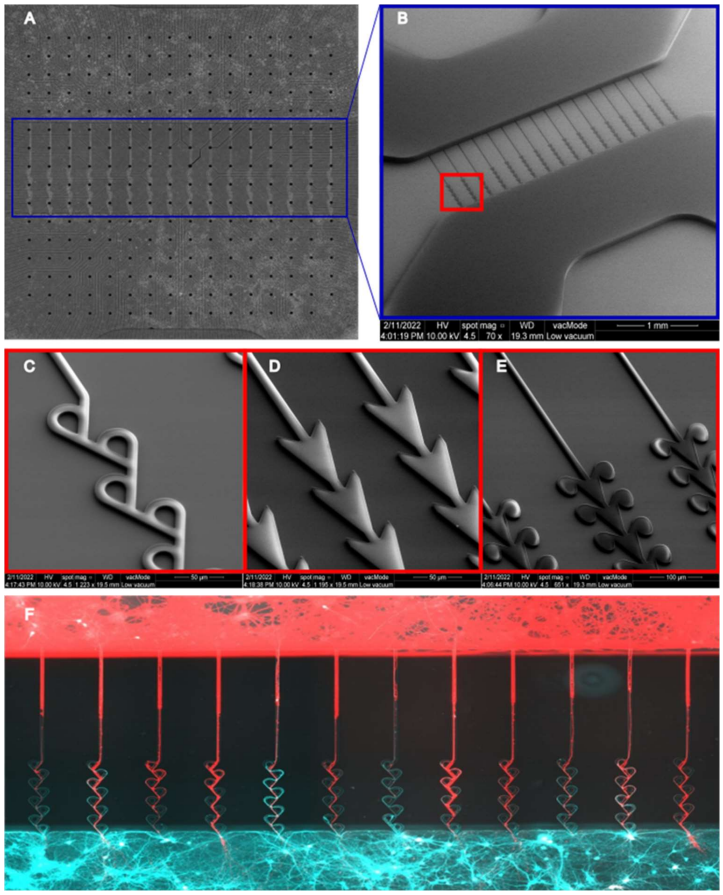

Figure III.2 - Representation of the structure and design of microchannels. (A) Whole Micro-Electrode Array (MEA) grid area shown in phase-contrast microscopy image. Electrodes pertaining to the microchannels highlighted in the blue rectangle; (B) Zoom-in microscopy image of the microchannels. It is observable that they are composed by a linear and an asymmetric part (highlighted in the red square). The three designs tested designs are presented in (C) tesla valves, (D) arrowheads and (E) rams. (F) Fluorescence image with different dyes for each population – "Source" is marked in red fluorescence while "Target" population is marked in blue fluorescence. Here, the tested design is a tesla valve and microchannels are dominated by red colored axons, which indicates a structural bias enforced by the design.

having moving components adjusting the flow rate it's not an alternative, much like the case on this study [65]. The principle through which these valves work it's purely structural - it's a sequence of twists and turns in interconnected channels that allow natural flow in one way while limiting the other (Fig III.3)

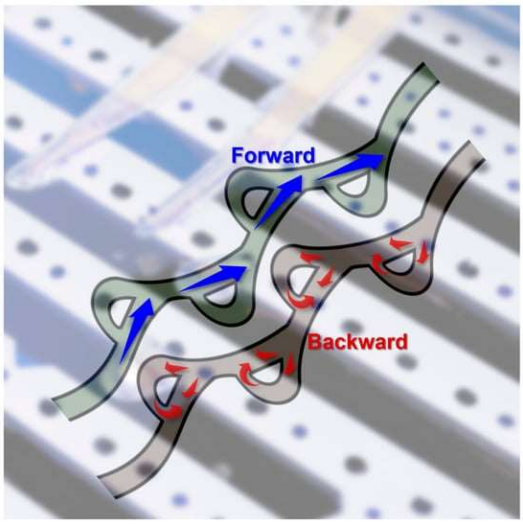

Figure III.3 -Depiction of the functioning principle of the Tesla valves, showing unidirectional bias in the flow of fluids, similar to the way they're expected to behave on the flow of information when used as asymmetrical structures of the channel. Taken from [65].

Arrowheads have been an alternative for signal propagation conditioning after the studies of *Peyrin et al*. In here, structural properties of the channels connecting two microfluidic channels were studied and evidence was found that axons follow along walls that are tangent to their path, whereas when they come in contact with something perpendicular, they pivot. This effect, combined with axonal stiffness, makes designs which have clear asymmetric structural ratios between their sides, effective in conditioning signal propagation directionality [23].

These results have been reproduced by other researchers that tested both of these – tesla valves [24] and arrowheads [25], [66] – in mainly structural studies, with results indicating that these designs do effectively hinder axonal growth in the undesired direction. From this point onwards, they will be designated as "Tesla" and "Arrows", respectively. Likewise, other architectures were implemented, however, they turned out to be less effective.

Hence, the creation of the rams was an alternative as to explore designs more effective in their blockage. Their difference in comparison with the arrowheads is that the first have their top extremities curled in on themselves. Then, they should work maintaining both principles in mind: while the arrow-like main component should direct growth of axons in the right direction, the twists in the extremities should lead the incorrect ones to a compartment where it is hard to escape from, much like Tesla's design.

Finally, there were also some microfluidics in which the linear design is maintain throughout the channels to work as controls. These straight channels should not present any type of bias in terms of events propagating on them as there is nothing conditioning the axonal growth, functioning as controls and, thus, validating the hypothesis that the conditioning was effectively a result of the structural blockage.

3.3 - Cell culture and preparation

Initially, it is important to acknowledge that all procedures which involved animal handling followed up-to-date Portuguese regulation on Animal Care (DL 113/2013) and EU Directive (2010/63/EU) on the safeguard of animals' protection for scientific research projects. DGAV's (Direção Geral de Alimentação e Veterinária) Ethics Committee, the Portuguese official authority on animal welfare and experimentation, approved the experimental protocol (reference 0421/000/000/2017) followed. It is also important to emphasize that all kinds of considerations were taken when considering the animal suffering and efforts were done to minimize the number of animals and animal harm.

The primary embryonic cells on this study were harvested from Wistar rat embryos (E18) as in [67] and tissues' dissection was done in a 15min bath of 0.6% (w/v) trypsin (1:250) in Hank's Balanced Salt Solution (HBSS) at 37 ◦C. After those had passed, a wash-out with culture medium and 10% fetal bovine serum was used to inhibit digestive properties of trypsin [21].

Mechanical dissociation of tissue fragments was done using a plastic pipette. Cells were suspended, filtered with a 40 µm strainer (Falcon) to exclude remaining tissue clumps, and counted. A following suspension of 100k viable cells in 4 µl was seeded on each of the somal compartments of the µEF. On the cell culture, a mixture of Neurobasal Plus medium with 0.5 mM glutamine, 2% (v/v) B27 Plus, and 1% (v/v) penicillin/streptomycin (P/S) was used [20]. A total of 11 independent experiments were conducted.

In between recordings, cultures were kept in a humidified incubator at 37 ◦C supplied with 5% CO_2.

3.4 - Electrophysiology recordings

In the electrophysiology experiments, recordings of the hippocampal neurons were performed at 11-21 DIV. Inspection for visual cues of contamination, cell death or axonal degeneration was done to discard µEFs whenever they failed this examination. 10 minutes of adjustment to recording conditions preceded every recording session [21].

The electrical equipment used for recordings was the commercial MEA2100-256 system (Multichannel Systems MCS, Germany). Temperature was maintained at 37 ◦C by an external temperature controller [21]. Two types of recordings were made, considering the level of experimenters' interaction with the system. Stimulation recordings were associated with a population-level stimulation, making use of the MEA2100-256's (Multichannel Systems MCS, Germany) internal stimulator to deliver, per trial, a single monophasic voltage pulse -600mV with a duration of 200 µs at 0.2Hz. These pulses were either applied to the 5 top or the 5 bottom electrode rows of the MEA's grid, meaning each experiment number-DIV-design triplet has two recordings associated with it, one for stimulation of the "Source" and the other for the "Target".

The sampling frequency used in the recordings was of 20 kHz and they lasted for 10min, for recordings of spontaneous activity, and 5 min, for recordings with electrical stimulation, unless stated otherwise. In terms of the timeline, stimulation recordings, whenever present, were done immediately after the end of spontaneous activity one.

It's important to understand that the purpose of using stimulation was to establish an initial proof of concept of structure-conditioned functional bias. Therefore, the focus was on the analysis of

Commented [PM57]: REALLY NEED YOUR ATTENTION TO CHECK THIS INFORMATION! I've based this chapter of "Bidirectional flow (…)" and my notes of the experiments as per your description @Ze

Commented [PMPTdM58R57]: Ok some information needs to be updated, following what is written in the section Materials and Methods of the "unidirectional" paper

Commented [jo59R57]: Agora está ok

Commented [jo60]: confirmar

Commented [PMPTdM61]: Still lacking a thing on the time line of experiments, explaining that after doing na experiment recording spontaneous activity, there are two other recordings of stimulation (whenever there's a corresponding stimulation recording), no?

Commented [jo62R61]: Penso que é suficientemente simples que uma frase chega

Commented [PM63R61]: Preciso de adicionar a ordem porque foram feitos?

Commented [jo64]: se só usares dados até DIV21 corrige isto

Commented [PM65R64]: Só vou usar isso!

different types of response on the unconditioned population to the outputs of the stimulated population, so only the timestamps of the first were taken into account.

On the other hand, spontaneous activity corresponds to the recording of neuronal populations' activity unperturbed by electrical stimulation. Here, it was relevant to comprehend how both interact with one another, meaning the data of the three sections of the MEA needed to be evaluated.

Finally, before discarding some of the cultures, tetrodotoxin (TTX) was applied in the top chamber, aiming to hinder the activity of the source population. TTX selectively binds to sodium channel pumps in the neuronal cellular membrane, inhibiting the rising of the cellular potential which is responsible for triggering neuronal AP propagation. Thus, it is expected that the presence of TTX at the emitter population diminishes the activity of the target population whose activity is now only self-motivated (in comparison to previous states when responses could be elicited through source population NB activity).

Commented [jo66]: Se não incluires resultados disto, apaga

Commented [PM67R66]: Devo incluir na forma que acabei por te falar na sexta. Mas se assim for tenho de reescrever

Commented [PMPTdM68R66]: Acabei por ainda não a ter feito pq ainda não tenho os esses dados analisados… o mais certo será talvez tirar a menos que, de facto encontre aqui alguma coisa …

3.5 - Software Analysis framework

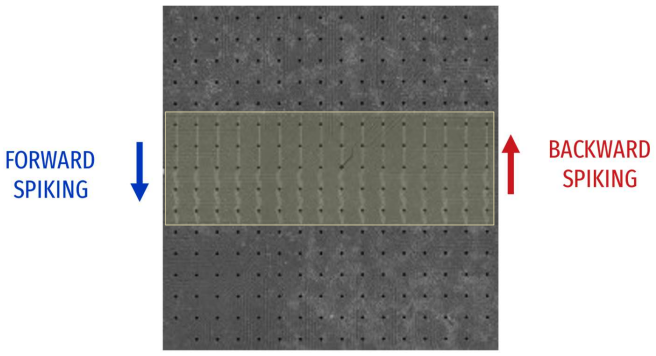

Figure III.4 - Illustration over the MEA-grid of the types of events looked for in microchannels (highlighted in the yellow box). These events take in consideration all electrodes in the channels.

The pipeline of analysis of each of these recordings began with the upload of the data to MATLAB from a HDF5 file. This is output by the Multichannel Systems Data Manager, after translation of the data from Multichannel Systems Experimenter software. Here, there was a second step of segmentation of the data in "Source" and "Target" populations and Microchannels, through a GUI where an activity heatmap is overlaid to ease the selection of the electrodes designated to each section.

Commented [jo69]: Na realidade a conversão para HDF5 é feita via outro software (Multichannel Systems Data Manager)

Commented [PM70R69]: Certo, corrigido já!

It's important to guarantee in this step that the same number of electrodes are considered for both populations to eliminate putative bias associated with uneven amount of activity in one vs the other.

Secondly, it matters to characterize spike propagation on the microchannels. For this section, two types of events are considered, forward and backward spiking according to their propagation direction [21].

In parallel, for the populations' analysis, the custom NB detection algorithm is run. Once more, these bursting events are considered to be hallmarks of population activity and the units of communication between the populations.

It, then, follows the calculation of the summed firing rate (SFR) vectors, crucial to the visual outputs, namely, the raster plot with microchannels directionality of events and NB information, the NB-trigger-averaging plot. There's also the plot of the information regarding the population-to-population communication. The final step is to calculate the histogram of the delays of forward and backward Population Driving Events (PDEs), to have a visual assessment of how biased the communication between the populations is in the recording.

In the following subsections, a detailed description of how each of these aforementioned steps were done is presented.

3.5.1) Action Potential detection and propagation

The initial steps for the analysis include the high pass filtering of the raw voltage with a 200 Hz cut off and the implementation of a spike detection algorithm within *Multi Channel Experimenter Software*. The hardware of Multi Channels Systems also does a low pass filtering of 3500 Hz, as per description of their user manual.

This software presents a myriad of up-to-date alternatives for the spike detection, namely, hard and adaptive thresholding or wavelet template matching. In fact, in NCN's spike times recordings is common practice to define as the spike detection algorithm the adaptive threshold alternative - 500ms of the pre-recording time are used to calculate the standard deviation of the noise in each channel. In the recording, a spike is detected whenever the voltage surpasses a user defined factor of this defined standard deviation (STD), usually 5 times the STD above the baseline level of activity.

While overall the method's adaptability to different firing regimes makes it the preferred alternative, for it to function properly there's a need to beware of the period to estimate the standard deviation, as it needs to be one when the network is "totally quiet".

Afterward, the spike trains were used to run the data analysis on *Matlab R2023b* with custom-made scripts and in-house functions. Data analysis starts by segmenting activity in the MEA in the sections of interest, as information from the chambers and the microchannels should be fundamentally different both in terms of activity and its processing. For the microchannels' analysis, the main reference followed was [21] and for the population's will follow analysis similar to what is done in [24].

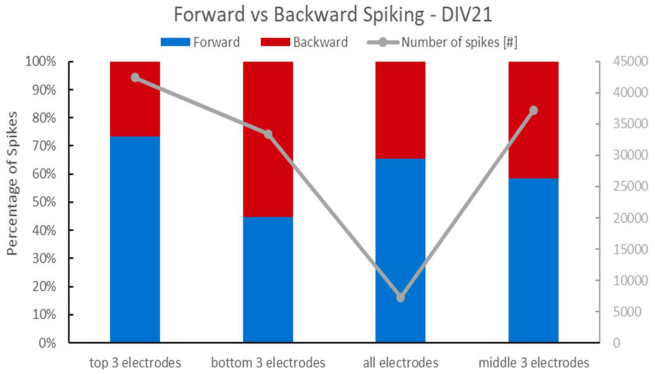

Figure III.5 - Stacked bar graph for the percentage of forward vs backward spiking PEs for a recording of the linear-only channels, illustrating the relevancy of choosing the right electrodes for the analysis of bias in the channels.

Commented [PMPTdM71]: I'm not sure if here i shouldn't add something like "usually, (a factor of) 5"

Commented [jo72R71]: Sim, 5x std

Commented [PM73R71]: Feito!

Commented [jo74]: Está aqui alguma confusão... O threshold do experimenter só é "adaptativo" para cada um dos eletrodos, mas não se atualiza passada a janela dos 500 ms que usa para cálculo

Commented [PM75R74]: Eu sei, mas tens razão não estava muito claro... ve agora plz

To make sure that this was, in fact, what was being seen and to check for what solution was best to overcome this problem, three other conditions were tested: analysis of only the 3 electrodes closest to the "Target", of the 5 electrodes associated with the microchannels and only the 3 middle electrodes.

These results, presented in Fig. III.5, lead to the following conclusions:

- evaluation only on the 3 electrodes closest to a population will be associated with a structural bias, due to elongating axons (i.e., ones which have not yet crossed the whole microchannel) of this population being accounted for, yet the equivalents for the opposite population are not. Thus, these results do not represent the full length of the microchannel.
- evaluation of the total of electrodes of the microchannels leads to a much smaller number of PEs. Still, in the case of hippocampal neurons as the ones on the recordings of this study, the number of detected propagating APs is still very high.
- evaluation using the 3 middle electrodes produce similar relationships as the use of the 5 electrodes, maintaining similar number of events as the other testing with 3 electrodes.

Either of these last two options have no structural reason to present a bias but involve downstream the use of electrodes associated with asymmetrical designs. As defined in [21], consecutive events from the same channel had to be at least 3ms apart from each other, to ensure that identified propagations would not be associated with burst activity either triggered by the population or the axons themselves. The delays between consecutive electrodes pertaining to the same event to be smaller than 1ms, value established previously on [21], on 2 electrode pairs.

Similar tests as the ones done for Fig. III.5 were made on recordings with asymmetric channels. Evaluation of the signal propagation considering the middle 3 electrodes led to the identification of propagating events that had to respect only propagation between 2 electrode pairs. The likelihood of mismatches happening is quite higher than when the 4 propagations must exist to consider an event. Both conditions had to be tested to check, however, the best alternative in terms of the equilibrium between the number of spikes vs reliability of the results.

It was then concluded that, even if the number of propagating spikes identified decreased by a factor of 10, the best alternative should be to consider all electrodes in the microchannels, as the number of events was still considerably high, and the results could be more confidently accepted.

Nonetheless, considering the objective of making a software tool that has transferability for other studies, for example, with Dorsal Root Ganglia (DRG) explants, [21] which do not fire as often, this might be a limiting factor.

At the population level, analysis had to take into account that the same number of electrodes should be used to avoid bias in the quantification of information transfer. This meant that, regardless of whether the microchannels start on 6th or 7th row, for the functional data analysis, "Source" population is only the top 5 rows and "Target", the 5 bottom ones.

3.5.2) Summed Firing Rate Vector

The visualization of the dynamics in the cultured neuronal networks is done, more often than not, through raster plots, where for each electrode-time of activation pair a marker is added to the graph. However, in these raster plots, small changes in the firing rate of the overall network might go unnoticed, which might be an issue for a better understanding of the initial and end points of high frequency activity such as the NB events.

Commented [jo76]: Simplifica

Commented [PM77R76]: Mais claro?

Commented [jo78]: Refere apenas que optaste por usar 5 eletrodos de forma a ter de satisfazer 4 propagações, ao invés de 2 (+ confiança nos resultados)

Commented [PM79R78]: Achas que assim ficou claro?

Commented [jo80]: aqui podes citar

Commented [PM81R80]: Citei já

Commented [PMPTdM82]: Should I add a figure here?

Commented [jo83R82]: Já tens mais à frente também

Commented [PM84R82]: Ok

With that in mind, most plots represented in this document resort to calculation of the summed firing rate of each of the 3 section of interest - Microchannels, “Source” and “Target” Population. Initially, using the spike train for every electrode, an instantaneous spike firing rate is calculated for every millisecond of the recording. Afterwards, the vectors of the instantaneous firing rate matrix respecting to the sets of electrodes relating to the populations are filtered with a causal linear filter with an unnormalized kernel size of 50ms. The analysis of the microchannels is similar, but two summed firing rates are obtained, one for the forward spiking and another for the backward.

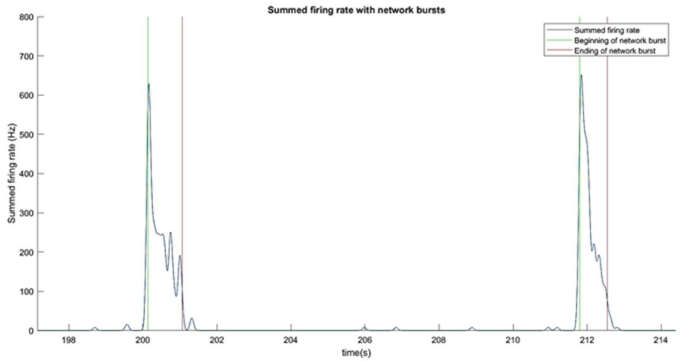

Figure III.6 - Zoom-in (20s window) of the summed firing rate vector of the activity of one of the populations at DIV 12. It is observable that the initial and final time of the network burst events calculated on the spike times, encompass well the summed firing rate peaks.

The use of a causal filter is justified for visualization purposes, because it’s the most logical way to assess that increases in firing rate do not occur before the timestamp at which the number of spikes actually starts to increase. Nevertheless, this elicits a delay in comparison to the real signal, which it’s important to beware of. On the other hand, the kernel is not normalized to allow to recapitulate how many spikes were in fact detected in a specific time bin.

In the end, this resulted in vectors which effectively represent changes in the firing rate of each section. They are particularly useful to distinguish NB activity from baseline, as one can observe in Fig. III.6.

3.5.3) Stimulation artifact

The need to control the timing of one of the population’s network drive to check for the response on the second required the used of some kind of stimulation, which, as mentioned, was performed by the internal electrical stimulator in the setup. However, it soon become obvious that the stimulation artifact was a problem on the stimulation recordings which need an extra step of pre-processing.

Indeed, to have a *proxy* to NB activity to compare registers where neurons were spontaneously active, a much higher number of electrodes than the ones regularly used on stimulation was essential, which lead, thus, to an artifact with a format and magnitude that has not yet been seen in other works within the group.

Raw voltage signals had to be analyzed in this case to ensure what was being detected by the online spike detector. By observing its timestamps near the stimulus, one can confirm what is stated

on the user manual of the recording system, which is blanking. This phenomenon is the result of the disconnection of the amplifier from the recording electrodes, done to avoid electrical damage to them as a result of the stimulation.

Reconnection of the amplifier to the electrodes generates a very large increase in the voltage in the following 200ms. However, the spike detection algorithm is not run on the raw voltage. In fact, as in previous projects in the group, a 6th order Butterworth filter in a bandpass configuration which should cut-off frequencies between 200-3000 Hz was used.

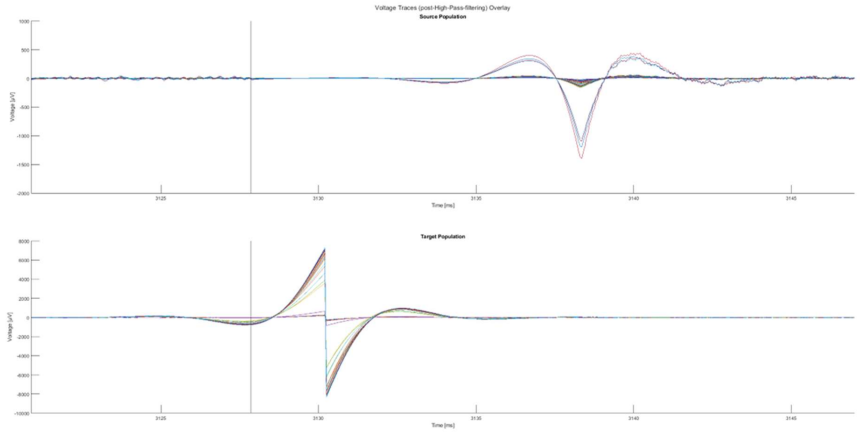

Figure III.7 - Filtered voltage traces of a "Source"-stimulated recording at DIV12, with the signals associated with the electrodes of the "Source" population represented on the top and the ones on the bottom with the "Target". The thin black vertical line represents the time of the stimulus.

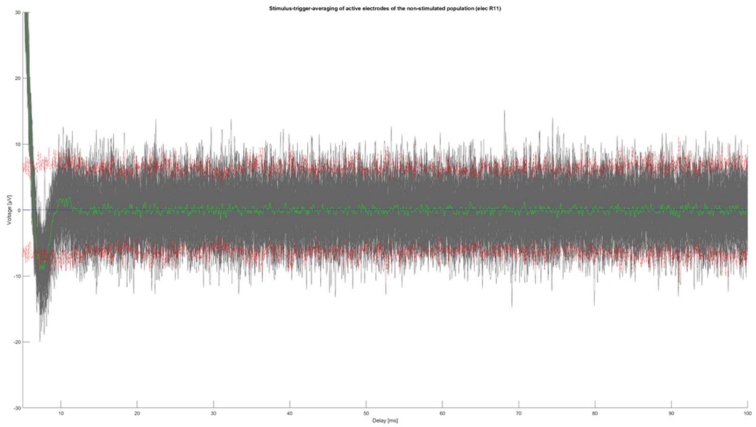

Figure III.8 - Stimulus-trigger-averaging of an electrode of the non-stimulated "Target" population starting at 5ms post-stimulus. In gray, the signal post-stimulus for all trials is drawn. The green line represents the average over all trials and the red ones are defined as the average ± standard deviation across trials.

So, at first, the analysis was run on the filtered signal and what was observed, by graphing the filtered signal for different electrodes, and afterwards, the post-stimulus trigger-averaging – see section *Event-trigger-Averaging* for further details - was that, to make sure that the analysis was not affected by stimulation residues, information pertaining to 20ms post-stimulus should be removed.

After removing this component, the idea was to observe and later quantify the response of the unstimulated population to the outputs of the stimulated population. A heatmap of the post-stimulus for each stimulation trial with the summed firing rate – see section *Summed Firing Rate vector* – of the unstimulated population's activity was drawn.

The existence of a vertical bar in the [20,70] ms period meant there was still some stimulation artifact residue, as neuronal response wouldn't be so consistent across trials. Following that, it was necessary to review the steps and check for the possible causes of that phenomenon.

One thing that was not taken in consideration was the fact that, to prevent delays in the signal output by the Butterworth filter, the filtering is done in a zero-phase format. This means that data is first run through the filter in a time-forward sequence but then the signal output by this first filter is re-run in a time-reversed way to the input of filter and the final output is the time-reversed version of this second filtering operation.

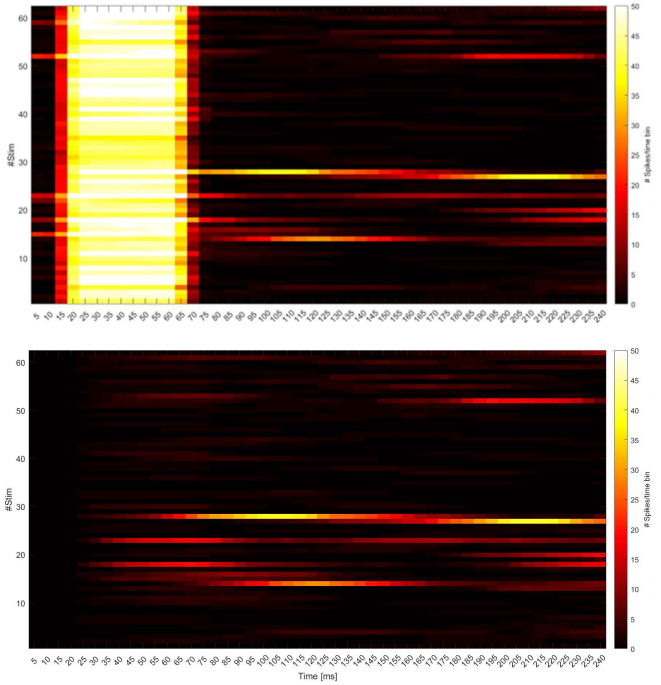

Figure III.9 – Post-Stimulus heatmaps of the "Target" response in a "Source"-stimulated recording. Top figure is the representation of the data without any type of processing, while on the bottom data of 50ms pre stimulus and 20ms post stimulus was removed. The main distinction on the figure by visual assessment is the removal of the vertical bar.

Nevertheless, this technique raised an issue: then, stimulation artifact was not limited to timestamps at and post-stimulus, due to the fact that the filtering introduced artifact residues on the

pre-stimulus timestamps. Indeed, reanalyzing Fig III.9 it's obvious that there is a large component of consistent response pre-stimulus which is likely to originate spikes.

This became a problem when the input for drawing the heatmap was the summed firing rate vector which has been referred to as having a delay in comparison to the original signal. Furthermore, it was interesting to understand that the bar-like had a size comparable to the kernel size of the operation which outputs the summed firing rate vector.

Due to the fact that the interest on the stimulation recordings is mainly understanding how unstimulated populations respond, removing 50ms worth of pre-stimulus spike timestamps might not be prejudicial. After removing both pre and post-stimulus spikes data, the heatmap had a much cleaner look and resulted in something much similar to what one could expect from graphing this information.

3.5.4) Network Burst detection

As previously mentioned, NBs are coordinated spontaneous activity of the neuronal networks. Due to the fact that synchronicity is a known key factor of information between clusters of neurons [68], [69], a pipeline to analyze spontaneous cell activity and their in-between populations electrophysiological communication must, for this reason, have algorithms to detect these types of events.

It has also been stated that the NB detection algorithm used in this work was based off an ISI-statistics-based adaptive threshold method first implemented by Pasquale [49]. Indeed, initial testings were conducted using this approach and they generally presented satisfactory results.

Nevertheless, when the dynamics of the network were more complex, meaning more electrodes were involved and each with distinctive firing regimes, the algorithm's performance decays, achieving levels of performance that hindered the ability to detect relationships between the populations' activity.

This was motivation enough to test changes in the parameters of the current published version of it and see how they would increase the performance of the NB detection for the neuronal cultures in this study.

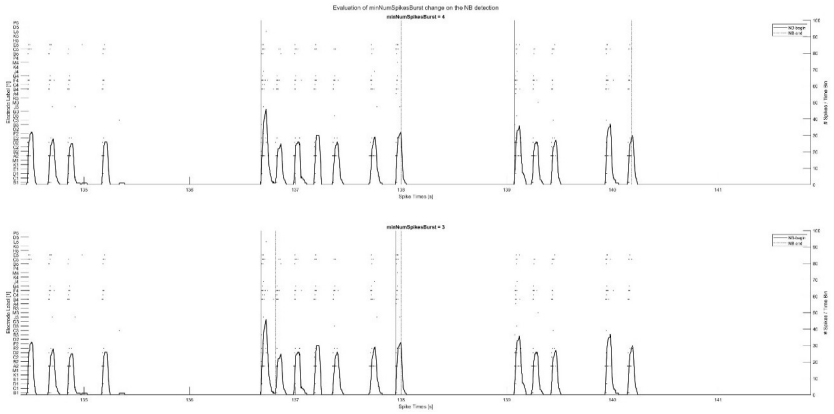

Figure III.10 - Zoom-in on the summed firing rate vector plotted against time in a spontaneous activity recording. Network burst detection performance is tested for *minSpikes* = 4 (top) and *minSpikes* = 3 (bottom). Through visual assessment, the value of 4 was selected.

Initially, the analysis began with observing the results after changes on the *minSpikes* parameter, as it is reported in the original manuscript that this should be changed according to the behavior of the cultured networks. In fact, through visual analysis on the recording software, NB-like activity was associated with a typical value between 3-4 spikes on each electrode. So, in order to decide on which value made the most sense, a subset of the recordings was run. The results are shown for one of them in Fig. III.10 and their across-recordings consistency led to setting it to 4.

The next step involved testing parameter *maxISITh* and *maxISImax* for values of *minPercElec* of 10% and 15% of the active electrodes. These were tested with increasing values due to, as compared to previous studies, there being more electrodes and naturally an increase in the number of cells bursting, Three settings were tested starting on the values defined on [49], *maxISITh* = 150 and maxISImax = 500 and, finally, *maxISITh* = 250 and maxISImax = 600.

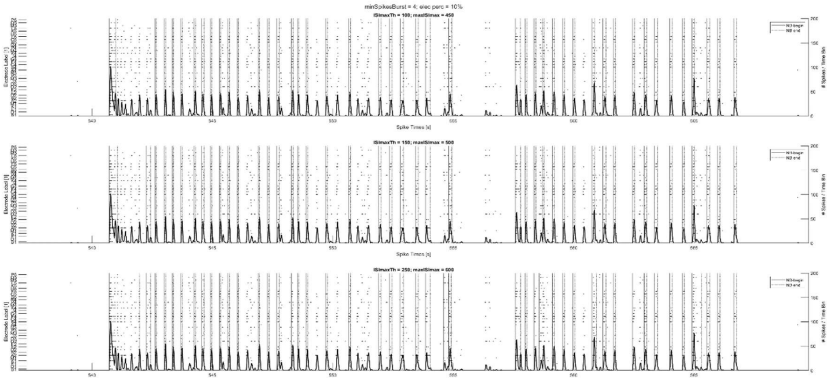

Figure III.12 - Zoom-in on the summed firing rate vector plotted against time in a spontaneous activity recording. Network burst detection performance is tested with *minSpikes* = 4 and *minPercElec* = 10% and, from top to bottom, *maxISITh* of 100, 150 and 250 and *maxISImax* of 450, 500 and 600, respectively. Here, only slight differences are detected but still the top one seems to work best.

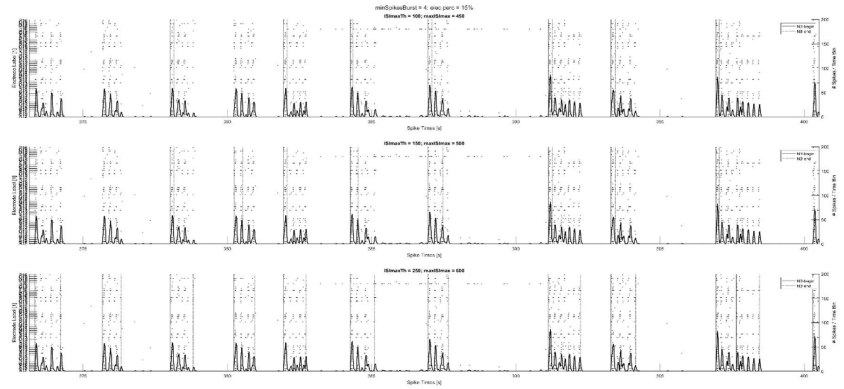

Figure III.11 - Zoom-in on the summed firing rate vector plotted against time in a spontaneous activity recording. Network burst detection performance is tested with *minSpikes* = 4 and *minPercElec* = 15% and, from top to bottom, *maxISITh* of 100, 150 and 250 and *maxISImax* of 450, 500 and 600, respectively. Here, the parameters of the bottom one deliver the best performance.

It soon became obvious that neuronal cultures had too diverse dynamics to consider a single set of values which enabled a generally good performance. After analyzing several recordings, selected randomly, patterns emerged indicating that whenever cultures had lower levels of activity a smaller percentage of electrodes and lower values of the thresholding worked the best while performance peaked for higher percentage of electrodes bursting and longer time thresholds in recordings with higher levels of activity.

It was then decided that the percentage of active electrodes should then be the decisive factor: for values lower than 50%, then the 1st case – Fig. III.11 - was selected and the parameters would be the smallest and if this value was equal to or higher than 50%, the 2nd set of parameters – Fig. III.12 would be the one used. This alternative increased the overall performance of the algorithm, following a visual assessment of distinct firing regimes.

Even if the produced results improved, there were rare cases where the performance was underperforming. For those, what happened was that the number of electrodes was not enough to characterize the level of activity of the network. To overcome this issue, an upper boundary of the value of *IBeITh* was set, meaning that whenever the result of the calculations already described in the characterization of the Pasquale's method resulted in values higher than 500ms, the method reevaluates the parameters and repeats the analysis. If the value was lowered, then the last analysis is kept, otherwise the original results are the ones used on the downstream analysis.

3.5.5) Population-to-population communication

One of the main goals of the project is to define a preferentially unidirectional flow of information for the population-to-population communication. Hence, it matters to gather all obtained data from the previous analysis in the same representation as is the temporal sequence of this events that should explain the modulation of one population over the other's activity.

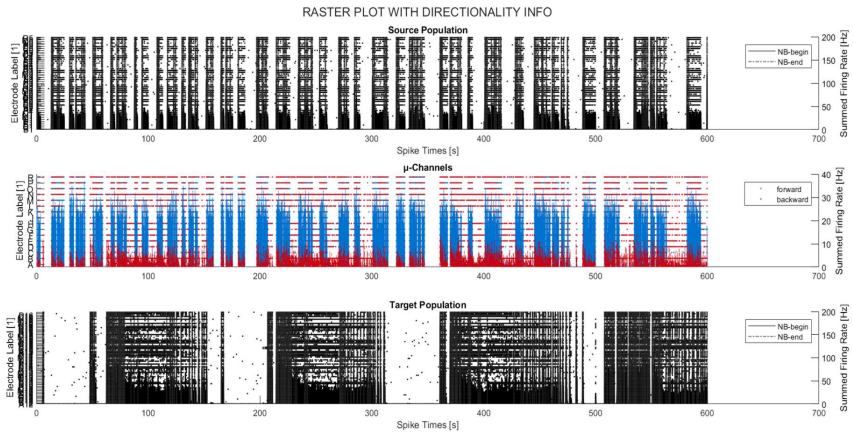

Figure III.13 - Raster plot of a spontaneous activity for each of the three sections on the µEF. On the populations' sections, along with the overlay of their respective summed firing rate vector, there are vertical lines representative of the initial and end time of the NBs. On the microchannels, instead of representing every point in which the electrode has a spike, the 3 linear electrodes are considered as a representative of the whole channel and only identified forward, and backward spiking events are drawn. Like in the populations, the summed firing rate vectors are also plotted.

This accomplishment was done in a graph where the raster plot was segmented in 3 sections, each for one of the areas of interest, and overlaid with the plot of the summed rate vectors and vertical lines in respect of the NBs initial and final times for the populations.

The study of the state-of-the-art allowed to identify two methods of defining this communication related to NBs or NB-like activity. Firstly, there were studies that defined a minimal percentage of time overlap between NB-like activity of one population and the other [70]. *Winter-Hjelm et al.* (2023) considered an event whenever the initial time point of the driving population happened with a delay of [20, 240] ms of the beginning of the driven population [24].

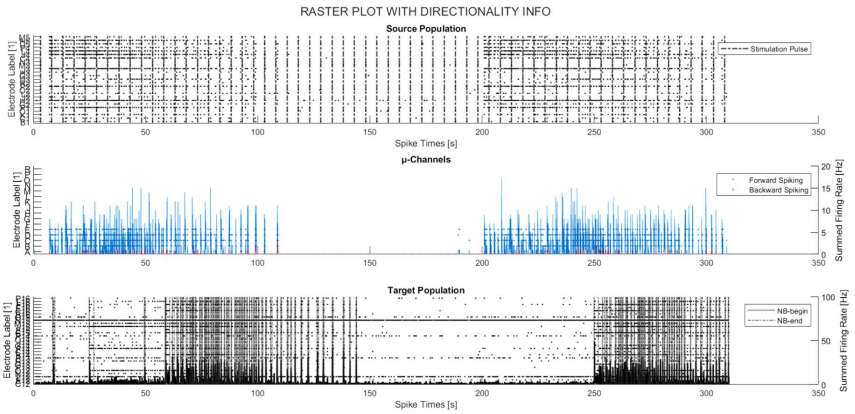

Figure III.14 - Raster plot of a stimulation recording, where the stimulated population was the "Source". The distinction over spontaneous recording is related to the stimulated population whose representation includes only the spikes and stimulation pulses timestamps.

In this study, after visual assessment of multiple raster plots like the one previously shown with directionality information, the 2nd option looked the most logical one. Thus, starting on the beginning of the recording time, time is run and the initial time of the NBs (regardless of which population it happens on) is used to check if there is a corresponding NB event on the other population with delays on the aforementioned interval.

Similarly to the analysis done in the microchannels, there are also putative forward and backwards events. In this case, forward corresponds to "Source" population' NB driving a "Target" population' NB and backward to the other way around. To distinguish between the events on the microchannels and the in-between populations events, the latter were defined as Population-Driving Events (PDEs).

There's, nevertheless, a phenomenon which was named "recurring waves" that deserves mentioning. In the spontaneous recordings, there is sometimes a sequence of NB-like activation in close succession in both populations. In other words, "recurring waves" it's when, for instance, a NB on the "Target", triggered by a NB on the "Source", triggers a second NB in the "Source" population. Therefore, because this reactivation seems to need less driving force to occur, for the sake of fair comparisons, each NB can only enter as part of the first PDE happening chronologically.

For stimulation recordings, the removal of peri-stimulus data meant that any possible NB-like activity associated with the outputs generated by stimulation could go unnoticed by conventional NB detection methods. To compare population-to-population communication with spontaneous activity, the non-stimulated population's ability to raise its activity above a certain threshold after stimulation

Commented [jo85]: referir que não veio da observação de um unico raster plot...

Commented [PM86R85]: Feito!

Commented [PMPTdM87]: Should I add a picture here?

Commented [jo88R87]: Acho que já se nota nesta Fig III. 14

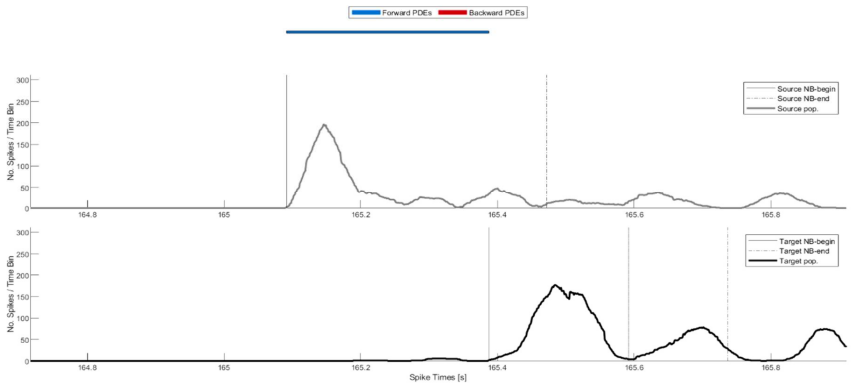

Figure III.15 - Zoom-in of the Evaluation of Population-Driving Events (PDEs) of a spontaneous activity recording, illustrating a Forward PDE.

was tested. The threshold was set at an average of 15 spikes in a 5ms time bin within the [20, 240] ms post-stimulus window. If this threshold was surpassed, the trial was identified as a response to stimulation. A percentage of these events, termed fidelity, was calculated for each recording. If the asymmetrical channels function as intended, the fidelity levels for "Source" population stimulation should be higher than for "Target" population stimulation, while controls should present similar values in both conditions.

3.5.6) Event-trigger Averaging

In order to evaluate the consistency of a response on electrophysiology, it is not uncommon to have an analysis where the 0 is set to be the time at which a certain event has begun and then average the signal across the different number of trials.

Commented [PMPTdM89]: Procurar referências em que se use análises similares

This type of analysis can be used on Event-Related potentials, in particular Sensory Evoked potentials, to extract consistent brain's electrical response to stimuli [71], [72], on study of synaptic strength and plasticity as a result of different triggering action potentials in patch-clamp recordings [73], on animal or human behavioural studies to understand how time-locked EEG signals change to activate certain cognitive processes or elicit specific behaviours [74] and on any other Stimulus-Response study.

That is called event-trigger averaging and, on these scenarios - where the objective is to assert how the outputs of one population condition the other's activity -, they are particularly useful. This translates, in the presented work, on using the stimulation timestamps on stimulation recordings and the initial time of NBs in the spontaneous activity recordings.

In what regards to stimulation, on the preliminary studies, this meant doing Post-Stimulus Trigger Averaging on the filtered voltage signal meaning, for each trial of stimulation, the 100ms after stimulus were drawn, overlaid on the same graph in gray. This filtered signal of every trial is summed and then divided by the total number of trials. The result is represented by the green line in Fig. III.6. Additionally, to hint at how spike detection algorithm would result, the mean (blue line) and a multiple of the standard deviation (red line) after stimulation artifact are plotted.

There's also a second type of assessment to be made which is important to check that is the populations' response to stimulation. So, the idea here was to use the timestamps of every trial and

check how consistent the response of the stimulated and non-stimulated populations was over trials. The stimulated will be excited directly by electrical stimulation so, as observed in Fig. III.16, its summed firing rate has a peak around the 50ms post stimulus every trial, translating in a peak also observable in the line resulting of the stimulus-trigger averaging. On the non-stimulated population, stimulation is not delivered directly but the increase in firing rate of the opposite stimulation must be enough to drive some events. In fact, when looking for it on the non-stimulated population' summed firing rate vector, even if the outputs of the stimulated population are not enough to drive a response every time there is stimulation, there are some trials where the non-stimulated population experiences an increase in its firing rate.

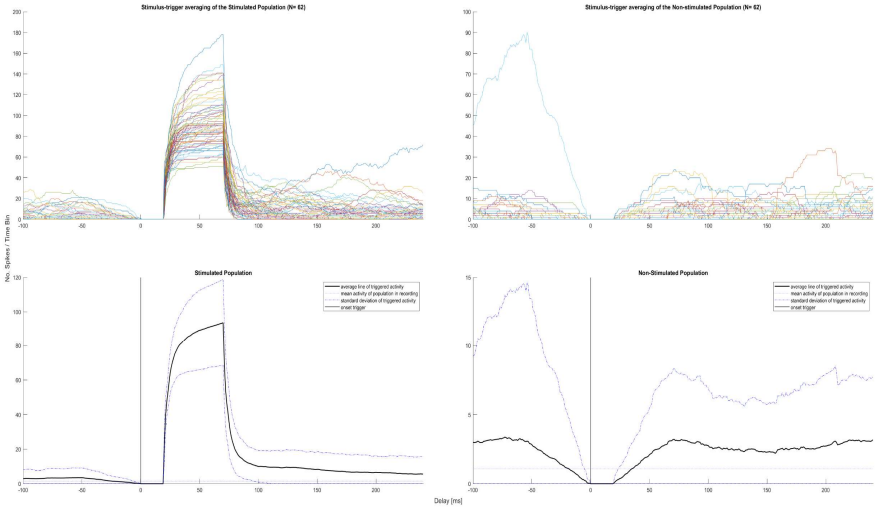

Figure III.16 - Evaluation of the bias on the population-to-population communication invoked by electrical stimulation, in this case of the "Target" population. The graphs on the left refer to the stimulated population while on the right the observed activity is related to the non-stimulated population. The top graphs represent all instances of the summed firing rate vector of the respective population on the 100ms before and the 240ms after, aligned by the beginning of stimulation pulse delivered. Bottom graphs, represent the average of the trials of the graphs on top of them, illustrating the consistency (or not) of this response. Information of the standard deviation across the different trials is marked on the blue dashed line. The mean activity is represented in the gray dotted line and represents the mean activity registered in the corresponding spontaneous activity recording, which is done immediately before the stimulation ones.

In the respective section on the *Results/Discussion*, this assessment went a bit further by analyzing whether this is distinct with stimulation of the "Source" population vs "Target" population' stimulation in terms of fidelity, as mentioned in the previous section.

On the other hand, the analysis of spontaneous activity recordings also could make use of this type of visual outputs. Indeed, to easily understand the bias of the connections established between the populations, an insightful idea is to perform NB-Trigger-Averaging of the summed firing rate vectors: the 0 is set for initial time of a NB of population A and then the previous and the following second of the summed firing rate activity of population B is plotted in the same graph for every NB of the first population. The signal of every trial is averaged and plot on a second plot alongside with the

mean activity of the population in recording and the standard deviation of triggered activity. Analogously, another two plots are drawn changing the triggered and triggering population, to check if the propagation is really biased or not.

In cases where the desired forward bias is present, the graphs should look like the ones in Fig. III.17. Here, the average line of triggered activity of the "Target" population (even considering the standard deviation) is considerably above the mean activity of this population in the recording in values between [60, 300] ms post-trigger. Simultaneously, the average line of triggered activity of the "Source" population has similar behaviour but for delays of the negative side of the graph, which means that, on average, the "Source" population has NB-like activity preceding a beginning of the NB of the "Target" population.

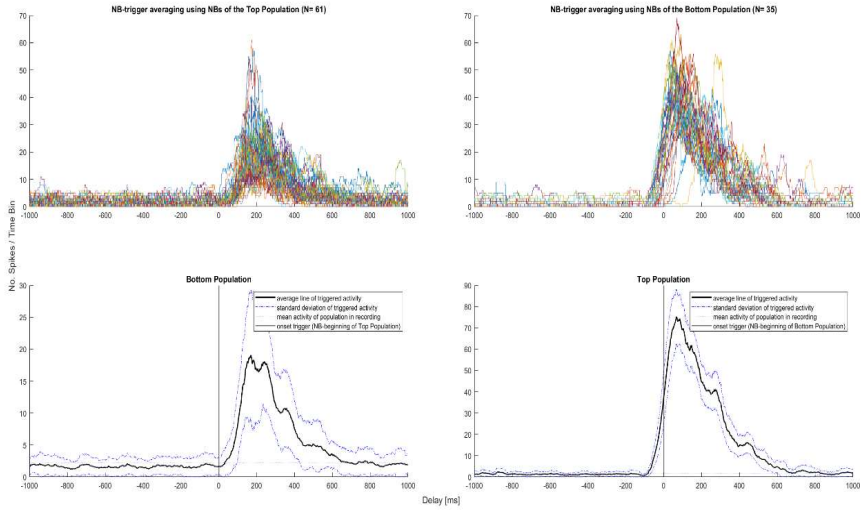

Figure III.17 - Evaluation of the bias on the population-to-population communication through NBs. The top graphs represent all instances of the summed firing rate vector of population B 1s after and another before, aligned by the beginning of NB of the population A. Bottom graphs, represent the average of the trials of the graphs on top of them, illustrating the consistency (or not) of this response. Information of the standard deviation across the different trials is marked on the blue dashed line. In this case, in particular there's a forward PDEs bias, due to the consistency of the graph pertaining to the bottom population on the [20, 240] ms post-NB-trigger window.

3.5.7) Spatial Profiles in population activity

Alongside with analyses done on the temporal domain, it is relevant to examine the spatial activation of the neuronal networks since it is known to play a crucial role in coding of neuronal information. Indeed, studies on the power of neuronal populations in decoding spatial information in visually guided eye movement tasks have revealed that decoding performance peaks during visual and motor epochs, showcasing the importance of this type of analysis [75]. On a similar note, complementing neuronal signals, astrocytes seem as the spatial position decoders, behaving as regulators on the coordination of the distinct brain circuits [76].

To this end, the spiking activity was discretised in 20ms bins for all 256 electrodes and the resulting bin vector, reshape to resemble the MEA matrix. The output of this operation is a 16x16xt, where t is the max number of 20ms bins the recording could hold. Hence, every entry of the matrix represents the sum of the number of spikes detected in the respective electrode inside that specific time bin. This approach allows for a more detailed spatial-temporal mapping of neuronal activity across the MEA.

Afterwards, following other published works which were doing similar studies, it mattered to see if there were any spatial profiles worth noting whenever an event indicative of neuronal populations' communication. – see section *Population-to-population communication* for additional information – was happening. The result is shown in Fig. III.18.

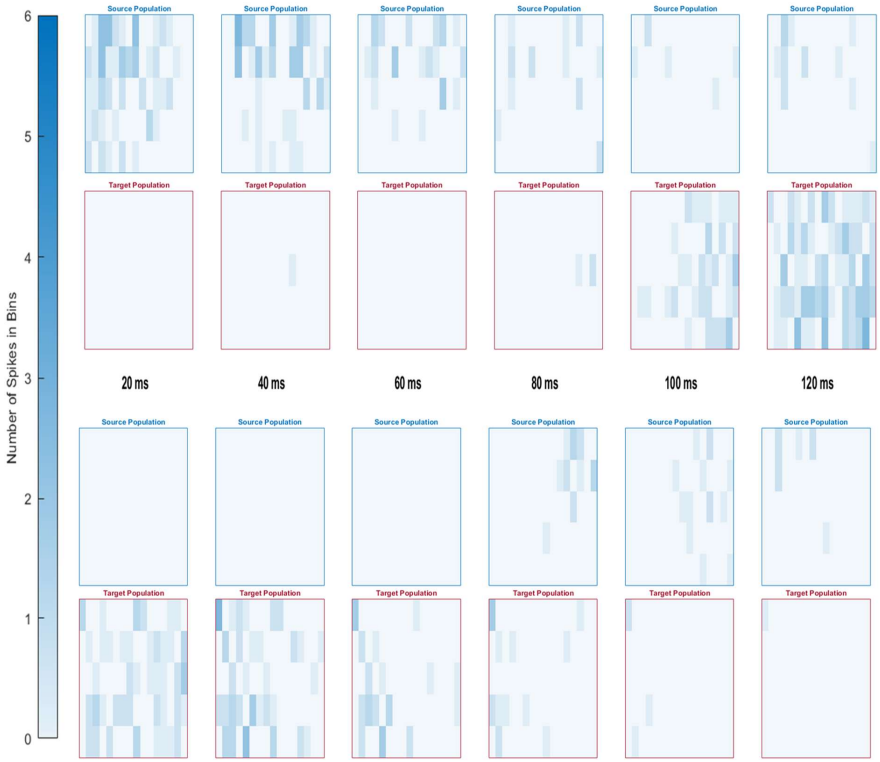

Figure III.18 - Heatmaps of the binned (20ms) activity of each electrode in the 120 ms following a network burst in the "Source" population, on top, and the "Target" population, on the bottom. Both events were taken from the same recording, where there was asymmetry in the microchannels design.

It is quite clear that for similar network-wide activities on both populations, there were different levels of activation on the other population. In fact, the shown NB-like activity, when initiated on the "Source" population was capable of driving the same type of behaviour on the "Target". Conversely, "Target" population's NB activity did not seem to result in a smaller, more localized response on the

"Source". This suggests a directional bias in the efficacy of communication between populations, likely influenced by the asymmetrical design of the microchannels.

Despite how intriguing following this line of inquiry further might have been, time constraints limited this analysis from going beyond what is presented in this section. As such, no statistical evaluation of the spatial coding of the signalling in neurons or more detailed insights were observed in the current study.

Future work should focus on doing a more granular analysis of the spatial profiles which could involve burst sorting and an analogous to the temporal Event-trigger averaging to classify and interpret the spatial-temporal patterns of MEA activity. By correlating the activity of specific electrodes or network bursts with the initiation of propagating events in the microchannels or across populations, researchers could gain deeper insights into the mechanisms underlying neural communication and network dynamics.

Integrating spatial analysis with temporal data and applying advanced computational methods will be essential for uncovering the complex patterns of neural communication and enhancing our understanding of the function of both *in vitro* and *in vivo* networks at multiple scales.

3.6 - Statistical analysis

To effectively reach conclusions on how much of the obtained results can be translated into novel knowledge on neuronal populations' communication, one must beware to assess how much of it is reproducible and unrelated to chance. In order to do that, statistical analysis of the obtained data was due. In fact, software – Graphpad Prism – specifically used to assert statistical significance of the results was used.

Regardless of which data was being analysed, the pipeline was nearly identical:

- Testing for normal distribution – the first assessment to be made was related to the type of distribution of the data. This had to do with what assumptions could be made about it, which, in turn, is used to define what statistical tests can be done on the following steps. The Shapiro-Wilk and the Anderson-Darling tests were, then, run, considering the small sample sizes of some experiments.
- Checking for unidirectional bias – in cases where the data analysed followed a normal distribution, paired t-tests were implemented. Otherwise, the data was run on a Wilcoxon matched-paired signed rank test.
- Assessing for differences across designs – finally, testing for different performance of the designs was ensured by Brown-Forsythe and Welch ANOVA, when data was normally distributed, and Kruskal-Wallis, when it was not. Post-hoc comparisons test analysis included Dunnett's and Dunn's, respectively, ran against controls.

The statistical analysis couldn't be carried out without first doing a preprocessing of the data. Indeed, inclusion criteria for the studies pertaining to the functional characterization of the MEA data were a minimum of 10% of active electrodes for both populations and a total sum of at least 100 propagating events (forward + backward) on the microchannels.

Note that an electrode is considered to be active if the mean firing rate across the whole recording is superior to 0.1 Hz, as widely accepted in the literature.

For all analysis, unless otherwise stated, the confidence level was defined as $p < 0.05$. The significance of the findings is represented by * when $0.001 < p < 0.05$, ** when $0.0005 < p < 0.001$, *** when $0.0001 < p < 0.0005$ and **** if $p < 0.0001$.

Chapter IV

Results/Discussion

The results output by the analysis done in the work for this thesis pertaining to two very distinct scenarios which are stimulation and spontaneous activity recordings. Their nature brings about implications and different conditional factors, nevertheless, both contribute for each result in their own way, increasing the confidence of the overall analysis through their consistency.

4.1 - Profiles of Activity in the Micro-Electrode Array

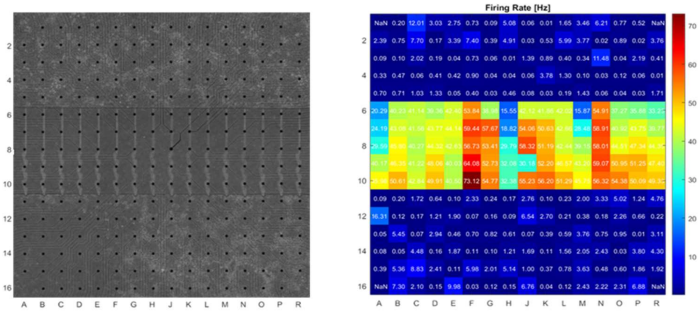

Figure IV.1 - Side-by-side illustration of the MEA grid (left) and its respective color-coded distribution of the mean firing rate (right)

The initial analysis led to distinguishing two profiles of activity, as it can be seen in Fig. IV.1. They were associated with the structure: the microchannels' electrodes present much higher mean firing rates than neuronal populations', probably due to the increase in SNR and number of signal sources (i.e., axons) [21], [77], [78].

The distinction reinforced the idea that analysis of both populations and microchannels should be made differently but simultaneously it made interesting to check if there were also differences in what regard to the activity of the populations, masked by the magnitude of the microchannels' activity.

Commented [jo90]: citar papers relevantes

Commented [PMPTdM91R90]: Citei estes. Parecem-me ser aqueles em que é mais claramente dito que há aumento de SNR

A before-after plot with the percentage of active electrodes in "Source" vs "Target" is calculated, using, for each design, data from the 3 different timepoints altogether. The results are shown in Fig. IV.2. For reference, the distribution is reflected on a box and whiskers plot underneath it. Recordings where the percentage of active electrodes of one population was inferior to 10% were discarded.

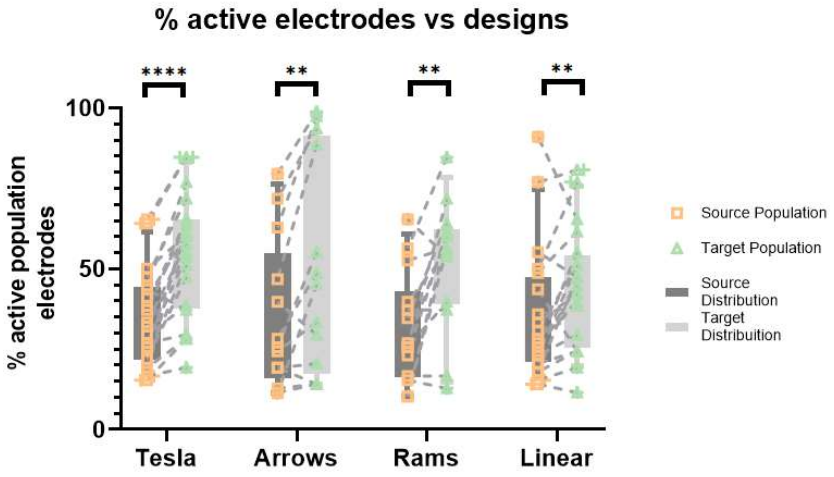

Figure IV.2 - Before-and-after plot for the percentage of active electrodes on the "Source" and "Target" populations on all spontaneous activity recordings where both populations had more than 10% of active electrodes. The distribution of the data is represented in the box and whiskers plot beneath it and recordings are each divided in its associated design. Regarding significance values, those were taken of the results of Wilcoxon Signed-Rank Test, whose test statistic is represented by W. Tesla had W = 184.0 and returned $p < 0.0001$, Arrows had W = 58, $p = 0.0098$, Rams had W = 58, $p = 0.0034$ and the control channels had W = 133, $p = 0.0054$. As for the median differences, they had values of 24.75, 28.21, 14.10 and 7.70, respectively.

It is easily observable that, regardless of the design, the percentage of active electrodes on the "Target" population is much higher, on average, than the one on "Source". The first step was to check for normality for the dataset composed by all recordings of each design, separating each population. As there were some datasets which did not follow normal distribution, a Wilcoxon Signed-Rank test was run for each design, looking for inter-population differences on the pooled data.

The results returned significant differences for all designs, including the control. While this is a point in favour of the asymmetric designs, because is an indirect measure of the "Source" inducing activity in the "Target", the same cannot be said about the controls where no extrinsic factor plays a role in the directionality of the events.

A detail worth noting is that the median difference is the smallest on the symmetric channels, meaning that the magnitude of the difference on the asymmetric channels is higher. In fact, the given difference represents 6 electrodes only for the controls and more than 12 for the remaining asymmetric ones.

It mattered also to check, motivated by the distinct order of magnitude in the median differences between asymmetrical and control designs, how the design factors in this difference, hence, a Kruskal-Wallis's test was made. Nonetheless, with a statistic test value of 5.047 and a p-value of 0.1684, no conclusions could be drawn.

In summary, this is first evidence that “Target” population’s activity is also being driven by the outputs of the “Source”. Likewise, other metrics of the network’s activity were used to evaluate if this bias is also shown – average across all recording time of the summed firing rate vectors and number of NBs in each population.

The first, shown in Fig. IV.3, after running a similar statistical analysis, obtained very similar results – significance of the population factor and non-significance on the design one.

The distinction between the average of the summed firing rate across the recording on the “Source” and “Target” population, however, proved to be equally relevant for every design. Once more, the controls did not present the expected behaviour and observable changes are of the highest level of significance. Nevertheless, the value of the median differences is higher for the rams which is the one expected to perform the best, as per unpublished data on structural/anatomical studies in these previously mentioned platforms.

Despite that, once more, this graph reinforces the idea that “Target” population is being conditioned by the activity of the “Source”.

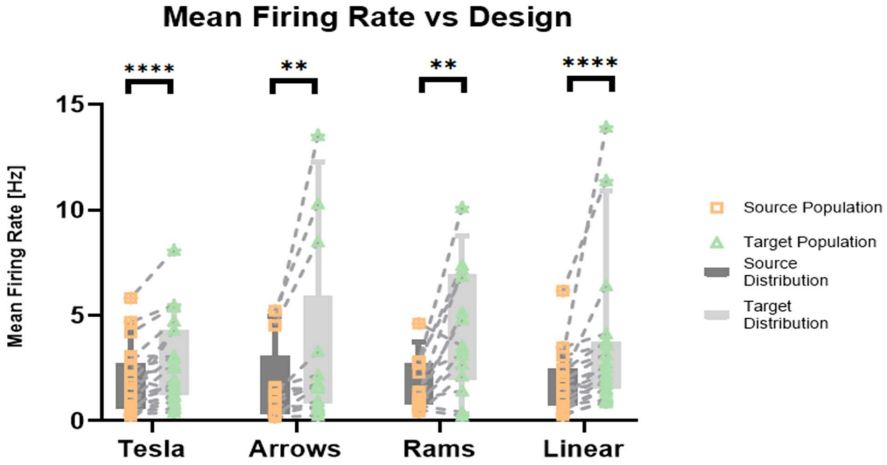

Figure IV.3 - Before-and-after plot for the mean of the summed firing rate on the “Source” and “Target” populations on all spontaneous activity recordings where both populations had more than 10% of active electrodes. The distribution of the data is represented in the box and whiskers plot beneath it and recordings are each divided in its associated design. Regarding significance values, those were taken of the results of Wilcoxon Signed-Rank Test, whose test statistic is represented by W. Tesla had W = 180.0 and returned $p < 0.0001$, Arrows had W = 72, $p = 0.0012$, Rams had W = 75, $p = 0.0031$ and the control channels had W = 190, $p < 0.0001$. As for the median differences, they had values of 0.7930, 0.6435, 2.504 and 0.8175, respectively.

In order to validate that the previous two findings were a result of “Target” population activation of the outputs of the “Source” population, the idea to do a paired comparison for the mean firing rate of each TTX recording with the respective spontaneous activity one emerged. The results on Fig. IV.4 show what was to be expected, which was, in general, a decrease in firing rate on the post-TTX by removing the activity on “Source” population, due to the effects of the neurotoxin.

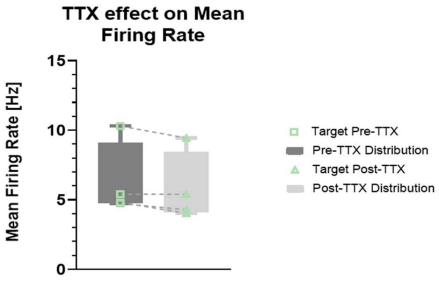

Figure IV.4 - Before-and-after plot for the mean of the summed firing rate on the "Source" and "Target" populations on the specific recordings which had also a TTX injection on the "Source" module associated with the recording. The distribution of the data is represented in the box and whiskers plot beneath it. A Wilcoxon Signed Ranked test was run but not enough data exist to find statistical relevancy on the visual difference.

Finally, when testing the frequency of NBs, presented in Fig. IV.5, the only significant difference found was on the arrows, where the "Target" seems to have a higher burst rate than the "Source". Due to the inter-culture variability, observable prior to statistical testing in the visual analysis of the raster plots with directionality information, identifying this relationship would be more complex. In other words, the dynamics of the segregated neuronal populations can be considerably distinct and, thus, generate burst rhythms and patterns that are themselves different, even if they come from the same cell isolation, meaning NB detection is dependent on these network dynamics that shift between one and the other. In fact, the significance of the results in the arrows is probably due to the small sample size, meaning that there is an inherent bias in the observed recordings which might not be real when considering a bigger and more representative sample size.

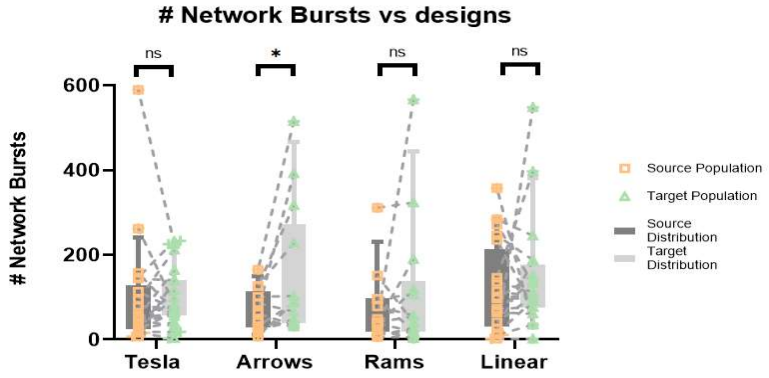

Figure IV.5 - Before-and-after plot for the number of network bursts on the "Source" and "Target" populations on all spontaneous activity recordings where both populations had more than 10% of active electrodes. The distribution of the data is represented in the box and whiskers plot beneath it and recordings are each divided in its associated design. Regarding significance values, those were taken of the results of Wilcoxon Signed-Rank Test, whose test statistic is represented by W. Tesla had W = 31 and returned p = 0.2884, Arrows had W = 59.0, p = 0.0199, Rams had W = 9, p = 0.3867 and the control channels had W = 21, p = 0.3433. As for the median differences in the Arrows which was the only significant difference found they had values of 30.0.

It is important to mention that these numbers of the NBs in one and the other population greatly influence the results of the Population-Driving Events. For example, if one population has a much smaller number than the other, the likelihood of the first presenting higher percentages of the events of population-to-population communication drastically increases, due to, firstly, there being an increase in the number of events that are caused by one another but a result of chance synchronicity (increase in the numerator), but also to the smaller number of events on the driver population (decrease in the denominator).

As such, the fact that in the majority of them there's no significant difference between them, actually works in favour of the proposed goals by not introducing a bias respecting the population-to-population communication. Otherwise, the starting point of one population would be different than the other which could potentiate a putative bias which would not necessarily be real.

Nevertheless, it's important to emphasize that in all performed statistical tests the pairing and the subject factor had high significance, meaning that the neuronal cultures themselves have a substantial impact on the measured activity parameters, that are not related to any extrinsic factor. Indeed, it's taken as a known fact that systematic differences in activity parameters among the different cultures can be linked to their biological variability - each neuronal culture may have unique characteristics or responses due to inherent biological differences. Furthermore, one needs also to consider the sensitivity of neuronal cultures to experimental variability, which is bound to happen, regardless of the caution/expertise of the experimenter, and that will also condition their activity.

Inspection of the activity colormaps of cultures of asymmetric designs vs symmetric ones motivated yet another analysis of cultures of asymmetric designs vs symmetric ones - the comparison of the mean of the firing rate of the top 2 vs the bottom 2 electrodes in every channel in each recording. Indeed, it comes as an indirect measure of the blockage factor of the asymmetrical designs, because, if there's blockage of the axons growing in the "Source" to "Target" directionality, some of those might not reach the top 2 electrodes, whilst the ones growing from the "Source" population should grow without any hindrance. For visual reference, please refer to Fig. IV.6.

Commented [jo92]: tens de ter cuidado com estas "informalidades" e ter uma linguagem mais "científica"... vem com o tempo :D

Commented [PMPTdM93R92]: É verdade :x acontece principalmente quando sinto que estou a repetir a mesma estrutura de frase pela 1000ª vez e a tentar escapar disso saem estas versões muito informais

Commented [jo94]: Boa!

Commented [PMPTdM95R94]: Obrigado!

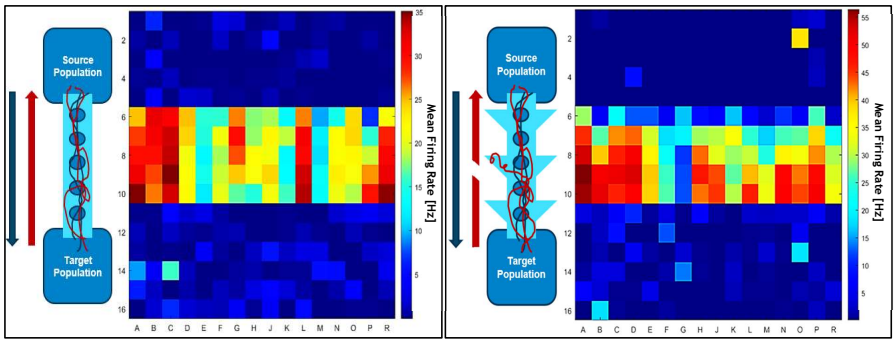

Figure IV.6 - Image showing how the design factor changes the level of activity in the microchannels. On the left, there's a depiction of a linear channel. Those have no structural motivation for showing difference between the top and bottom activity in the microchannels. This is followed by a colormap of the mean firing rate in each electrode on the MEA grid, showing a homogeneous profile in the channels which corresponds to the middle section (electrodes number 6-10). On the right, there's a depiction of an asymmetrical channel, represented by an arrow-like design. As can be observed in the corresponding colormap of the mean firing rate, the top activity (electrodes number 6 and 7) is lower than the activity on the bottom (electrodes number 9 and 10), as expected, due to the presence of backward (red) axons which do not reach the top electrodes.

This means that the level of activity on the top 2 electrodes must be rather lower than the 2 bottom 2 electrodes on asymmetrical designs and comparable in the control ones.

As such, it mattered to analyse different recordings and evaluate whether or not this was a statistically significant effect. Likewise, if that proved to be true, it would be important to consider if the designs performed differently from each other.

A single datapoint per chip was used for this analysis for each experiment-design-chip triplet to ensure that a bias associated with a certain culture was not favoured over others which for different reasons had less timepoints.

For the sake of observing the structural factor to its utmost potential, the maximum number of axons had to be observed which meant exploring the most mature timepoint of the network DIV17 onward of all experiments with a specific design.

Initial analysis of this data pertaining to the type of profile observed in the microchannels, when using the sum of the activity in all microchannels for each of the 5 electrode numbers of all included recordings led to preliminary conclusions that not all designs have the same ability to functionally block activity in the microchannels, as seen in Fig. IV.7.

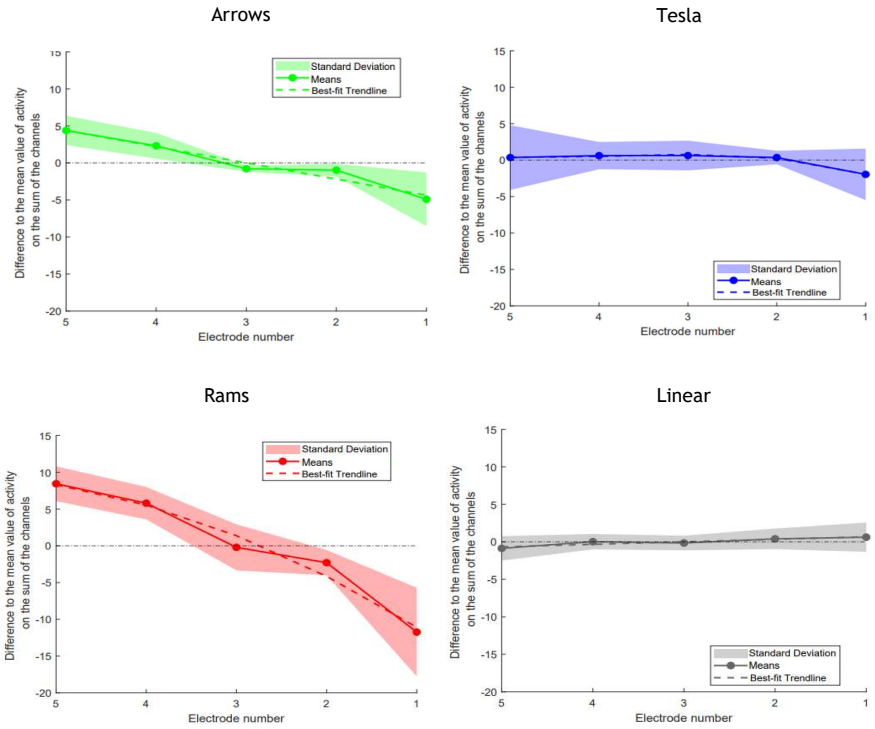

Figure IV.7 - Profile of activity inside the microchannels considering the sum on every channel on the corresponding electrode number for each of the designs. Each point is the mean of all recordings of that design post-DIV12 in its most mature state and there's a colorized information for the standard deviation across recordings. A best-fit regression was adjusted to the mean datapoints to get the corresponding equation for each design. The numbering of electrodes increases with the distance to "Source" population chamber.

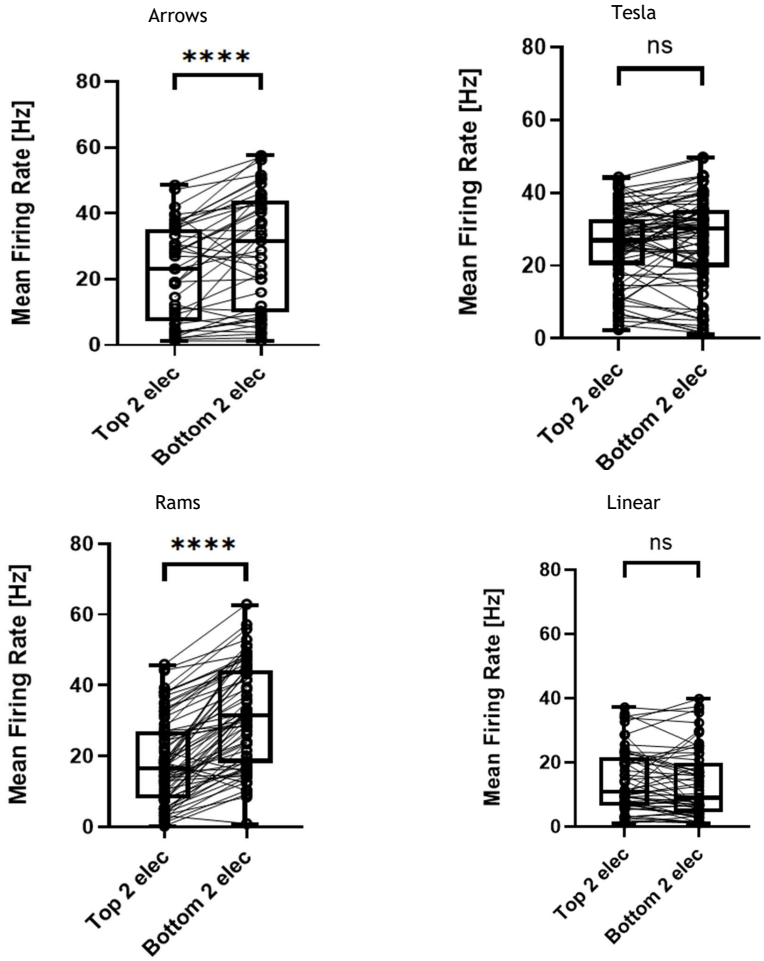

Figure IV.8 - Before-and-after plot of the Mean of the Firing Rate in Hz of the top 2 electrodes vs the 2 bottom ones on the microchannels. The data was pooled of all spontaneous activity recordings corresponding to the highest level of maturity of a given network. The distribution of the data is represented in the box and whiskers plot beneath it and recordings are each divided in its associated design. Regarding significance values, those were taken of the results of Wilcoxon Signed-Rank Test, whose test statistic is represented by W. The test was one-tailed and run with bottom 2 electrodes vs top 2 electrodes. Tesla had W = 671.0 and returned p = 0.0508, Arrows had W = 713.0, $p < 0.0001$, Rams had W = 2671, $p < 0.0001$ and the control channels had W = - 314.0, p = 0.1074. As for the median differences in the Arrows and the Rams which were the only significant differences found they had values of 5.790 and 11.54, respectively.

The graphs include also the calculation of a trendline for the data of each design in an attempt to get a slope value to compare the different designs. This best-fit approach tried to modulate the trendline of the data to a polynomial equation with a maximum degree of 3.

In this sense, the rams had a linear trendline with -4.85 slope (R^2 = 0.95) which was considerably higher than the -2.19 registered on the arrows (R^2 = 0.95). Interestingly enough, the linear channels had a slope of 0.34 (R^2 = 0.85), which considerably smaller than both others and, sufficiently low to be close to a constant value – what was first expected from a channel which has no factor to hinder axonal growth in whichever direction.

However, the R^2 value for a linear regression for the tesla was below 0.5, defeating the purpose of doing a quantitative evaluation of all designs through this methodology. Instead, the presented trendline for this design was of 3rd degree, making it much harder to do any comparison.

To this end of quantifying the structural blockage bias and the level of significance of their difference, the comparison of the mean of firing rate of the top 2 electrodes against the mean of the firing rate of the bottom 2 was performed for all channels which had means above 1 Hz.

Once more, tests for normality failed on some conditions, which is something to be expected in the cases where the structural blockage is effectively working, as lower levels of activity are more likely to happen then higher ones. The results of this trend of the backward blockage bias evaluation can be observed in Fig. IV.8.

The results were consistent with expectations: the controls did not exhibit any significant differences, while most asymmetric designs demonstrated evidence of inducing a bias in the communication within the microchannels. However, the Tesla design did not yield any significant changes, suggesting it may not be effective for the proposed blockage.

To actually get a better grasp as to how performance can be compared between designs, two other metrics were collected from this same data – the mean of the fold change of every bottom over top mean and the percentage of "blocked" channels across all considered channels on a recording. For a channel to be considered as having a "backward blockage bias" its' fold change value had to be higher than 1 (i.e., the mean of the bottom activity had to be superior to the one on the top).

These definitions mean that the expected values for the control are, on the average of the recordings, 1 for the mean fold change – the profile of activity on the straight microchannels should be close to homogeneous – and 50 % - half of the channels should show one type of directionality and the other half the other direction.

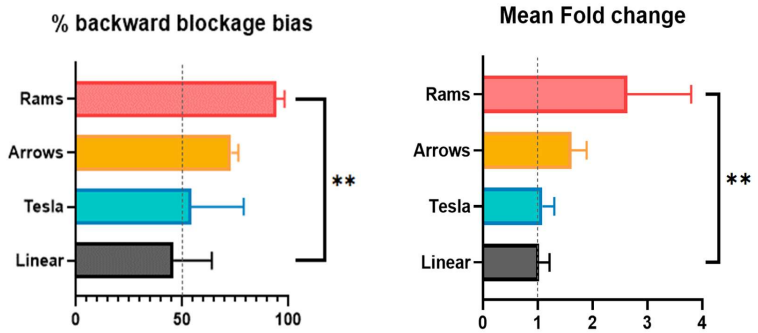

Figure IV.9 - Horizontal bar graphs presenting, from left to right, the percentage of the backward blockage bias and the mean fold change in the analyzed microchannels. The results presented correspond to the mean of the values obtained from each recording and the error bar corresponds to the standard deviation. The dotted line corresponds to what one should expect from the controls. On the left, the significance value, after the Kruskal-Wallis test returned p = 0.0002 and a statistic of 13.33, was taken from Dunn's multiple comparison with the adjusted p-value = 0.0016. Running a similar analysis on the right, the results were a p = 0.0006 and a statistic of 12.47 on the Kruskal-Wallis and an adjusted p-value of 0.0062 on the post-hoc analysis.

The results are presented above on Fig.IV.9. and what one can conclude, after running a Kruskal-Wallis and a Dunn's multiple comparison test, is that the Rams is the best performer, delivering both the highest number of channels with a blockage bias and the highest fold-change of bottom-to-top-activity. Moreover, these values are identified as statistically significant.

It was also possible to verify that the even if there looks like there's a difference on the Tesla and the Arrows vs the linear channels, those designs did not present a performance good enough to be considered a significant difference.

On the case of the Tesla, when grouping that with previous results, this probably means that their blockage factor is not that relevant, even if it's possible to get some cultures that present some type of bias. On the other hand, the issue with the Arrows could be derived from the fact that only 3 values are sampled for this analysis, which greatly reduces the chances of a statistical discovery to be found on this type of testing.

4.2 - Forward vs Backward spiking

Commented [PM96]: Adicionar aqui dados do TTX. "As a proof of concept we silenced one of the populations"

Then, the microchannels' activity was characterized. Initially, taking in consideration what had already been observed in the structural-anatomic studies, yet unpublished data, the idea was to avoid using electrodes associated with the asymmetrical designs, as those might have had very complicated axonal shapes, translating into complex dynamics on the activation of electrodes. This would add an extra layer of caution when creating a function identifying the directionality of the spikes in the microchannels.

Initially, forward spiking was defined as activity detected in the electrodes of the linear part of the asymmetrical microchannels closest to the "Source" population, while backward spiking was defined as the same sequence occurring in the opposite order. However, when analyzing control recordings with exclusively linear profiles, these definitions required reevaluation. It was expected that linear channels would exhibit a roughly 50/50 ratio of forward and backward events, as no structural elements favor a communication direction. Contrary to this expectation, some conditions showed a 70/30 bias towards forward spiking. This discrepancy might be due to an inherent bias in the analysis, where the "Source" population's axons needed to grow less in length than those of the "Target" population to be considered forward propagating events.

The final decision was, as mentioned earlier, to use all electrodes in the microchannels. As a proof of concept, to understand if what was being measured was axons of one population communicating with the other, the mean of the TTX recordings was compared to its pre-TTX spontaneous activity counterpart for the means of all DIV21 recordings of asymmetric channels, in terms of the percentage of PEs. The results are shown in Fig. IV.10.

Firstly, it is important to be reminded that TTX is a neurotoxin whose role on neuronal activity inhibition and its nearly 100% effectiveness have been well documented in the literature. Applying it on the "Source" chamber, meant the silencing of all activity related to this population in the 4 recordings, with 0 electrodes active on this module.

From the graph, it is also possible to observe that the use of this drug drastically diminished both the PEs originated by the "Source" population – its values where close to 0, as intended – but also the overall number of propagating events. This second finding implies that some of the neurotoxin might have flown in the microchannels. Finally, it's relevant to observe that the 99.999% mean of backward spiking on the post-TTX bar for the total of the analysed recordings validates the used method for the

evaluation of PEs in the microchannels, because the silencing of one of the populations meant the silencing also of the activity in the respective direction of propagation.

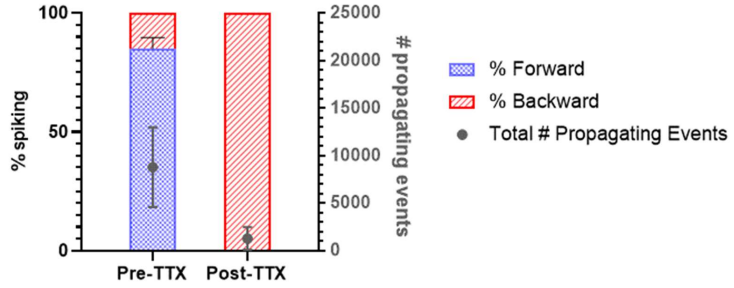

Figure IV.10 - Stacked bar plot showing the difference in the bias of PEs, comparing the mean of the spontaneous activity DIV21 with the mean of 4 post-TTX on asymmetric channel recordings. Note that there are some forward PEs occurring in these experiments, even if it's not observable here.

When the assessment of the results in certain studies to ensure that the developed methods were optimally translating data into meaningful outcomes was finished, results of the overall data could be verified.

It was interesting to notice the consistency across recordings on the activity on the microchannels, which was much more frequently happening on the "Source"-"Target" directionality than the other way around, regardless of the DIV or asymmetric design being analyzed. This is important because the microchannels are the only way the populations can contact with one another, so it's to be expected that this conditions the activity generated on the "Target" population as a result of the outputs of the "Source".

However, there was a need to quantify this bias. In a first approach, data of the count of each type of events pertaining to all recordings of each design was considered, as long as the sum of the number of propagating events in both directions was higher than 100.

To ensure comparability between different datapoints the values had to be normalized to percentages of the types of spiking activity. The graph produced on Fig. IV.11 represents the data as per its associated design.

The asymmetric designs had on average, at least, nearly 4 times more forward spiking than backwards and the controls had a mean of 56.66% of forward spiking, close to the 50/50 relationship one could expected from this design. The lack of normality found on the datasets enforced the assessment with a Wilcoxon Signed-Rank test on paired percentual data for each design to test for significant differences on the one-tailed difference between backward and forward propagating events.

The test, first, validated that the control channels, which had W = -64.00 and a p-value of 0.1227, had no significant difference in the type of spiking activity and likely the distinction observed might be a result of chance. On the other hand, all asymmetric designs presented considerable differences – Tesla had W = -136.0 and p-value lower than 0.0001, Arrows had W = -78.00 and p-value of 0.0002 and the Rams had W = -91.00 and p-value of 0.0001. The medians of differences values were -60.08, -71.60 and -85.30, respectively, showcasing again that there is inter-design performance variability.

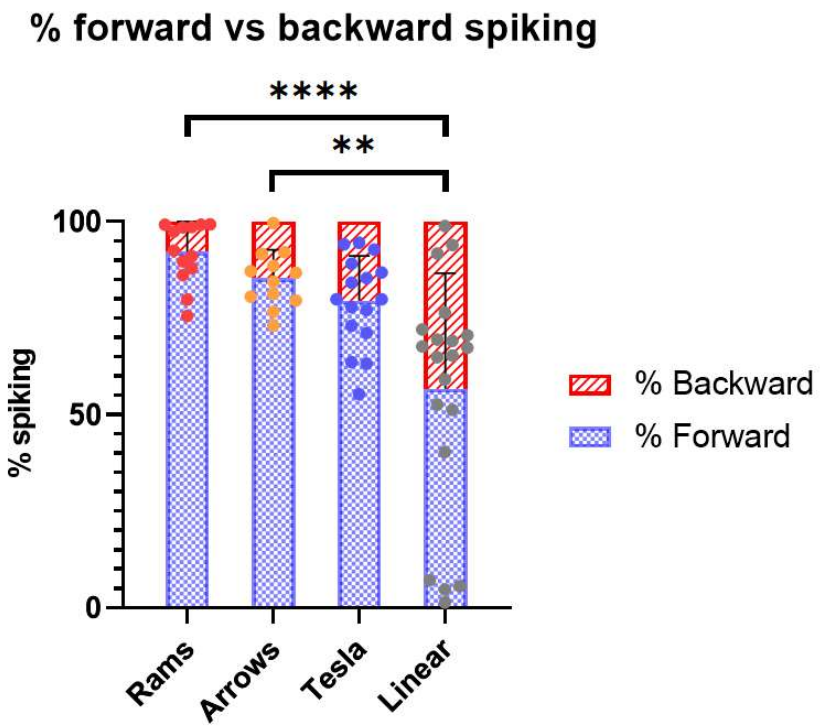

Figure IV.11 - Stacked bar plot showing the difference in percentage between forward and backward spiking events, across all recordings. The 10% electrode activity exclusion criterion was

Afterwards, a Kruskal-Wallis comparing the percentage of forward spiking of the different designs was run, returning a test statistic of 24.42 and an approximate p-value inferior to 0.0001, meaning the highest possible significance, and the results are shown in the graph.

The designs which had statistically relevant performances over the controls were the Arrows (adjusted p-value = 0.0048 and Z = 3.155) and the Rams (adjusted p-value < 0.0001 and Z = 4.723), as per the Dunn's multiple comparisons test.

Then it also matters to check how for each design did the bias changed across DIVs. Furthermore, intuitively, it's important to keep the data paired to consider the longitudinal analysis in the same culture, due to the networks' inter-culture variability.

The longitudinal analysis returned a lot of interesting insights, regarding many aspects of the communication and, particularly, about reproducibility.

Firstly, as with all previous analysis, some of the distributions analyzed here were not normal, so parametric tests were not performed. Another point was that, even if the means change a little across the timepoints, the Kruskal-Wallis tests on the 4 designs presented a p-value higher than 0.7, meaning that these differences might be related to chance. Moreover, after visual analysis of the percentage changes on different recordings what is observed is that they do look very similar across the different timepoints.

This is an important insight as the bias remains very similar at different timepoints, regardless of the increase on the number of propagating events, in general terms, observed between DIVs 12 and 17. It also led to the conclusion that maturation of the axons does not present any kind of turnover which reflects on the bias of the signal propagation.

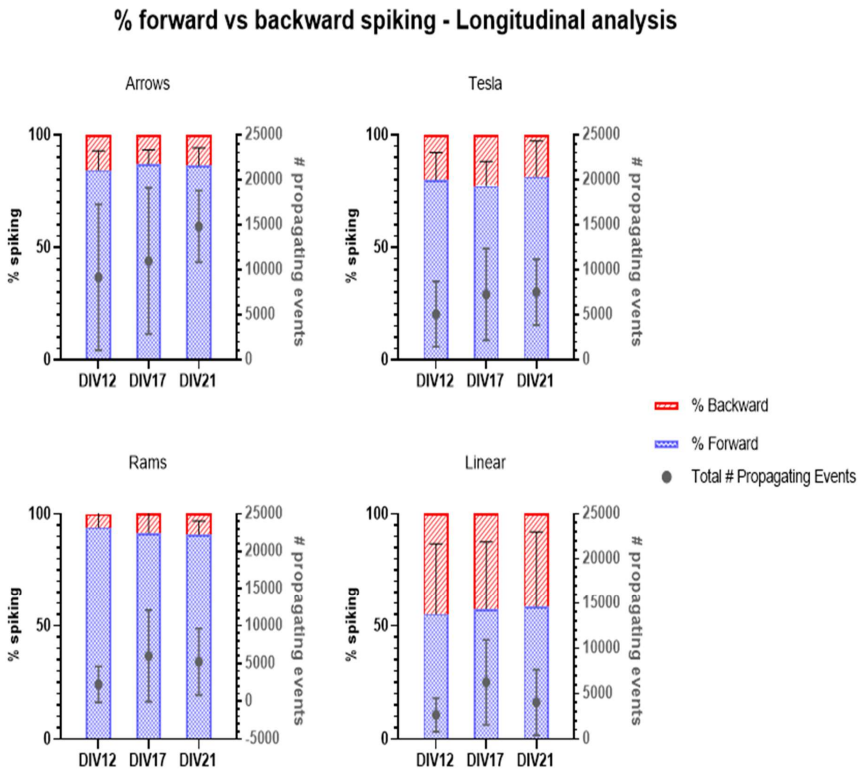

Figure IV.12 - Results of the longitudinal analysis of the percentage of spiking propagating events in the microchannels are presented in the vertical stacked bar plot. The values of the percentages are divided according to their respective DIV and associated design and plotted against the left y-axis. On the right Y-axis, the number of propagating events of is presented, considering its mean and its standard deviation, in each timepoint. Although statistical tests were run, there was no significance finding to report on the Kruskal-Wallis tests evaluating distinctions on the percentage of forward spiking across time in a said design.

4.3 - Stimulation-Driven Interpopulation Neural Dynamics

Population Driving Events are defined as the NBs on one population which have a [20, 240] ms delay to NBs on the other population. The defined window of causality was based on the current literature [24]. The first value is higher than 0 as it's an estimation of how long it could take from a

NB to start in one population, it being in full swing while it also starts being conducted by the axons on the microchannels and, finally, originating a NB-like activity on the driven population. On the other hand, 240 is set as the end value to refrain from considering events whose delay is far too long to infer any causality.

Commented [jo97]: Referir que baseámos na literatura para chegar a esta window

Commented [PMPTdM98R97]: Certo, referenciado !

In a first instance, it was relevant to study the ability of the cultures to do information transmission from population to population through NB-like activity, resorting to electrical stimulation. This analysis serves a proof of concept that population-to-population communication might be a result of higher synchronicity events.

By doing stimulation recordings' preliminary analyses, by visual assessment of the peri-stimulus heatmap of the summed firing rate vector, it was possible to confirm that, indeed, electrically stimulating one population allowed for, in some trials, a response in the other. This fact is also observed on the stimulation-trigger averaging plot on Fig. III.16.

Nonetheless, as already described in previous sections, what is needed here is to figure out how it could be translated into a quantitative analysis, as three relevant questions of the principles of neuronal communication had still to be answered, before any following analysis on the population-to-population communication of the recordings of spontaneous activity:

1) the longitudinal analysis of this connection's strength – is the strength of the connections between the two populations changing over time?
2) the conditioning factor of the designs on creating a preferably unidirectional type of communication – are the propagating events on the microchannels and its observed bias replicated on the communication between neuronal populations?
3) the conditioning factor of the designs and whether different designs result in different effectiveness in communication – are the different designs associated with different performances on this type of communication too?

After stimulation, the approach involved examining how the mean of the summed firing rate vector of the non-stimulated population changed in 5ms bins within the [20, 240] ms window.

The only asymmetric design for which he had 3 instances of time (DIV 12, 17 and 21) in recordings with stimulation was the Rams, thus this data was used to perform a longitudinal study. The pre-established concept was that, over time, the strength of the connections between the networks would grow, reaching a peak.

The results on this can be observed in Fig IV.13. On both populations, the given culture would start with the lowest response ratio on DIV12, reach their maximum at DIV17 and fall down at DIV21.

Nevertheless, these results also hinted at the fact that stimulation of the "Source" population produced more frequent and overall stronger response in the "Target" population, proving there is some functional blockage by the Rams. As such, the fidelity for each of the represented recordings was calculated.

To ensure fairness, equivalent peri-stimulus heatmaps for the stimulated population were created to visualize whether stimulation was, in fact, consistently triggering NB-like activity, which it did for the recordings presented in the Fig. IV.13.

Despite these recordings and what resulted from similar analysis like Fig. III.16 on these same experiments, neuronal cultures did not respond to electrical stimulation on every trial. Therefore, due caution should be taken for the sake of comparability in what concerns to the analysis of propagation events on stimulation recordings.

This meant that fidelity metric evaluation needed a first step of understanding what trials of the non-stimulated population were associated with a response on the stimulated population to stimuli, to consider a propagation.

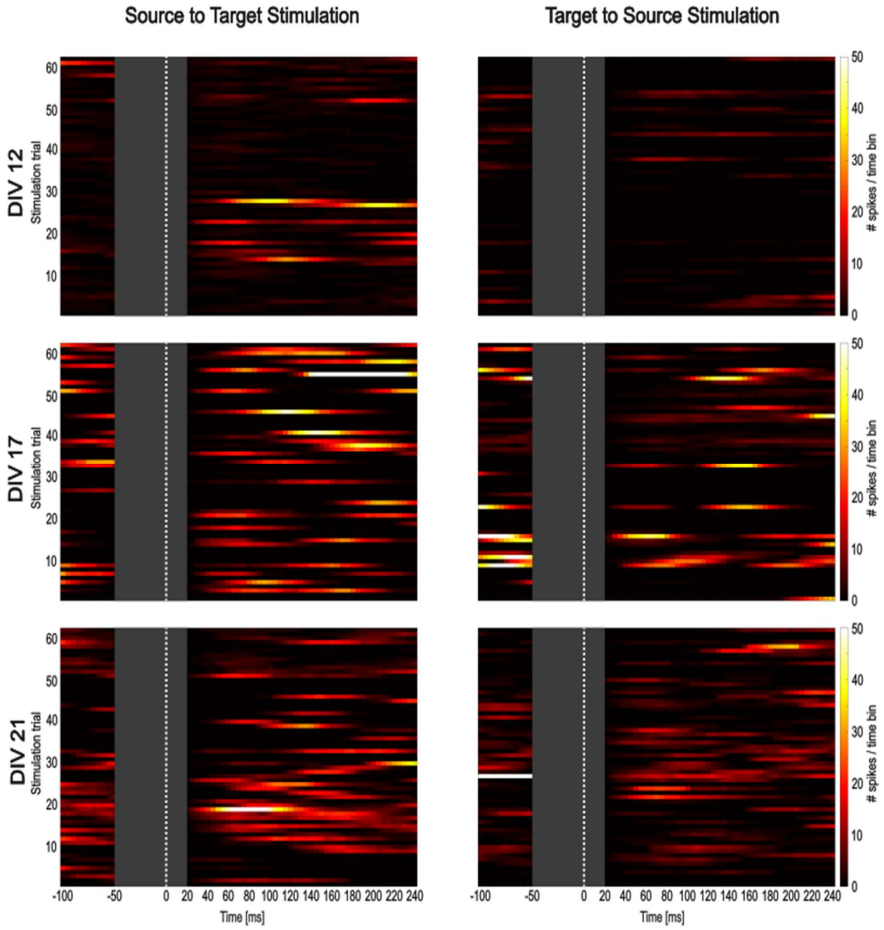

Figure IV.13 - Peri-stimulus (marked with the dotted white line at 0 ms) heatmaps of stimulation recordings at DIV12, 17 and 21 with a Rams design in the microchannels. On the left, the recordings correspond to the evaluation of the "Target" population's response through the outputs of a stimulated "Source" population and, on the right, the populations' roles are reversed. The grey area corresponds to an area of the heatmap which would draw on spike data that had to be removed because it was related with the stimulation artifact.

Two fidelity values were then calculated for each recording, one related to the stimulation response of the stimulated population – fidelity of stimulation response – and a second related to the non-stimulated response of the stimulated population' outputs – fidelity of propagation. The first is a ratio of how many of the stimulation trials generated a NB-like activity. A list of the trials number

which passed the 15 spikes set threshold is recollected. Hence, the second is the index of how many of these NB-like events induce a response on the target stimulation.

As it can be seen in Fig IV.14, the visual assessment of the previous figure is confirmed and there is, indeed, a functional bias as per validation through this measure.

To have, however, a better comprehension of the ability to communicate evolves throughout time, in future work one should focus on having other datapoints valid for analysis which are associated with other designs.

Likewise, graphs like the one on Fig. IV.14 are also good at providing proof that asymmetric designs might be effectively hindering population-to-population signal on the expected directionality, as proven by a one-tailed paired t-test of the "Target" population stimulation vs "Source" stimulation, with a value of 0.0185.

Hence, light begins to be shed on the two posed questions on the beginning of this chapter, as evidence of time changes in the ability of neuronal communication are found, alongside with the functional blockage factor on what has been so far the best performer at hindering axonal growth in the undesired directionality.

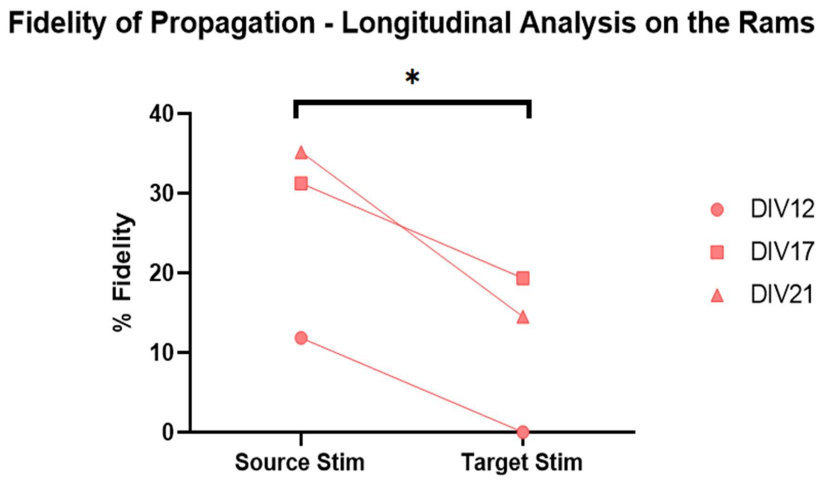

Figure IV.14 - Before and after plot of the fidelity metric for the recordings of a Rams experiment. The 3 datapoints are presented with the values of the corresponding stimulation protocol paired. After validating the normal distribution with a Shapiro-Wilk test, the pairs were run using a one-tailed paired t-test, which resulted in a p-value of 0.0185 and a means difference of -14,81 between "Target" and "Source" stimulation values. The 95 % confidence interval was [-27.42, -2.93].

Furthermore, it was important to see how the remaining designs performed and if there were significant differences in their performance. Moreover, for all asymmetric designs, the same datapoint - the DIV21 experiment with stimulation - was used for the comparison. Once more, this analysis further corroborated the microchannel asymmetry as a blocking factor. All recordings which had on both populations' fidelity of stimulation response higher than 50% were taken into account.

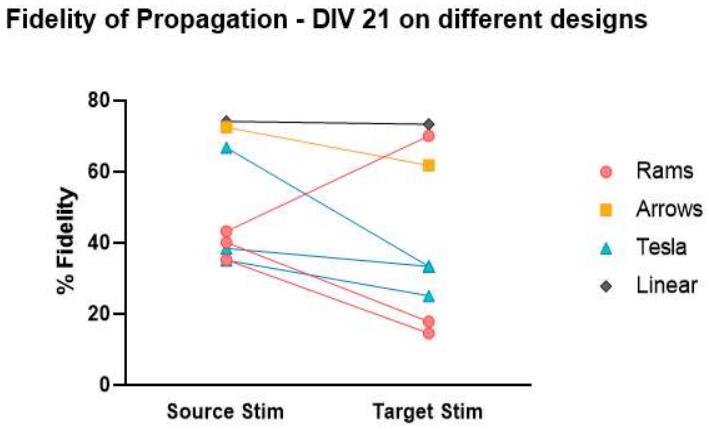

Figure IV.15 - Before-and-after plot of the fidelity metric for the recordings at DIV21 of the different designs. The sample size on this experiment was prohibitive for statistical analysis, so no data regarding that is presented.

As per what was to be expected, one can visually assess that not all asymmetric designs seem to show a considerable difference, as it can be observed in Fig. IV.15. Yet, the lack of a significant sample power for this graph prevented the discovery of any insights, because of inter-culture variability. For instance, in both Tesla and Rams which had 3 cultures, one of the recordings looks like an outlier when compared to the other two, as they seem to have a consistent slope except for those ones.

Finally, to ensure that the functional bias achieved here was a result of having asymmetry in the microchannels, control experiments were made with all linear channels. These do not have any reason to show unidirectionality, unless it's imposed by the way the populations connect with each other spontaneously as no structural factor motivates it. Those were also included in Fig. IV.13 and show very similar values on both conditions. Here, the remaining two cultures had to be removed from analysis as they had nearly 0 values of fidelity of stimulation response on "Source" population stimulation.

In the end, this concludes the analysis as the third and final question gets answered as best as possible with the given recordings – the functional blockage observed in the previous section which was different on the different manifests in a not so significant form here in the population-to-population propagation.

Lastly, after careful analysis of the fidelity of stimulation response on the recordings of asymmetric designs which shown a relevant percentage of forward spiking bias on the microchannels, one could observe that, while for "Target" stimulation the ratio would consistently be 100%, "Source" stimulation always had smaller values.

In other words, "Target" stimulation seemed to always elicit NB-like activity, a result which was not found on "Source" stimulation. It was, therefore, hypothesized that it could have a relationship with the synaptic activity in the "Target" module, either an increase in excitation synapses or a decrease in the inhibition ones. In fact, results on Fig. IV.14 are consistent with immunostaining

findings done on recent studies, corroborating the latter [79]. This emphasizes the need to, on further studies, do phenotypical analysis of the cultures explored.

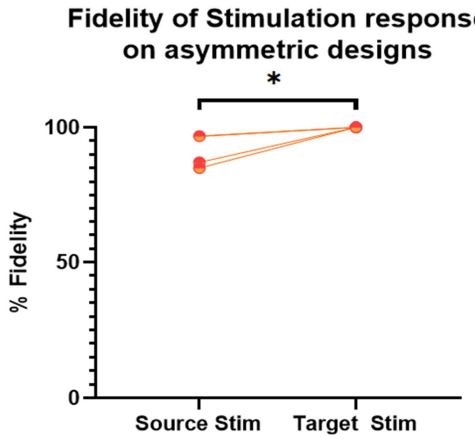

Figure IV.16 - Before-and-after plot of the fidelity metric for the recordings at DIV21 of the asymmetric designs which had already shown to act as functional blockers meaning the Arrows and the Rams. The data followed normal distribution as per the results of the Shapiro-Wilk test. Then, a paired t-test is run resulting in a p-value of 0.0348 for the one-tailed difference of "Target" Stimulation vs "Source" Stimulation values. The mean of differences was 8.615 and the 95% confidence interval [-1.282, 18.51].

4.4 - Forward vs Backward Population Driving Events

Finished the proof of concept by ending the analysis on the stimulation recordings, it was relevant to define if it had a parallel with spontaneous activity. So, here, the spontaneous activity recordings are studied in what regards to NB-like activity of one population generating the same type of activity on the other.

Commented [jo99]: Acho que isto merece o seu sub-chapter próprio

Commented [PM100R99]: Dividi em 2 subchapters diferentes a análise com estimulação e da atividade espontânea

For the spontaneous activity recordings, the lack of indirect forms of electrical stimulation allowed for detection of NBs to be performed on more conventional ways. In this case, as previously mentioned, these synchronous events were detected using a custom variation of the Pasquale's method [49].

Once more, the propagation was evaluated inside the [20, 240] ms window, but on this type of recordings, considering the delays between NBs of both populations. As such, what was taken into consideration here was the percentage of NBs which elicit a NB response on the other population over the total number of events on the first. This analysis considered both the forward and backward PDEs.

On the initial studies, every recording was considered whenever the previous established inclusion criteria, pertaining to the percentage of active electrodes and the number of events on the microchannels, were met.

Taking into account the overall of the forward vs backward PDEs, the Shapiro-Wilk normality test run returned all conditions as non-normally distributed, meaning the data had to be analyzed with a Wilcoxon Signed Ranked Test in the pairs and then a Kruskal-Wallis should be implemented to compare the inter-design performance, if the one-tailed p-value associated with the backward vs forward events difference is significant.

The only design which presented a significant difference was the Arrows, with a p-value of 0.034 and a sum of signed ranks equal to -66.00 and a median of the differences = -6.680. This meant that comparison between designs wouldn't make sense in these conditions. But soon it became clear that some type of filtering or exclusion criteria must be considered to get any insights on this type of population-to-population communication.

One important thing to beware of regarding this test is the fact that their intrinsically dependent on how well the NB detection algorithm performs and it's undeniable that some cultures NB activity was not described as well as it should have been for this assessment to be made unequivocally, particularly when inter-culture variability plays a huge role.

Another important disclaimer is that chance level is directly linked to the number of NBs of the driven population, as it increases the likelihood of there being a small delay between NBs in both populations without the existence of causality. Since there's some variability in what concerns to the number of NBs in different recordings, to ensure meaningful comparisons in the analysis, further studies should include a chance level indicator for each recording. Moreover, it is interesting to note that there were no significant differences detected on the number of NBs between "Source" and "Target" population, hence, no bias should be created in the results.

Therefore, considering that the goal is to consider the bias in a type of communication which should be predominantly but not exclusively unidirectional, datapoints for which at least one of the type of events was not occurring were discarded. Even with this exclusion criteria, there was a minimum of 6 recordings for each design, so the studies still have enough statistical power for conclusions to be significant. The data is plotted on Fig. IV.17.

The data remained not normally distributed, however, at this point, the results of the Wilcoxon Signed-Rank test were better aligned with what were the expectations, with significant differences for the asymmetric designs except for Tesla and no bias detected on the linear channels.

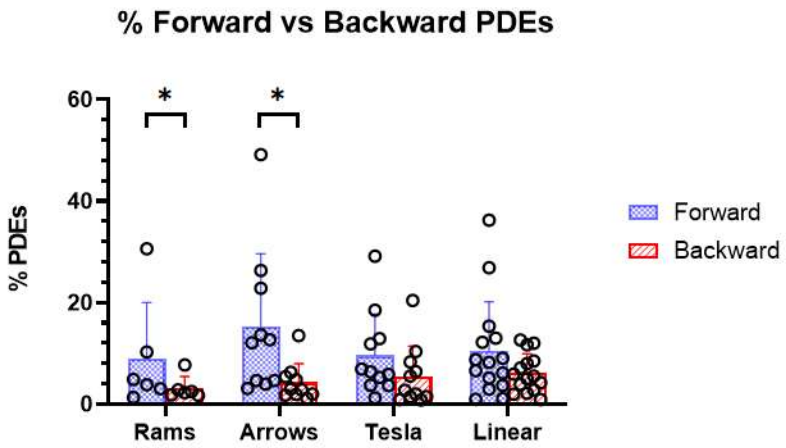

Figure IV.17 - Side-to-side bar plot showing the difference in percentage between forward and backward PDEs, across all recordings. All the inclusion and exclusion criteria were kept.

Firstly, on the Rams, the p-value was 0.0469, the sum of signed ranks = -17.00 and a median of differences of -2.325. For the Arrows, the p-value was 0.0137, the sum of signed ranks = -43.00 and a median of differences of -6.535.

Similarly to what had been done on the percentage of events on the microchannels, it also matters to check how for each design did this bias changed across DIVs. Once more, paired nature of the data must be taken into account on the longitudinal analysis reproduced on Fig. IV.18.

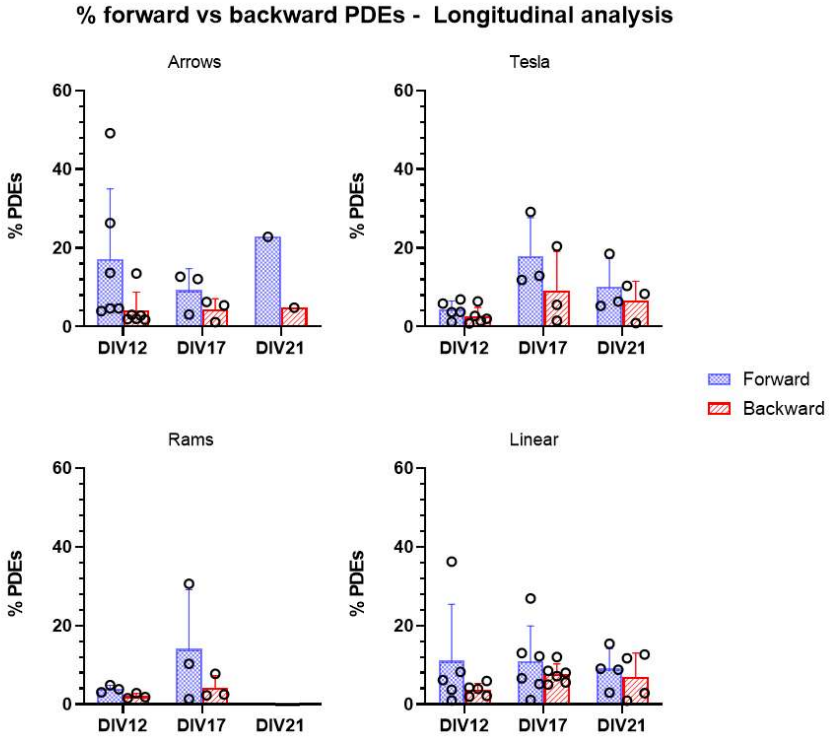

Figure IV.18 - Results of the longitudinal analysis of the percentage of population driving events (PDEs) are presented in the side-to-side bar plot. The values of the percentages are divided according to their respective DIV and associated design and plotted against the left y-axis, considering their mean and standard deviation, in each timepoint. Although statistical tests were run, there was no significance finding to report on the Kruskal-Wallis tests evaluating distinctions on the percentage of forward activity across time in a said design.

The first insight one can take from these bar plots is that, as opposed to what had been seen on the microchannels activity regarding the observable changes in the mean across time, here the time factor seems to be more important than on the microchannels, with greater variations through time.

However, that was not the case, when statistical analysis was performed. Firstly, as with most of previous analysis, some of the analyzed distributions were not normal, so parametric tests were discarded. Much like the analysis of events on the microchannels, Kruskal-Wallis tests on the 4 designs presented a p-value higher than 0.7, attributing to chance the differences observed. Future work should increase the number of evaluated cultures to ensure if the given changes across time are, in fact, not related with the lack of statistical power in a dataset that is for already presented reasons very variable of itself.

4.5 - Delays of the Population Driving Events

Lastly, on the assessment of the population-to-population communication on spontaneous recordings, a relationship between the asymmetric designs and the delay between a driving NB and response seemed to emerge as one can observe in Fig. IV.19. Indeed, it would make sense to have on the asymmetric designs, a higher delay for the backward events as they had to surpass the blocking factor on that directionality, due, not only to a lesser number of axons expected to reach the other population but also to the fact that they need to travel a greater distance (i.e. has to go through twists and curls).

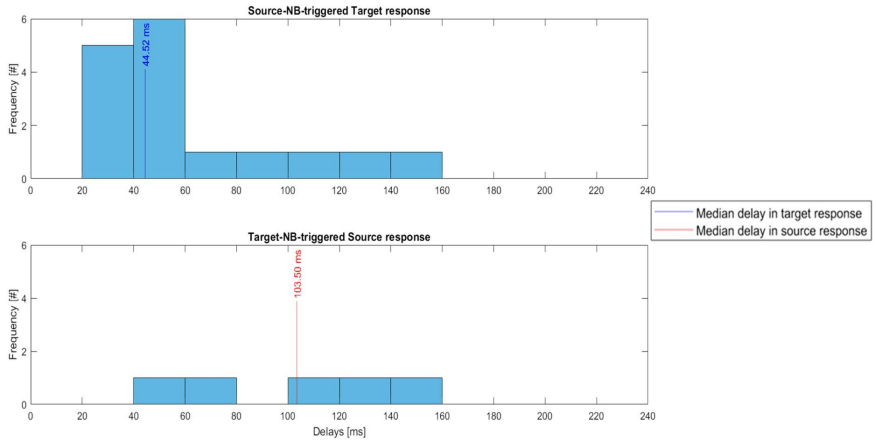

Figure IV.19 - Histograms of the delays of Population Driving events for a recording with asymmetric channels. On top, the representation for forward PDEs and, on the bottom, for backward events. In each histogram, a colored line is represented showing the median of the total delays.

The histograms of the delays of PDEs are an important tool on the characterization of the population-to-population communication, because not only do they show, for most recordings of the asymmetric channels, a higher number of forward events than backwards, but also display a lower median time for response in forward events.

Hence, for the data used for the last analysis, the median time values for both forward and backward events were taken and the framework of statistical testing reproduced, starting with an overall pool of the data and, afterwards, a longitudinal study.

Before stepping into to the observation of the results, it's of utmost importance to recall the impact the performance of the NB detection has on the data. Alongside, the already presented points, in this study, the temporal precision of the algorithm is increasingly more relevant, since events are in the [20,240] ms window and so their difference, if it exists would be most likely in the order of dozens of milliseconds.

The first results are presented in Fig. IV.20. Visually one can quickly assert that for the data in the graph there's no relationship between the delays of one type of event vs the other, regardless of the design.

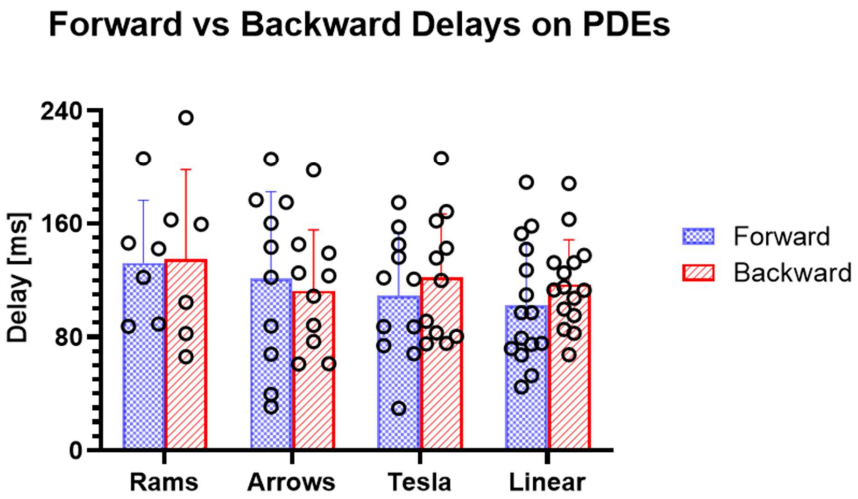

Figure IV.20 - Side-to-side bar plot showing the difference in delays between forward and backward population driving events (PDEs), across all recordings. All the inclusion and exclusion criteria were kept.

The statistical results corroborate it – the Wilcoxon Signed Rank test resulted in p-values over 0.35 for all designs for the one-tailed difference between forward and backward PDEs. As such, no Kruskal-Wallis test was performed. Note that, once more, normal distribution assumptions could not be made.

Nonetheless, one should beware that for recordings annotated as of perfect or particularly good NB detection – as per visual assessment by the author -, indeed, were better at revealing the expected bias, meaning that likely the results would have been more aligned with expectations, in case the algorithm of NB detection had a better performance. Therefore, further studies should take this in consideration.

Finally, as for the longitudinal analysis, it is displayed on Fig. IV.21. Here, after confirming non-normal data distribution, Wilcoxon Signed Ranked tests were run comparing forward and backward delays and did not result in any findings, meaning there's no statistically relevant relationship on their difference.

In the end, inter-culture variability and the sub-optimal performance of the NB detection algorithm on some of the recordings rendered a putative relationship between the delays of the two distinct events impossible to discover.

Furthermore, further studies should focus on increasing the sample size for every datapoint to make sure that there's enough statistical power to either validate or decline the proposed hypothesis with a greater certainty. Alternatively, other NB detection algorithms could be tested to see if they deliver a performance which makes the use of the current data more useful in finding this interplay between the times of the neuronal populations.

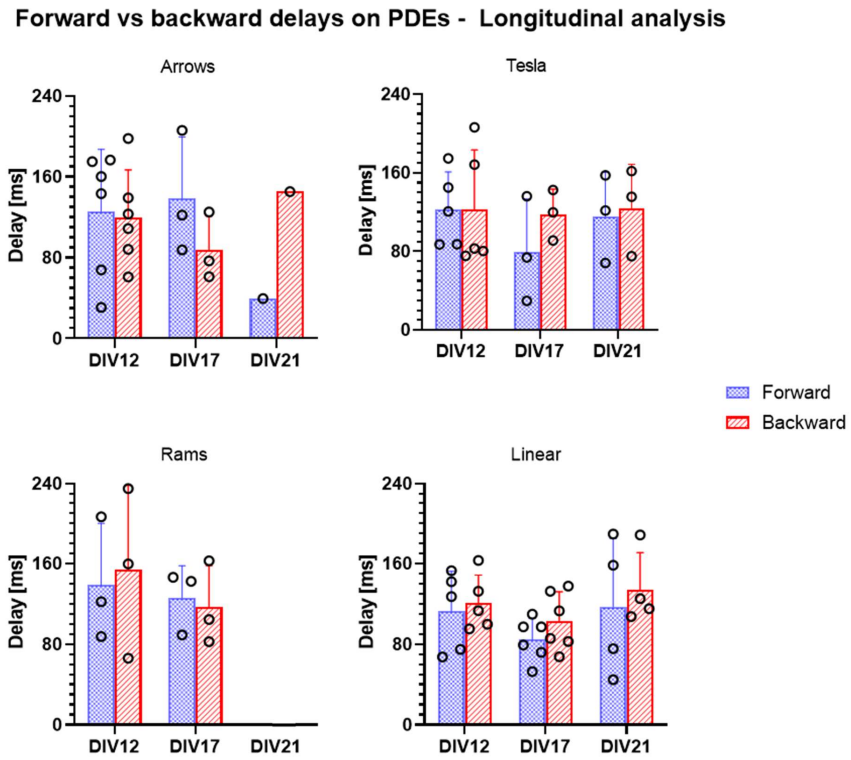

Figure IV.21 - Results of the longitudinal analysis of the delays of the types of PDEs are presented in the side-to-side bar plot. The values are divided according to their respective DIV and associated design and plotted against the left y-axis, considering their mean and standard deviation, in each timepoint. Although statistical tests were run, there was no significance finding to report on the Wilcoxon Signed Ranked tests evaluating the differences of forward vs backward activity across time in any design.

Chapter V

Conclusions

Commented [PMPTdM101]: Here I present the conclusions in a very general way… probably once I'm finished with the results, I'll add a few extra pragraphs for that

Commented [jo102R101]: Sim, tens mesmo de fazer isso para destacar os resultados principais

The comprehensive study of the brain is seldom done considering the whole system, due to its complexity. As a result, functional studies of the nervous system are broken down in bottom-up approaches where the main goal is to understand the behaviour of different neuronal and glial cells and how they work together to form cohesive and responsive networks.

In vitro technologies appear as an alternative by offering a controlled and accessible environment which mimics *in vivo* systems with a sought-after simplified complexity. In fact, the combined use of Microfluidics and MEAs grants researchers a platform for the study of modular neuronal networks, by reading the electrophysiological behavior of the cells in a controlled environment.

Throughout this study, the importance of these technologies in providing complex yet valuable data is recurrently emphasized, while also highlighting the interest in developing novel algorithms and strategies to get the most out of it. The state-of-the-art research has laid the groundwork on creating meaningful metrics, descriptive of the neuro-electrophysiological activity of the cultures and their dynamics across time. Moreover, in the literature it was possible to observe the purpose of establishing a relationship between metrics and functionality, shedding light on how functional neuronal communities are activated in bursts, seemingly the most relevant factor in population-to-population neuronal communication *in vitro*. The value of these technologies in delivering intricate yet useful data is frequently underlined in this study, along with the need to create cutting-edge algorithms and tactics to maximize their potential. The foundation for developing relevant metrics that describe the neuro-electrophysiological activity of the cultures and their dynamics over time has been established by sem ser kresearch. Moreover, in the literature it was possible to observe the purpose of establishing a relationship between metrics and functionality, shedding light on how functional neuronal communities are activated in bursts, seemingly the most relevant factor in population-to-population neuronal communication in vitro.

Indeed, this thesis' main goal on the development of software tools aimed at decoding the electrophysiological communication between segregated neuronal populations and tailored for analyzing action potential propagation within single cells and its relationship with network-wide communication has been achieved, as recordings associated with different µEF designs on the microchannels connecting them have been promptly characterized. As such, it was relevant to

describe the influence of these distinct structural motifs on the networks' behavior and, on the other hand, the correlation between population-level and axonal activity in these different settings.

The implemented methodologies allowed to validate the significance of network architecture in determining the efficiency of neuronal communication. Through rigorous computational analysis, it was demonstrated that the use of asymmetrical designs successfully created an effective functional bias in communication between populations.

At first, the analysis of the spiking activity along the microchannels demonstrated the effectiveness of asymmetric microchannel designs in creating a functional bias, when considering that asymmetric designs exhibited nearly four times more forward spiking than backward spiking, while control channels displayed something close to a 50/50 distribution. The Rams and the Arrows significantly outperformed the controls, in terms of the percentage of forward spiking, as per statistical results. Longitudinal analysis across DIVs 12, 17, and 21 revealed that the forward spiking bias remained consistent over time despite an increase in the number of propagating events. This consistency highlights the reliability and reproducibility of the induced functional biases in asymmetric designs for long-term experiments.

Additionally, higher synchronicity events, such as NB activity, provided further insights, in terms of the studies of population-level neuronal communication under both stimulated and spontaneous conditions. Significant findings about the nature of neuronal interactions were revealed.

For the stimulated condition, visual assessments and statistical analyses confirmed a functional bias, with asymmetric designs effectively promoting the expected directionality of signal propagation. This was evidenced by significant differences in the chance of propagation between the "Target" and "Source" populations. The analysis included a longitudinal component to assess how communication evolved over time, where, the "Rams" proved to have a higher chance of having a propagation event on "Source" stimulation (i.e. source-to-target propagation) than on the "Target" one (i.e. target-to-source propagation), providing a strong indication of the effectiveness of this asymmetric design in modulating population-to-population neuronal communication.

Comparative analysis of different designs at DIV21 further supported the conclusion that microchannels' asymmetry functions as a blocking factor, even if the lack of additional points prevented the discovery of any statistical significant result. It reinforced, nonetheless, the notion that asymmetric designs have the ability to hinder undesired directional growth and maintain a functional bias over time.

Finally, when considering the communication through PDEs, significant differences were also found for the "Rams" and the "Arrows", indicating a forward PDEs bias. In the end, the "Rams" design was shown to be the most successful in the majority of direct and indirect metrics of functional blockage, indicating that it might offer a superior choice for enforcing a favored path for information flow in neural transmission.

These results pave the way for a more in-depth comprehension of the signal propagation and interdependency of firing units: at the cellular level, relating to soma-axonal interplay, and at the population level, understanding network dynamics. Details on how structure factors in on the propagation of APs have been uncovered too – for the different tested designs, the results show different levels of efficiency on their capability to block neuronal population-to-population communication. Then, the "Rams" was proven to be the most effective of all the tested designs on most of the calculated metrics.

Furthermore, it's important to note the clinical relevance of the work done and the role it might play in exposing neuronal circuitry dynamics changes that can be linked to neuropathophysiological conditions. Considering recent studies' assessment of how symptomatology manifests only after the

neuronal networks are damaged beyond repair, this type of analysis becomes paramount to better grasp how neuronal communication alterations might reproduce in observable symptoms.

In summary, this thesis brings about trends in neuronal signal transmission, thus contributing to the ever-growing pool of knowledge pertaining to neuronal circuitry and, particularly, to neuronal networks established using "brain-on-chip" technologies. It offers insights into their strong suits and associated challenges, but also about potential for further exploration – read the following *Further studies* subchapter. As the neuroscience field keeps growing, these techniques will play a pivotal role in unveiling the mist in which brain activity is still shrouded in and in pushing forward clinical interventions for neuropathies.

5.1 - Further studies

Although the project has been successful in delivering advances on the current understanding of neuronal communication while providing valuable insights into the dynamics of neuronal network interactions, there are still a number of directions to investigate. Focus on extending these findings on several avenues for further exploration must be done to build upon the groundwork laid by this study.

Firstly, improvements can be done on the technical part of the presented implementation, namely, in what regards to NB detection. In here, only rather simple adaptive threshold-based methods were tested and selection of the one of Pasquale was based off performance. Had time not been a constraint and more methods of NB detection could have been tested, particularly machine learning and deep learning approaches, with the goal of making detection more robust and reliable on the more complex dynamics of particular *in vitro* neuronal cultures.

On the other hand, complementary studies could be of use. For example, single-cell RNA sequencing techniques to obtain a more thorough characterization of the neuronal populations involved in the recordings is one avenue for additional research. This method would specifically assist, for example, in figuring out what proportion of excitatory and inhibitory neurons are present in each recording, which could be responsible for a degree of culture-to-culture variability. Deeper understanding of the underlying mechanisms of neural communication may result from a knowledge of the distinct contributions made by these various neuronal phenotypes to the observed network dynamics and functional connectivity patterns.

Recently, the emerging field of protocols related with differentiation of induced pluripotent stem cells (iPSCs) has shown promise in controlling excitatory-inhibitory balance in *in vitro* neuronal cultures, by conditioning the phenotype of those same cells [80], [81], [82]. Thus, researchers are able to define proportions of excitatory and inhibitory neurons on their networks, which, in turn, enables to study the effects of their compositions on network behaviour and neuronal communication. One must also weight in how such controlled environments can help on building pathophysiological models of neurological disorders characterized by imbalances in excitatory and inhibitory signalling, adding on the clinical value of this work.

Likewise, investigating the function of non-neuronal cells in the workings of neural networks offers still another important line of inquiry. In general, primary cultures are not exclusively composed by neurons, meaning glial cells (e.g. astrocytes) are also in the experimental setup. Nevertheless, their functions in regulating neuronal activity and maintaining network integrity may become clearer, if studies were conducted adding an extra layer of complexity to the setup with an astrocytic module. Hence, the addition of these cells to said structure will enhance the comprehension of larger cellular

connections in the nervous system and how they influence neuronal function and connectivity, by having them in co-cultures.

This becomes particularly relevant in a neuron-centric perspective most common in the field of neurosciences, where most studies are exclusively done in neurons or with neuronal cultures which do not discriminate what types of cells are there.

Moreover, it is interesting to think that, analogously to the tests done on this thesis with TTX for the blockage of neuronal activity, there are other chemical compounds, such as Temozolomide, Cytarabine and 5-Fluorouracil, which have been shown to diminish astrocyte proliferation and inhibit their activity [83]. Manipulation of the system with conjugations of these drugs might reveal a lot about how their activity interplays and what is the impact of not neglecting the characterization of the astrocytic activity in most neuronal culture studies.

Indeed, recent studies have shown that in *in* vitro chemically induced epileptic-like conditions in neuron-astrocytes co-cultures, the latter present a protective function of the neuronal firing patterns [84], once more, highlighting the need for this kind of translational research.

Please note that, calcium imaging studies, which are frequently used for characterizing these cells' activity, are also associated with the analysis of spiking activity. More often than not, the type of analyses run on calcium imaging are very similar in nature as the one implemented here for the NB activity of neurons. Furthermore, the metrics which were taken from the recordings of spontaneous APs in neurons, for instance, the ratio of events propagating after a trigger, have a parallel in this second type of studies. Minor adaptations to the software developed as part of this project might make it fit to recollect relevant information from this data.

It is also imperative that computational techniques for data integration and analysis continue to progress. Increasing the complexity of techniques for feature extraction and network connection analysis will enhance the analytical power to process multi-scale neural data. Even if this kind of work was implemented on this thesis, only by developing on the groundworks stablished here can one get a more complete knowledge of neural communication and the complex patterns within neuronal networks by integrating additional data at the molecular, cellular and network levels. It would be interesting to explore the ability to perform online spike sorting of axonal conduction signals, thereby enabling the use of closed-loop experiments, and, for clinical settings, understand how to perform connectivity inference to prevent/act on neuropathology patients. Likewise, within the context of this work, it would be beneficial to correlate the activity of specific electrodes or network bursts (NBs) with the initiation of propagating events, either in the microchannels or in the other population.

Additionally, implementing burst sorting or other types of spatial profiling of MEA activity, like the one initiated on Fig. III.18, would provide deeper insights into the spatiotemporal dynamics of neuronal networks. This approach could help identify distinct patterns of activity across different regions of the MEA, revealing how localized bursts of activity contribute to overall network behaviour. Such detailed analyses are essential for understanding the functional organization of neural circuits and could lead to the development of more targeted and effective interventions for neurological disorders.

Longitudinal studies on network dynamics represent another important area for future research. By tracking the evolution of neuronal interactions through time, researchers can identify long-term patterns and potential shifts in network functionality, especially under different physiological and pathological states. These studies will provide valuable insights into the stability and plasticity of neuronal networks and their relationship with structural motifs.

In the end, the fundamental findings, product of this study, can be translated into clinical applications, which in turn means there's a need to integrate them alongside known disease models.

Commented [jo103]: Acho que só deves referir isto na discussão

Commented [PMPTdM104R103]: Passei para aqui, parece-te um local válido para estar?

Commented [jo105]: Esta frase aparece sem grande contexto... Talvez esteja melhor na discussão/perspetivas futuras

Commented [PMPTdM106R105]: Passei para lá

Utilizing these models to study the alterations in neuronal communication associated with specific neurological disorders could help identify potential biomarkers related with the neuronal function. For example, in models of Alzheimer's disease, aberrant neuronal communication patterns, such as disrupted network synchronization and altered spike propagation, could be investigated to identify early biomarkers for cognitive decline. By understanding these alterations, targeted therapies could be developed to restore normal communication patterns and potentially slow the progression of the disease [85], [86].

This will contribute to the development of strategies aimed at mitigating the impacts of these disorders on neuronal networks, ultimately paving the way for new therapeutic approaches.

By pursuing these further studies, researchers can continue to deepen their understanding of neuronal communication and increase the impact of the current studies on clinical settings.

References

[1] M. Cerina, M. C. Piastra, and M. Frega, “The potential of in vitro neuronal networks cultured on micro electrode arrays for biomedical research,” *Progress in Biomedical Engineering*, vol. 5, no. 3. Institute of Physics, Jul. 01, 2023. doi: 10.1088/2516-1091/acce12.

[2] D. Lonardoni, H. Amin, S. Di Marco, A. Maccione, L. Berdondini, and T. Nieus, “Recurrently connected and localized neuronal communities initiate coordinated spontaneous activity in neuronal networks,” *PLoS Comput Biol*, vol. 13, no. 7, p. e1005672, Jul. 2017, doi: 10.1371/journal.pcbi.1005672.

[3] M. Chiappalone, A. Novellino, I. Vajda, A. Vato, S. Martinoia, and J. van Pelt, “Burst detection algorithms for the analysis of spatio-temporal patterns in cortical networks of neurons,” *Neurocomputing*, vol. 65–66, no. SPEC. ISS., pp. 653–662, Jun. 2005, doi: 10.1016/j.neucom.2004.10.094.

[4] D. Eytan and S. Marom, “Dynamics and effective topology underlying synchronization in networks of cortical neurons,” *Journal of Neuroscience*, vol. 26, no. 33, pp. 8465–8476, Aug. 2006, doi: 10.1523/JNEUROSCI.1627-06.2006.

[5] D. Lonardoni, S. Di Marco, H. Amin, A. Maccione, L. Berdondini, and T. Nieus, “High-density MEA recordings unveil the dynamics of bursting events in Cell Cultures,” in *Proceedings of the Annual International Conference of the IEEE Engineering in Medicine and Biology Society, EMBS*, 2015, pp. 3763–3766. doi: 10.1109/EMBC.2015.7319212.

[6] T. Fardet, M. Ballandras, S. Bottani, S. Métens, and P. Monceau, “Understanding the generation of network bursts by adaptive oscillatory neurons,” *Front Neurosci*, vol. 12, no. FEB, 2018, doi: 10.3389/fnins.2018.00041.

[7] M. E. J. Obien, K. Deligkaris, T. Bullmann, D. J. Bakkum, and U. Frey, “Revealing neuronal function through microelectrode array recordings,” *Frontiers in Neuroscience*, vol. 9, no. JAN. p. 423, 2015. doi: 10.3389/fnins.2014.00423.

[8] D. Cabrera-Garcia, D. Warm, P. de la Fuente, M. T. Fernández-Sánchez, A. Novelli, and J. M. Villanueva-Balsera, “Early prediction of developing spontaneous activity in cultured neuronal networks,” *Sci Rep*, vol. 11, no. 1, p. 20407, 2021, doi: 10.1038/s41598-021-99538-9.

[9] M. I. Ham, L. M. Bettencourt, F. D. McDaniel, and G. W. Gross, “Spontaneous coordinated activity in cultured networks: Analysis of multiple ignition sites, primary circuits, and burst

phase delay distributions," *J Comput Neurosci*, vol. 24, no. 3, pp. 346–357, Jun. 2008, doi: 10.1007/s10827-007-0059-1.

[10] M. Gandolfo, A. Maccione, M. Tedesco, S. Martinoia, and L. Berdondini, "Tracking burst patterns in hippocampal cultures with high-density CMOS-MEAs," *J Neural Eng*, vol. 7, no. 5, p. 056001, Oct. 2010, doi: 10.1088/1741-2560/7/5/056001.

[11] J. Shao, Y. Liu, D. Gao, J. Tu, and F. Yang, "Neural Burst Firing and Its Roles in Mental and Neurological Disorders," *Frontiers in Cellular Neuroscience*, vol. 15. Sep. 27, 2021. doi: 10.3389/fncel.2021.741292.

[12] Y. S. Vakilna, W. C. Tang, B. C. Wheeler, and G. J. Brewer, "The Flow of Axonal Information Among Hippocampal Subregions: 1. Feed-Forward and Feedback Network Spatial Dynamics Underpinning Emergent Information Processing," *Front Neural Circuits*, vol. 15, Aug. 2021, doi: 10.3389/fncir.2021.660837.

[13] N. A. Steinmetz, C. Koch, K. D. Harris, and M. Carandini, "Challenges and opportunities for large-scale electrophysiology with Neuropixels probes," *Current Opinion in Neurobiology*, vol. 50. pp. 92–100, 2018. doi: 10.1016/j.conb.2018.01.009.

[14] P. Alcami and A. El Hady, "Axonal Computations," *Frontiers in Cellular Neuroscience*, vol. 13. Sep. 18, 2019. doi: 10.3389/fncel.2019.00413.

[15] J. C. Mateus, M. M. Sousa, J. Burrone, and P. Aguiar, "Beyond a Transmission Cable—New Technologies to Reveal the Richness in Axonal Electrophysiology," *Journal of Neuroscience*, vol. 44, no. 11, p. e1446232023, Mar. 2024, doi: 10.1523/JNEUROSCI.1446-23.2023.

[16] L. Huang and G. van Luijtelaar, "Search For New Targets Of Deep Brain Stimulation For Epilepsy Treatment," *J Neurol Res Ther*, vol. 1, no. 2, pp. 23–33, Mar. 2016, doi: 10.14302/issn.2470-5020.jnrt-15-800.

[17] X.-M. Zhang and J. Zhu, "Kainic Acid-Induced Neurotoxicity: Targeting Glial Responses and Glia-Derived Cytokines," *Curr Neuropharmacol*, vol. 9, no. 2, pp. 388–398, May 2011, doi: 10.2174/157015911795596540.

[18] D. A. Hosford and J. O. McNamara, "Basic mechanisms of the epilepsies," *Current Opinion in Neurology and Neurosurgery*, vol. 3, no. 2. pp. 262–265, 1990. doi: 10.7326/0003-4819-72-6-969_2.

[19] R. Habibey, J. E. Rojo Arias, J. Striebel, and V. Busskamp, "Microfluidics for Neuronal Cell and Circuit Engineering," *Chemical Reviews*, vol. 122, no. 18. American Chemical Society, pp. 14842–14880, Sep. 28, 2022. doi: 10.1021/acs.chemrev.2c00212.

[20] M. Katsuno, K. Sahashi, Y. Iguchi, and A. Hashizume, "Preclinical progression of neurodegenerative diseases," *Nagoya Journal of Medical Science*, vol. 80, no. 3. Nagoya University, pp. 289–298, Aug. 01, 2018. doi: 10.18999/nagjms.80.3.289.

[21] J. C. Mateus *et al.*, "Bidirectional flow of action potentials in axons drives activity dynamics in neuronal cultures," *J Neural Eng*, vol. 18, no. 6, p. 066045, Dec. 2021, doi: 10.1088/1741-2552/ac41db.

[22] S. Na *et al.*, "Microfluidic neural axon diode," *Technology (Singap World Sci)*, vol. 04, no. 04, pp. 240–248, Dec. 2016, doi: 10.1142/s2339547816500102.

[23] J. M. Peyrin *et al.*, "Axon diodes for the reconstruction of oriented neuronal networks in microfluidic chambers," *Lab Chip*, vol. 11, no. 21, pp. 3663–3673, Nov. 2011, doi: 10.1039/c1lc20014c.

[24] N. Winter-Hjelm, Å. Brune Tomren, P. Sikorski, A. Sandvig, and I. Sandvig, "Structure-function dynamics of engineered, modular neuronal networks with controllable afferent-efferent connectivity," *J Neural Eng*, vol. 20, no. 4, Aug. 2023, doi: 10.1088/1741-2552/ace37f.

[25] P. M. Holloway, G. I. Hallinan, M. Hegde, S. I. R. Lane, K. Deinhardt, and J. West, "Asymmetric confinement for defining outgrowth directionality," *Lab Chip*, vol. 19, no. 8, pp. 1484–1489, Apr. 2019, doi: 10.1039/c9lc00078j.

[26] T. Alejandre-García, S. Kim, J. Pérez-Ortega, and R. Yuste, "Intrinsic excitability mechanisms of neuronal ensemble formation," *Elife*, vol. 11, 2022, doi: 10.7554/eLife.77470.

[27] A. Tanwar, H. A. Gandhi, D. Kushwaha, and J. Bhattacharya, "A review on microelectrode array fabrication techniques and their applications," *Materials Today Chemistry*, vol. 26. p. 101153, 2022. doi: 10.1016/j.mtchem.2022.101153.

[28] Axion Biosystems, "Neural Characterization and Development." Accessed: Oct. 25, 2023. [Online]. Available: https://www.axionbiosystems.com/applications/neural-activity/neural-characterization-and-development

[29] Netri, "Netri Devices | Software." Accessed: Oct. 02, 2023. [Online]. Available: https://netri.com/netri-devices/products/software/

[30] 3Brain, "Brainwave 5." Accessed: Oct. 02, 2023. [Online]. Available: https://www.3brain.com/products/software/brainwave5

[31] J. E. Chung *et al.*, "High-density single-unit human cortical recordings using the Neuropixels probe," *Neuron*, vol. 110, no. 15, pp. 2409-2421.e3, Aug. 2022, doi: 10.1016/j.neuron.2022.05.007.

[32] M. Toledo-Rodriguez and H. Markram, "Single-Cell RT-PCR, a Technique to decipher the electrical, anatomical, and genetic determinants of neuronal diversity," *Methods in Molecular Biology*, vol. 1183, pp. 143–158, 2014, doi: 10.1007/978-1-4939-1096-0_8.

[33] H. Kida, Y. Sakimoto, and D. Mitsushima, "Slice patch clamp technique for analyzing learning-induced plasticity," *Journal of Visualized Experiments*, vol. 2017, no. 129, Nov. 2017, doi: 10.3791/55876.

[34] T. Guillamón-Vivancos, D. Vandael, D. Torres, G. López-Bendito, and F. J. Martini, "Mesoscale calcium imaging in vivo: evolution and contribution to developmental neuroscience," *Frontiers in Neuroscience*, vol. 17. Frontiers Media SA, 2023. doi: 10.3389/fnins.2023.1210199.

[35] M. Robbins, C. N. Christensen, C. F. Kaminski, and M. Zlatic, “Calcium imaging analysis - how far have we come?,” *F1000Research*, vol. 10. NLM (Medline), p. 258, 2021. doi: 10.12688/f1000research.51755.1.

[36] W. N. Ross, K. Miyazaki, M. A. Popovic, and D. Zecevic, “Imaging with organic indicators and high-speed charge-coupled device cameras in neurons: some applications where these classic techniques have advantages,” *Neurophotonics*, vol. 2, no. 2, p. 021005, Dec. 2014, doi: 10.1117/1.nph.2.2.021005.

[37] T. Nöbauer, R. Prevedel, F. Schlumm, M. Hoffmann, M. Molodtsov, and A. Vaziri, “Whole-brain dynamics of neuronal circuits enabled by sculpted light and light field microscopy,” in *International IEEE/EMBS Conference on Neural Engineering, NER*, 2015, pp. 869–872. doi: 10.1109/NER.2015.7146762.

[38] S. R. Schultz, C. S. Copeland, A. J. Foust, P. Quicke, and R. Schuck, “Advances in Two-Photon Scanning and Scanless Microscopy Technologies for Functional Neural Circuit Imaging,” *Proceedings of the IEEE*, vol. 105, no. 1. Institute of Electrical and Electronics Engineers Inc., pp. 139–157, Jan. 01, 2017. doi: 10.1109/JPROC.2016.2577380.

[39] L. Qiu, B. Zhang, and Z. Gao, “Lighting Up Neural Circuits by Viral Tracing,” *Neuroscience Bulletin*, vol. 38, no. 11. pp. 1383–1396, Nov. 16, 2022. doi: 10.1007/s12264-022-00860-7.

[40] L. Fenno, O. Yizhar, and K. Deisseroth, “The development and application of optogenetics,” *Annu Rev Neurosci*, vol. 34, pp. 389–412, Jul. 2011, doi: 10.1146/annurev-neuro-061010-113817.

[41] M. Hariz and P. Blomstedt, “Deep brain stimulation for Parkinson’s disease,” *Journal of Internal Medicine*, vol. 292, no. 5. John Wiley and Sons Inc, pp. 764–778, Nov. 01, 2022. doi: 10.1111/joim.13541.

[42] C. Liu *et al.*, “An action potential initiation mechanism in distal axons for the control of dopamine release,” *Science (1979)*, vol. 375, no. 6587, pp. 1378–1385, Mar. 2022, doi: 10.1126/science.abn0532.

[43] R. D. Traub, M. A. Whittington, N. Maier, D. Schmitz, and J. I. Nagy, “Could electrical coupling contribute to the formation of cell assemblies?,” *Rev Neurosci*, vol. 31, no. 2, pp. 121–141, Feb. 2020, doi: 10.1515/revneuro-2019-0059.

[44] J. Wouters, F. Kloosterman, and A. Bertrand, “Towards online spike sorting for high-density neural probes using discriminative template matching with suppression of interfering spikes,” *J Neural Eng*, vol. 15, no. 5, p. 056005, Oct. 2018, doi: 10.1088/1741-2552/aace8a.

[45] I. Magrans de Abril, J. Yoshimoto, and K. Doya, “Connectivity inference from neural recording data: Challenges, mathematical bases and research directions,” *Neural Networks*, vol. 102. Pergamon, pp. 120–137, Jun. 01, 2018. doi: 10.1016/j.neunet.2018.02.016.

[46] K. Heiney, J. C. Mateus, C. D. F. Lopes, E. Neto, M. Lamghari, and P. Aguiar, “µSpikeHunter: An advanced computational tool for the analysis of neuronal communication and action

potential propagation in microfluidic platforms," *Sci Rep*, vol. 9, no. 1, p. 5777, 2019, doi: 10.1038/s41598-019-42148-3.

[47] M. Aghagolzadeh, A. Mohebi, and K. G. Oweiss, "Sorting and tracking neuronal spikes via simple thresholding," *IEEE Transactions on Neural Systems and Rehabilitation Engineering*, vol. 22, no. 4, pp. 858–869, Jul. 2014, doi: 10.1109/TNSRE.2013.2289918.

[48] A. M. Kamboh and A. J. Mason, "Computationally efficient neural feature extraction for spike sorting in implantable high-Density recording systems," *IEEE Transactions on Neural Systems and Rehabilitation Engineering*, vol. 21, no. 1, pp. 1–9, Jan. 2013, doi: 10.1109/TNSRE.2012.2211036.

[49] V. Pasquale, S. Martinoia, and M. Chiappalone, "A self-adapting approach for the detection of bursts and network bursts in neuronal cultures," *J Comput Neurosci*, vol. 29, no. 1–2, pp. 213–229, 2010, doi: 10.1007/s10827-009-0175-1.

[50] T. P. Patel, K. Man, B. L. Firestein, and D. F. Meaney, "Automated quantification of neuronal networks and single-cell calcium dynamics using calcium imaging," *J Neurosci Methods*, vol. 243, pp. 26–38, Mar. 2015, doi: 10.1016/j.jneumeth.2015.01.020.

[51] J. P. Dominguez-Morales, S. Buccelli, D. Gutierrez-Galan, I. Colombi, A. Jimenez-Fernandez, and M. Chiappalone, "Real-time detection of bursts in neuronal cultures using a neuromorphic auditory sensor and spiking neural networks," *Neurocomputing*, vol. 449, pp. 422–434, Aug. 2021, doi: 10.1016/j.neucom.2021.03.109.

[52] N. S. Narayanan and M. Laubach, "Methods for studying functional interactions among neuronal populations," *Methods in Molecular Biology*, vol. 489, pp. 135–165, 2009, doi: 10.1007/978-1-59745-543-5_7.

[53] R. Segev, I. Baruchi, E. Hulata, and E. Ben-Jacob, "Hidden Neuronal Correlations in Cultured Networks," *Phys Rev Lett*, vol. 92, no. 11, p. 118102, Mar. 2004, doi: 10.1103/PhysRevLett.92.118102.

[54] A. F. Meyer, J. Poort, J. O'Keefe, M. Sahani, and J. F. Linden, "A Head-Mounted Camera System Integrates Detailed Behavioral Monitoring with Multichannel Electrophysiology in Freely Moving Mice," *Neuron*, vol. 100, no. 1, pp. 46-60.e7, Oct. 2018, doi: 10.1016/j.neuron.2018.09.020.

[55] M. Bisio, A. Bosca, V. Pasquale, L. Berdondini, and M. Chiappalone, "Emergence of bursting activity in connected neuronal sub-populations," *PLoS One*, vol. 9, no. 9, p. e107400, Sep. 2014, doi: 10.1371/journal.pone.0107400.

[56] F. Miraglia *et al.*, "Brain Connectivity and Graph Theory Analysis in Alzheimer's and Parkinson's Disease: The Contribution of Electrophysiological Techniques," *Brain Sciences*, vol. 12, no. 3. p. 402, Mar. 18, 2022. doi: 10.3390/brainsci12030402.

[57] C. Miehl, S. Onasch, D. Festa, and J. Gjorgjieva, "Formation and computational implications of assemblies in neural circuits," *Journal of Physiology*, vol. 601, no. 15. pp. 3071–3090, 2023. doi: 10.1113/JP282750.

[58] D. Poli, V. P. Pastore, and P. Massobrio, “Functional connectivity in in vitro neuronal assemblies,” *Frontiers in Neural Circuits*, vol. 9, no. OCT. Frontiers Research Foundation, Oct. 07, 2015. doi: 10.3389/fncir.2015.00057.

[59] A. Tauste Campo, “Inferring neural information flow from spiking data,” *Computational and Structural Biotechnology Journal*, vol. 18. Elsevier B.V., pp. 2699–2708, Jan. 01, 2020. doi: 10.1016/j.csbj.2020.09.007.

[60] IEEE Information Theory Society and Institute of Electrical and Electronics Engineers, *2020 IEEE International Symposium on Information Theory : proceedings : July 21-26, 2020, Virtual, Los Angeles, California, USA*. Pistacaway, New Jersey: IEEE, 2020.

[61] Z. C. Chao, D. J. Bakkum, and S. M. Potter, “Region-specific network plasticity in simulated and living cortical networks: comparison of the center of activity trajectory (CAT) with other statistics.,” *J Neural Eng*, vol. 4, no. 3, pp. 294–308, Sep. 2007, doi: 10.1088/1741-2560/4/3/015.

[62] N. M. Timme and C. Lapish, “A tutorial for information theory in neuroscience,” *eNeuro*, vol. 5, no. 3. Society for Neuroscience, May 01, 2018. doi: 10.1523/ENEURO.0052-18.2018.

[63] M. Ursino, G. Ricci, and E. Magosso, “Transfer Entropy as a Measure of Brain Connectivity: A Critical Analysis With the Help of Neural Mass Models,” *Front Comput Neurosci*, vol. 14, Jun. 2020, doi: 10.3389/fncom.2020.00045.

[64] E. Neto *et al.*, “Compartmentalized microfluidic platforms: The unrivaled breakthrough of in vitro tools for neurobiological research,” *Journal of Neuroscience*, vol. 36, no. 46, pp. 11573–11584, Nov. 2016, doi: 10.1523/JNEUROSCI.1748-16.2016.

[65] A. Purwidyantri and B. A. Prabowo, “Tesla Valve Microfluidics: The Rise of Forgotten Technology,” *Chemosensors*, vol. 11, no. 4. MDPI, Apr. 01, 2023. doi: 10.3390/chemosensors11040256.

[66] C. Forró *et al.*, “Modular microstructure design to build neuronal networks of defined functional connectivity,” *Biosens Bioelectron*, vol. 122, pp. 75–87, Dec. 2018, doi: 10.1016/j.bios.2018.08.075.

[67] C. D. F. Lopes, J. C. Mateus, and P. Aguiar, “Interfacing microfluidics with microelectrode arrays for studying neuronal communication and axonal signal propagation,” *Journal of Visualized Experiments*, vol. 2018, no. 142, Dec. 2018, doi: 10.3791/58878.

[68] M. Lodi, F. Della Rossa, F. Sorrentino, and M. Storace, “Analyzing synchronized clusters in neuron networks,” *Sci Rep*, vol. 10, no. 1, Dec. 2020, doi: 10.1038/s41598-020-73269-9.

[69] I. Belykh and M. Hasler, “Mesoscale and clusters of synchrony in networks of bursting neurons,” *Chaos*, vol. 21, no. 1, 2011, doi: 10.1063/1.3563581.

[70] T. B. DeMarse, L. Pan, S. Alagapan, G. J. Brewer, and B. C. Wheeler, “Feed-forward propagation of temporal and rate information between cortical populations during coherent activation in engineered in vitro networks,” *Front Neural Circuits*, vol. 10, no. APR, Apr. 2016, doi: 10.3389/fncir.2016.00032.

[71] D. X. Wang and C. E. Davila, “Subspace Averaging of Auditory Evoked Potentials,” in *Proceedings of the Annual International Conference of the IEEE Engineering in Medicine and Biology Society, EMBS*, 2019, pp. 656–659. doi: 10.1109/EMBC.2019.8857818.

[72] T. Pander, S. Pietraszek, and T. Przybyła, “A Novel Approach to Robust Weighted Averaging of Auditory Evoked Potentials,” in *Information Technologies in Biomedicine, Volume 4*, E. Piętka, J. Kawa, and W. Wieclawek, Eds., Cham: Springer International Publishing, 2014, pp. 321–332. doi: 10.1007/978-3-319-06596-0_30.

[73] L. Badel, W. Gerstner, and M. J. E. Richardson, “Spike-triggered averages for passive and resonant neurons receiving filtered excitatory and inhibitory synaptic drive,” *Phys Rev E Stat Nonlin Soft Matter Phys*, vol. 78, no. 1, Jul. 2008, doi: 10.1103/PhysRevE.78.011914.

[74] J. Shen, N. Liu, D. Li, and B. Zhang, “Behavioral Analysis of EEG Signals in Loss-Gain Decision-Making Experiments,” *Behavioural Neurology*, vol. 2022, 2022, doi: 10.1155/2022/3070608.

[75] M. R. Heusser, C. Bourrelly, and N. J. Gandhi, “Decoding the Time Course of Spatial Information from Spiking and Local Field Potential Activities in the Superior Colliculus,” *eNeuro*, vol. 9, no. 6, pp. 1–13, 2022, doi: 10.1523/ENEURO.0347-22.2022.

[76] S. Curreli, J. Bonato, S. Romanzi, S. Panzeri, and T. Fellin, *Complementary encoding of spatial information in hippocampal astrocytes*, vol. 20, no. 3. 2022. doi: 10.1371/journal.pbio.3001530.

[77] C. D. F. Lopes, J. C. Mateus, and P. Aguiar, “Interfacing microfluidics with microelectrode arrays for studying neuronal communication and axonal signal propagation,” *Journal of Visualized Experiments*, vol. 2018, no. 142, Dec. 2018, doi: 10.3791/58878.

[78] N. Goshi, G. Girardi, F. da Costa Souza, A. Gardner, P. J. Lein, and E. Seker, “Influence of microchannel geometry on device performance and electrophysiological recording fidelity during long-term studies of connected neural populations,” *Lab Chip*, vol. 22, no. 20, pp. 3961–3975, 2022, doi: 10.1039/d2lc00683a.

[79] Y. Pigareva, A. Gladkov, V. Kolpakov, V. B. Kazantsev, I. Mukhina, and A. Pimashkin, “The Profile of Network Spontaneous Activity and Functional Organization Interplay in Hierarchically Connected Modular Neural Networks In Vitro,” *Micromachines (Basel)*, vol. 15, no. 6, p. 732, May 2024, doi: 10.3390/mi15060732.

[80] S. Wang, R. Hesen, B. Mossink, N. Nadif Kasri, and D. Schubert, “Generation of glutamatergic/GABAergic neuronal co-cultures derived from human induced pluripotent stem cells for characterizing E/I balance in vitro,” *STAR Protoc*, vol. 4, no. 1, p. 101967, Mar. 2023, doi: 10.1016/j.xpro.2022.101967.

[81] A. G. Nadadhur *et al.*, “Multi-level characterization of balanced inhibitory-excitatory cortical neuron network derived from human pluripotent stem cells,” *PLoS One*, vol. 12, no. 6, p. e0178533, Jun. 2017, doi: 10.1371/journal.pone.0178533.

[82] A. A. Galiakberova *et al.*, “Different iPSC-derived neural stem cells shows various spectrums of spontaneous differentiation during long term cultivation,” *Front Mol Neurosci*, vol. 16, May 2023, doi: 10.3389/fnmol.2023.1037902.

[83] C. Gottschling, E. Dzyubenko, M. Geissler, and A. Faissner, “The indirect neuron-astrocyte coculture assay: An in vitro set-up for the detailed investigation of neuron-glia interactions,” *Journal of Visualized Experiments*, vol. 2016, no. 117, Nov. 2016, doi: 10.3791/54757.

[84] A. Ahtiainen, B. Genocchi, J. M. A. Tanskanen, M. T. Barros, J. A. K. Hyttinen, and K. Lenk, “Astrocytes exhibit a protective role in neuronal firing patterns under chemically induced seizures in neuron–astrocyte co-cultures,” *Int J Mol Sci*, vol. 22, no. 23, p. 12770, Nov. 2021, doi: 10.3390/ijms222312770.

[85] S. F. Kazim *et al.*, “Neuronal network excitability in alzheimer’s disease: The puzzle of similar versus divergent roles of amyloid B and TAU,” *eNeuro*, vol. 8, no. 2. p. ENEURO.0418-20.2020, Mar. 2021. doi: 10.1523/ENEURO.0418-20.2020.

[86] K. Kudo *et al.*, “Neurophysiological trajectories in Alzheimer’s disease progression,” *Elife*, vol. 12, Mar. 2024, doi: 10.7554/eLife.91044.